Sclerochronological $\delta^{18}O$ and $\delta^{13}C$ patterns in shells of the aquatic gastropod *Radix* sp. as a new climatic and hydrologic archive for the Tibetan Plateau in sub-seasonal resolution

Dissertation
zur Erlangung des akademischen Grades
Doktor der Naturwissenschaften
"doctor rerum naturalium"
(Dr. rer. nat.)
am Fachbereich Geowissenschaften der Freien Universität Berlin

in Form einer kumulativen Arbeit

vorgelegt von

Linda Taft

Berlin, 2013

Eidesstattliche Erklärung

Hiermit erkläre ich, dass ich die vorgelegte Arbeit selbständig und ohne fremde Hilfe verfasst und andere als die angegebenen Hilfsmittel nicht benutzt habe. Die Beiträge der Co-Autoren der wissenschaftlichen Veröffentlichungen sind in Kapitel 1.6 dargelegt. Ich erkläre, dass ich die Arbeit erstmalig und nur am Fachbereich Geowissenschaften der Freien Universität Berlin eingereicht habe und keinen entsprechenden Doktorgrad besitze. Der Inhalt der dem Verfahren zugrunde liegenden Promotionsordnung ist mir bekannt.

Linda Taft   Berlin, 25.07.2013

Acknowledgements

This dissertation would not have been possible without the support and help of numerous people to whom I would like to express my gratitude.

First of all, I would like to thank my supervisor Prof. Dr. Frank Riedel (FU Berlin) for his constant encouragement and support over the years. I greatly benefited from the inspiring discussions as well as from his constructive criticism, his broad knowledge, his encouragement, his beliefs and his great ideas! I also wish to thank Dr. Uwe Wiechert (FU Berlin) for critical discussions and Prof. Dr. Pavel Tarasov (FU Berlin) for constructive suggestions and motivation. Special thanks go to Prof. Dr. Steffen Mischke (FU Berlin and University of Potsdam) for his constructive reviews and his encouragement. It is always a pleasure to work with you! Furthermore, I am grateful to the Deutsche Forschungsgemeinschaft (DFG) for funding my PhD position as part of the Priority Program 1372 "Tibetan Plateau (TiP): Formation-Climate-Ecosystems"

Many thanks go to Parm von Oheimb, Thomas Wilke (both University of Gießen), Guoliang Lei (Fujian Normal University, Fuzhou, China) and Hucai Zhang (Yunnan Normal University, Kunming, China) for a great field trip across the Tibetan Plateau in 2009.

For support in preparation and analytical work I would like to express my gratitude to Maike Glos, Franziska Slotta and Matthias Friebel (all FU Berlin). Furthermore I would like to thank Jan Evers (FU Berlin) for creating some figures for the manuscripts.

I thank Christian Leipe for always listening to my major and minor problems, the great time, atmosphere and countless cups of tea in our office. It is a pleasure to share an office room with you! I will thank my friends and colleagues from the Department of Palaeontology (FU Berlin) for all that support and perfect distraction during our lunch-breaks and Wednesday coffee-meetings.

Finally and most important, I would like to thank with all my heart my family! Stephan, for your great moral, and often professional, support, patience and love. Our daughter Lotte, who joined us in the last year of my PhD time, for her smiles and childlike curiosity. You are the greatest happiness for me!

Table of contents

<u>List of figures</u>

List of abbreviations

a.s.l.	above sea level
C	carbon
CAM	Carrara marble
DEM	digital elevation model
DFG	Deutsche Forschungsgemeinschaft
ENSO	El Niño Southern Oscillation
GFZ	GeoForschungsZentrum
IAEA	International Atomic Energy Agency
KKS	Kaiserstuhl carbonatite
km²	square kilometre
LM	Laaser marble (in-house reference material)
m	metre
ml	millilitre
µg	microgram
O	oxygen
SEM	scanning electron microscopy
TIC	total inorganic carbon
TIP	DFG Priority Program 1372 "Tibetan Plateau: Formation-Climate-Ecosystems"
TOC	total organic carbon
TP	Tibetan Plateau
ü.M.	über dem Meer
V-PDB	Vienna PeeDee Belemnite
V-SMOW	Vienna Standard Mean Ocean Water

Abstract

The Tibetan Plateau (TP) is the largest elevated land mass on earth with a mean elevation of 4500 m a.s.l. The uplift started about 50 million years ago with the collision of the Indian and Eurasian plates. The TP has become a major focus of palaeoclimatic and palaeoenvironmental research during the last two decades because it influences not only the atmospheric circulation in Asia but also on a global scale. During the north hemispheric summer the TP heats up causing a low-pressure area over central Asia. It is generally accepted that this process results in a big land-ocean-circulation, the Indian and East Asian monsoon, which transports moist air masses from the Indian and Pacific Ocean to the Asian mainland. However, these triggering factors have recently come under scientific discussion again. Moreover, the TP is a barrier for the westerly wind circulation, which is split into a northern and a southern branch at the western margin of the TP. Open research questions concern the chronology of single uplift processes of the TP and how they affect monsoon intensity, moisture transport pathways and global circulation patterns. The TP is sometimes called the "water tower" of Asia because it is the source area of major Asian rivers such as the Indus, Brahmaputra, Mekong, Yangtze and Yellow rivers on which billions of people depend. The water regimen primarily depends on monsoon precipitation and glacier dynamics. Thus, an understanding of the atmospheric and hydrologic patterns and processes in this region is essential for evaluating future climate predictions, particularly with emphasis on "Global Change" that implicates the anthopogenic factor. Of importance is not only a deeper understanding of modern climate and environmental dynamics. Reconstructing former climate events and trends is an important tool to comprehend the entire spectrum of interactions, dynamics and scales. For this purpose, temporal high-resolution climate archives are essential because they mirror both general long-term trends and short-term (extreme) events. Suitable archives are tree rings with a resolution of one year, varves and ice cores with a seasonal resolution. However, the application of these archives to the TP is limited because most of the plateau area is treeless, most lakes do not have varves and glaciated areas are difficult to access and limited to high mountain ranges.

In the doctoral thesis presented here, aragonitic shells of the aquatic gastropod *Radix* were investigated in order to test whether they represent a suitable high-resolution archive for climatic and hydrologic patterns on the TP. ^{18}O and ^{13}C ratios of the shells are in equilibrium with the ambient lake waters and therefore allow conclusions about climatic and ecological conditions. In order to obtain the highest temporal resolution, the shells were sampled in equal distance along the ontogenetic order of the whorls. Using this method, up to 31 sub-samples per shell could be measured for oxygen and carbon isotope compositions.

Abstract

The doctoral thesis is structured in three consecutive sections. The study started with the question if sclerochronological $\delta^{18}O$ and $\delta^{13}C$ values of modern *Radix* shells mirror modern climatic and hydrologic conditions on the TP and if it is therefore a promising archive for palaeoclimate reconstructions. Shells from three different localities at two lakes which are influenced by the monsoon system were isotopically analysed.

The second step was a regional enlargement of the study in order to test if the isotope values of recent shells represent different lake settings within the atmospheric circulation. To answer this question, shells from seven lakes were analysed. Some of the lakes are located in the monsoon region, some are influenced by the westerly wind system and some are located in their transition zone.

The application to fossil shells was the final step of this study. A limnological multi-proxy study on a sediment core from Lake Karakul in Tajikistan (Mischke et al., 2010) provided first results of climate and environmental conditions in the lake catchments for the last 4200 cal yr BP. 21 fossil *Radix* shells from the core were isotopically analysed and the results were compared to $\delta^{18}O$ values of authigenic aragonite and ostracod calcite in order to test whether lake level changes were mainly triggered by glacial meltwater as was previously suggested by Mischke et al., (2010).

The results of these three working steps are published in two international peer-reviewed journals. A third manuscript has been submitted.

The sclerochronological isotope patterns indicate seasonal changes of temperature, precipitation, evaporation, biological productivity within the lakes, exchange with the atmosphere and input of allochthonous CO_2 from the catchment. Furthermore, it is possible to distinguish between precipitation and meltwater fluxes. Isotopic bulk values allow conclusions about lake setting characteristics and long-term trends. The study results have shown that 1) modern $\delta^{18}O$ and $\delta^{13}C$ compositions of the shells mirror modern climate and hydrologic conditions on the TP and are thus a promising tool for palaeoclimatic reconstructions, 2) shells from lakes which are influenced by the monsoon system show a distinct monsoon signal in the sclerochronological patterns, 3) modern $\delta^{18}O$ and $\delta^{13}C$ compositions of the shells mirror different lake settings within the atmospheric circulation, independent of the lake character and, 4) late Holocene $\delta^{18}O$ and $\delta^{13}C$ compositions of fossil shells from Lake Karakul in Tajikistan indicate changes of temperature and meltwater flux since 4200 cal yr BP.

The results of this doctoral thesis contribute to a better understanding and evaluation of atmospheric circulation patterns and hydrologic conditions on the TP. The aquatic gastropod *Radix* is a further suitable archive for palaeoclimatic and palaeoenvironmental studies which
2

differs from the already existing archives by its particularly high resolution. With the aid of the sclerochronological approach it is possible to distinguish between precipitation and meltwater.

Open research questions exist concerning the dynamic and the evolution of the palaeo-monsoon on the TP and in surrounding regions as well as the uplift history of the TP which can also be highlighted by using fossil *Radix* shells.

Kurzfassung

Das Tibetplateau (TP) ist die höchstgelegene zusammenhängende Landmasse der Erde. Die Hebung des Plateaus begann vor ungefähr 50 Millionen Jahren durch die Kollision der Indischen mit der Eurasischen Platte. Aufgrund des großen Einflusses auf die asiatischen und globalen atmosphärischen Zirkulationsmuster war das TP innerhalb der letzten Jahrzehnte zunehmend im Fokus paläoklimatischer Studien. Durch die Höhe des Plateaus, die durchschnittlich ca. 4500 m ü.M. beträgt, wirkt es im nordhemisphärischen Sommer wie eine Heizfläche, was das Tiefdruckgebiet über Zentralasien verstärkt. Es ist allgemein anerkannt, dass dieser Vorgang zu einer großen Land-Seewind-Zirkulation führt, die feuchte Luftmassen vom Indischen und Pazifischen Ozean auf das asiatische Festland transportiert (Indischer und Ostasiatischer Monsun), obwohl es jüngst erneute Diskussionen über die auslösenden Faktoren gibt. Zudem stellt das TP eine Barriere für die globale Westwindzirkulation dar, die im Bereich des westlichen Plateaus in einen nördlichen und einen südlichen Zweig gesplittet wird. Offene Forschungsfragen bestehen hinsichtlich der zeitlichen Abfolge der einzelnen Hebungsprozesse des Plateaus und wie diese sich auf Monsunintensität, Feuchtigkeitstransportwege und globale Zirkulationsmuster ausgewirkt haben. Das TP ist Quellgebiet einiger großer asiatische Flüsse wie beispielsweise Indus, Brahmaputra, Mekong, Yangze und Gelber Fluss, deren Wasserführung wesentlich von Monsunniederschlägen und Gletscherdynamik abhängen und die das Leben von mehr als einer Milliarde Menschen beeinflussen. Das TP wird deshalb auch der „Water Tower" Asiens genannt. Das Verständnis von atmosphärischen und hydrologischen Mustern und Prozessen in dieser Region ist folglich essentiell, um zukünftige Klimaprognosen zu bewerten, insbesondere unter dem Aspekt von „Global Change", was den anthropogenen Faktor mit einbezieht. Dabei ist jedoch nicht nur das Prozessverständnis moderner Klima- und Umweltdynamiken von Bedeutung. Auch die Rekonstruktion von Klimaereignissen und –trends in der Vergangenheit sind ein wichtiges Werkzeug um die ganze Bandbreite von Wechselwirkungen, Dynamiken und Größenordnungen zu erfassen und zu verstehen, und um diese Erkenntnisse in zukünftige Prognosen mit einfließen zu lassen. Dafür sind zeitlich hochaufgelöste Archive wichtig, die nicht nur generelle Trends abbilden

sondern auch relativ kurzfristige (extreme) Klimaereignisse widerspiegeln. Geeignete Archive sind Baumringe mit einer Auflösung von einem Jahr, Warven mit einer saisonalen Auflösung oder Eisbohrkerne mit einer bestenfalls saisonalen Auflösung. Die Verwendung dieser Archive ist auf dem TP jedoch nur eingeschränkt möglich, da der größte Teil des Plateaus baumlos ist, die meisten Seen keine Warven aufweisen und sich Vergletscherungen auf einige wenige Gebiete beschränken. Zudem sind weite Teile des Plateaus nur unter erschwerten Bedingungen zugänglich.

In der vorliegenden Dissertation wurde untersucht, ob die aragonitischen Gehäuse der aquatischen Gastropode *Radix* solch ein geeignetes Archiv für hochauflösende klimatische und hydrologische Muster auf dem TP darstellen. Als Klima- und Umweltproxy wurden ^{18}O und ^{13}C Verhältnisse analysiert, da sich die Isotopenwerte der Gehäuse im Gleichgewicht mit den Habitaten innerhalb der Seen befinden und somit Rückschlüsse auf die klimatischen und ökologischen Gegebenheiten erlauben. Um eine besonders hohe zeitliche Auflösung zu erreichen, wurden die Gehäuse in einem gleichmäßigen Abstand entlang der ontogenetischen Wachstumsspirale beprobt. Mit dieser Methode konnten bis zu 31 Einzelproben pro Gehäuse gewonnen werden, die isotopisch analysiert wurden.

Die Dissertation ist in drei thematisch aufeinander aufbauende Abschnitte strukturiert. Am Anfang stand die Frage, ob sclerochronologische δ^{18}O und δ^{13}C Muster rezenter *Radix*gehäuse die rezenten klimatischen und hydrologischen Gegebenheiten widerspiegeln und somit ein vielversprechendes Archiv für paläoklimatische Rekonstruktionen darstellen. Dafür wurden je zwei Gehäuse an drei unterschiedlichen Lokalitäten zweier Seen die sich im Monsuneinfluss befinden, isotopisch analysiert. Der folgende Arbeitsschritt bestand aus einer regionalen Ausdehnung der Untersuchungen um herauszufinden, ob die Isotopenmuster in rezenten Gehäusen auch die unterschiedlichen klimatischen Gegebenheiten der Seen widerspiegeln die sich aufgrund verschiedener Positionen innerhalb der atmosphärischen Zirkulation ergeben. Hierfür wurden insgesamt jeweils zwei Gehäuse von sieben Seen beprobt, die teils dem Monsuneinfluss, teils dem Einfluss des Westwindsystems und teils keinem von beiden Systemen exakt zugeordnet werden können. Der abschließende Schritt bestand aus der Beprobung von 21 fossilen *Radix*gehäusen aus einem Bohrkern der im östlichen Becken des Lake Karakul in Tajikistan geborgen wurde, welcher die letzten 4200 Jahre vor heute abdeckt. Unter diesen drei Aspekten sind drei Manuskripte entstanden, die bereits zum überwiegenden Teil in international peer-reviewed Zeitschriften veröffentlicht wurden.

Diese sclerochronologischen Isotopenmuster geben Hinweise auf saisonale Änderungen von Temperatur, Niederschlägen, Evaporation, biologischen Aktivität innerhalb des Sees, Austausch mit der Atmosphäre und Eintrag von allochthonem CO_2 aus der Umgebung. Darüber hinaus ist es möglich, Niederschläge von Schmelzwassereinträgen zu unterscheiden. Aber auch die isotopischen Durchschnittswerte erlauben Rückschlüsse auf die Lage des Sees innerhalb der atmosphärischen Zirkulation, den Seentyp (offenes oder geschlossenes System) und klimatische Langzeittrends. Die Untersuchungsergebnisse haben gezeigt, dass 1) die modernen $\delta^{18}O$ und $\delta^{13}C$ Zusammensetzungen der Gehäuse die modernen klimatischen und hydrologischen Gegebenheiten auf dem TP widerspiegeln und somit ein vielversprechendes Werkzeug für paläoklimatische Studien darstellen, 2) die Gehäuse die aus Seen stammen die im Monsuneinfluss liegen, ein deutlich ausgeprägtes Monsunsignal in ihren sclerochronologischen Mustern aufweisen, das aus einem abrupten Anstieg der $\delta^{18}O$ Werte und einem anschließenden graduellen Abfallen der Werte besteht, 3) die Isotopenmuster der rezenten Gehäuse die Lage der Seen innerhalb der atmosphärischen Zirkulation zeigen, unabhängig vom Charakter des Sees und 4) dass die spätholozänen $\delta^{18}O$ und $\delta^{13}C$ Zusammensetzungen der Gehäuse aus dem Lake Karakul-Bohrkern sowohl Änderungen der Temperatur als auch der Schmelzwassereinträge anzeigen und somit Rückschlüsse auf das Klima und die Gletscherentwicklung im Einzugsgebiet für die letzten 4200 Jahre vor heute erlauben.

Die Studienergebnisse die im Rahmen der vorliegenden Dissertation entstanden sind tragen dazu bei, die atmosphärischen Zirkulationsmuster und die hydrologischen Gegebenheiten auf dem TP besser zu verstehen und zu bewerten. Mit der aquatischen Gastropode *Radix* ist ein weiteres geeignetes Archiv für paläoklimatische Studien entstanden, das sich von den vielen bereits vorhandenen Archiven auf dem TP durch seine besonders hohe zeitliche Auflösung unterscheidet. Zudem ist es mithilfe der sclerochronologischen $\delta^{18}O$ und $\delta^{13}C$ Muster möglich, unterschiedliche Klima- und Umweltparameter voneinander zu unterscheiden. Hier sei insbesondere die Möglichkeit der Unterscheidung von Schmelzwasser und Niederschlag betont.

Offene Forschungsfragen betreffen vor allem Dynamik und Verlauf des Paläo-Monsuns auf dem TP und den umliegenden Regionen sowie die Hebungsgeschichte des TP, die ebenfalls mithilfe fossiler *Radix*gehäuse beleuchtet werden kann.

1. Introduction

1.1 Preface

The TP is the largest elevated land mass on earth with a mean elevation of 4500 m a.s.l. (Sato, 2009) spanning an area of about 3 million km² (Royden et al., 2008). The uplift of the plateau started about 50 million years ago with the collision of the Indian and Eurasian plates (Tapponnier et al., 2001; Royden et al., 2008; Wang et al., 2012). Although there are still quite different opinions about the uplift processes (Gloaguen and Ratschbacher, 2011; Xiao et al., 2012), it is generally accepted that the TP modifies global and regional climate and influence the Asian Monsoon intensities (An et al., 2001; Gupta et al., 2003; Harris, 2006; Molnar et al., 2009; Chen et al., 2010). It holds the headwaters of major south-east Asian rivers, e.g. Indus, Brahmaputra, Mekong, Yangtze and Yellow rivers on which about 1 billion people depend (Xu et al., 2008; Hua, 2009; Immerzeel et al., 2010; Piao et al., 2010) as well as more than 1,000 lakes (Hou et al., 2012) exceeding a total area of ca. 30,000 km² (Kong et al., 2007). Due to its climate sensitivity, the TP acts as a key region for palaeoclimate and palaeoenvironmental studies and an understanding of its natural climate variability is essential for evaluating anthropogenic impacts on modern and future climate (Crowley, 2000; Henderson et al., 2003).

For this reason, the Deutsche Forschungsgemeinschaft (DFG) has initiated a Sino-German Priority Program to combine studies on the interaction of the three major forcing mechanisms: plateau formation, climate evolution and human impact *(http://www.tip.uni-tuebingen.de/index/php/de/)*. These parameters have been analysed on different time scales and resolutions. The sub-project from which the dissertation presented here resulted is titled: ***Age, development and limnology of extant Qinghai-Tibetan Plateau lakes: A reconstruction based on phylogeography and paleoecology of the gastropod genus** Radix*.

Tectonics and climate dynamics have created thousands of lakes which are scattered on the TP representing important archives for palaeoclimatic and palaeoenvironmental as well as for phylogeographical studies. Only in the case of a few lakes is it known since when they have existed. The sub-project aims at a better understanding of age and dynamics of modern lakes on the TP and seeks to unravel the interplay of climate, lake development, phylogeography and palaeoenvironment within a broader spatial and temporal context. The aquatic gastropod genus *Radix* represents the biological and palaeontological object of research. *Radix* is one of the very

few invertebrate taxa with plateau-wide distribution and one of the first invaders of a newly developed lake (von Oheimb et al., 2011). The sub-project is subdivided into two parts: 1) generating a chronology of major genetic events by using molecular dating methods linked to geological, limnological and climate data from the TP; 2) establishing *Radix* as a (palaeo-) environmental and (palaeo-) climate archive in a sub-seasonal resolution by using geochemical approaches. The first part has been conducted by project-members from the University of Giessen, Germany. The second part is subject of my doctoral thesis which includes two already published international peer-reviewed papers and one submitted manuscript (see chapter 1.5).

1.2 Scientific background

1.2.1 Regional setting and climatic relevance of the Tibetan Plateau
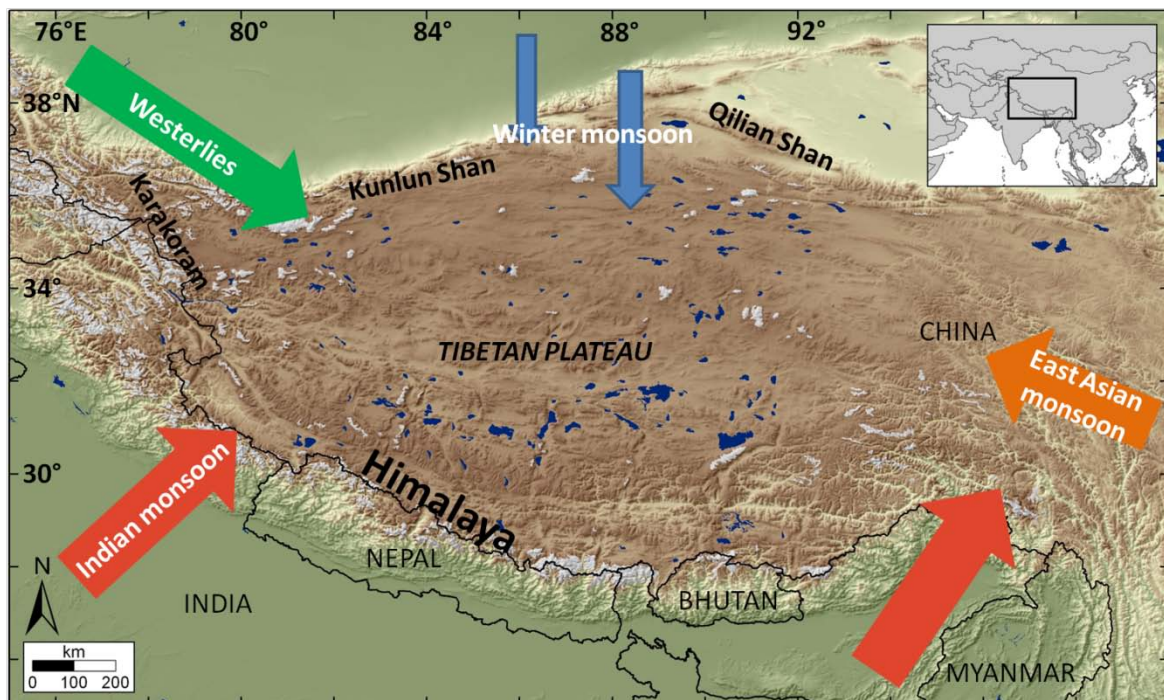
Figure 1: Overview map of the Tibetan Plateau and surrounding mountain ranges, including the dominant circulation systems. The basemap was created by Christian Leipe (FU Berlin) using ArcGis.

Politically, the TP covers the provinces of Xizang (Autonomous Region of Tibet) and parts of Qinghai and Xinjiang of the People's Republic of China. The TP is located between 74°-98° E and 28°-40° N and is bounded by the Himalaya mountain range to the south rising up to more than 8.000 m a.s.l. in places (Figure 1). To the north the TP is bordered by the Kunlun Shan and Qilian Shan ranges and the Karakoram Mountains in the west. Large intermontane basins are located in the north and north-east of the TP.

It is widely accepted that the uplift of the TP began about 50 million years ago, caused by the collision of the Indian and Asian plates (Wang et al., 2012); however, controversy still exists regarding the processes, mechanisms and evolution of the uplift (Gloaguen and Ratschbacher, 2011). The plateau formation occurred in several uplift phases that were associated with the evolution of the Asian monsoon system (see below; An et al., 2001; Harris, 2006; Yanai and Wu, 2006). Due to its immense size and elevation, the TP is an orographic barrier to the atmospheric circulation on the northern hemisphere and it highly influences the climates of Asia (Kutzbach et al., 1989; An et al., 2001).

More than 1,000 lakes are scattered on the plateau (Hou et al., 2012). In the northern and western part of the TP most lakes are saline or hypersaline with poor biological diversity. Fresh water lakes are primary located in the eastern and southern area where the influence of the Asian monsoons dominates (Yu et al., 2001). Since when lakes on the TP have existed is known only in the case of a few lakes and only approximately. After Kuhle (1998) the TP was covered with a 2.4 million km² ice sheet during the last glacial (LG) which spread over almost the entire TP. This would mean that all extant lakes must have developed after the last glacial maximum (LGM). This is in contrast to many studies in which lake sediments of Pleistocene age have been investigated (e.g. Yan et al., 1999; Wang et al., 2002; Opitz et al., 2012). However, many lakes are fed by meltwater and thus mirror the glacial history of their catchments, which in turn provides information about climate conditions.

The modern climate on the TP is characterized by a marked gradient in continentality and aridity from the south and east to the north and west (He et al., 2004; Wu et al., 2006; Chen, 2012). Steppe, semi-desert and desert regions are located in the extreme continental northern and western plateau area and well-vegetated mountain regions characterize the southern and eastern plateau (Wu et al., 2006). The mean annual air temperatures are in a range between 12°C on the south-eastern TP and below 0°C on the central and western TP (Domrös and Peng, 1988). Mean annual precipitation varies from ca. 600 mm on the monsoon influenced south-eastern TP to 50 mm on the central and western TP (Domrös and Peng, 1988). Due to the lack of meteorological stations climate data for the central plateau region and high mountain areas in particular are not available.

The TP is located in a transition zone between four circulation systems: the Indian summer monsoon, the East Asian summer monsoon, the Asian winter monsoon and the westerlies and is therefore particular vulnerably to past and present climate change (Figure 1; Wang et al., 2010). The TP blocks the mid-latitude westerlies and splits the jet stream into a northern and southern

branch. During the summer, a strong latitudinal temperature gradient exists in the upper troposphere caused by partial heating of the atmosphere over the plateau which fuels the monsoon circulation (Morill et al., 2006). Low atmospheric pressure over the TP and high atmospheric pressure over the relatively cold water surfaces cause the initiation of summer monsoon circulation (Clemens et al., 1991). Moisture sources are the Arabian Sea and the Bay of Bengal for the Indian monsoon, the South China Sea and the Pacific Ocean for the East Asian monsoon and the North Atlantic, Mediterranean Sea, Black Sea and Caspian Sea for the westerlies (Clemens et al., 1991; Aizen et al., 1996; Wu et al., 2006). The two sub-systems, the Indian monsoon and the East Asian monsoon, can roughly be divided at 105°E (Wang et al., 2005). During the winter the climate on the TP is characterized by cold and dry air masses from the Siberian anticyclone caused by a cooling of the Asian continent and relatively warm ocean surfaces. The onset of the Indian and East Asian monsoon circulation is identified for about 9-8 million years ago (An et al., 2001). Even though it is widely accepted that the heating of the plateau area is the dominant control of the monsoon system, a more recent study identifies the Himalaya mountain range, rather than the TP, as the dominant thermal forcing (Boos and Kuang, 2010). This demonstrates that many open questions still exist concerning moisture transport onto the plateau and related driving mechanisms.

Extreme events of summer monsoon precipitation can cause severe floods or droughts that impact nearly half of the world's population (Morrill et al., 2006). Studying palaeoclimate records on the TP is therefore a fundamental step towards understanding how the TP has influenced the atmospheric circulation (Kong et al. 2007) and how changes of the monsoon circulations have affected human history. However, studying the Asian monsoon circulations is crucial not only in a regional but in a global context (e.g. Wang et al., 2005; Wang, 2009; Caley et al., 2011) because the system interacts with other circulation patterns, e.g. El Niño-Southern Oscillation (ENSO; Wang et al., 2005) and the North Atlantic thermohaline circulation (Overpeck et al. 1996; Morrill et al., 2003). This may also explain the teleconnections of the Asian monsoon with the African and South American monsoon systems (Morrill et al., 2003; Dykoski et al., 2005).

Studying the palaeo-moisture availability on the TP may help in the investigation of precipitation trends in respect of long-term developments and allow scenarios of future moisture availability. However, archives which record high-resolution palaeo-moisture signals are scarce and mainly restricted to a few areas. Nevertheless, archives in a high resolution (annual, monthly, weekly) are essential because they mirror not only a long-term trend but also extreme events such as intense monsoon precipitation, strong meltwater fluxes or extreme temperatures. Therefore, an archive

which can be found plateau-wide and records different climate parameters in a sub-seasonal resolution has been lacking.

1.2.2 O and C isotope compositions of aquatic gastropod shells as a palaeoclimate proxy

Information about past climate and environmental conditions and changes can be obtained through various proxies. These are geochemical or physical signals recorded in biological or geological structures which reflect the environment in which they formed (Gröcke and Gillikin, 2008). Usually, they can record a time series of climatic or environmental information because they typically accrete or deposit sequentially through time (Gröcke and Gillikin, 2008). Such climatic and environmental proxies are for example ice cores, tree rings, mollusc shells, mammal teeth, corals, fish otoliths, speleothems and varves (e.g. Thompson et al., 2000, 2006; Bräuning, 2001; Brauning and Mantwill, 2004; Schöne et al., 2004; Grimes et al., 2003; Dykoski et al., 2005; Cai et al., 2010; Schlolaut et al., 2012; Schöne and Gillikin, 2013). However, most of the TP area is treeless, most studied lake sediments do not have varves and caves and glaciers are only existent in some particular areas (Bräuning and Mantwill, 2004; Johnson et al., 2006; Thompson et al., 2006; Liu, J. et al., 2011). Molluscs are attractive environmental recorders due to their abundance in diverse environments and their sequential skeletal deposition (McConnaughey and Gillikin, 2008) and often good state of preservation.

The study of oxygen and carbon isotope compositions in carbonate shells of aquatic gastropods is a widely used approach in palaeoclimate research (e.g. Abell, 1985; Abell and Williams, 1989; Bonadonna et al., 1999; Leng et al., 1999; Schmitz and Andreasson, 2001; Hailemichael et al., 2002; Jones et al., 2002; Latal et al., 2004; Gajurel et al., 2006; Stevens et al., 2012). In general, the isotope composition of freshwater snail-shell carbonate reflects that of lake water and the temperature in which the carbonate has precipitated, providing a useful tool for environmental and limnologic studies (Fig. 2; Fritz and Poplawski, 1974; Leng et al., 1999; Leng and Marshall, 2004). The O- and C-isotope composition of the lake water is primarily dependent on the isotope composition of precipitation and inflow, temperature, water residence time, evaporation, exchange with atmospheric CO_2, input of allochthonous CO_2, biological productivity in the water column, photosynthesis of aquatic plants and oxidation of organic matter at the lake bottom (Figure 2). The O-isotope composition of precipitation is related to the rainout history of the atmospheric moisture, air temperature and the so-called "amount effect" (Dansgaard, 1964; Rozanski et al., 1993; Lee and Fung, 2007). This effect appears in the oxygen isotope compositions of precipitation in monsoon influenced regions such as the south-eastern TP. The effect is

characterized by decreasing $^{18}O/^{16}O$ ratios with increasing monthly or annual mean precipitation. Such characteristic "monsoon signals" are also represented in the sclerochronological ^{18}O shell patterns of the Tibetan gastropod *Radix* (Taft et al., 2012, 2013). The reasons for the "amount effect" are still under discussion but the effect is probably caused by a high relative loss of light oxygen isotopes when raindrops evaporate below the cloud base in arid regions (Lee and Fung, 2007).

Beside *Radix* only *Gyraulus* (Pulmonta, Planorbidae) and *Pisidum* (freshwater bivalve) could be found in the harsh TP environments, the diversity of aquatic invertebrates being generally very low. However, only *Radix* is a suitable organism for the approach presented here due to the shell size and life span.
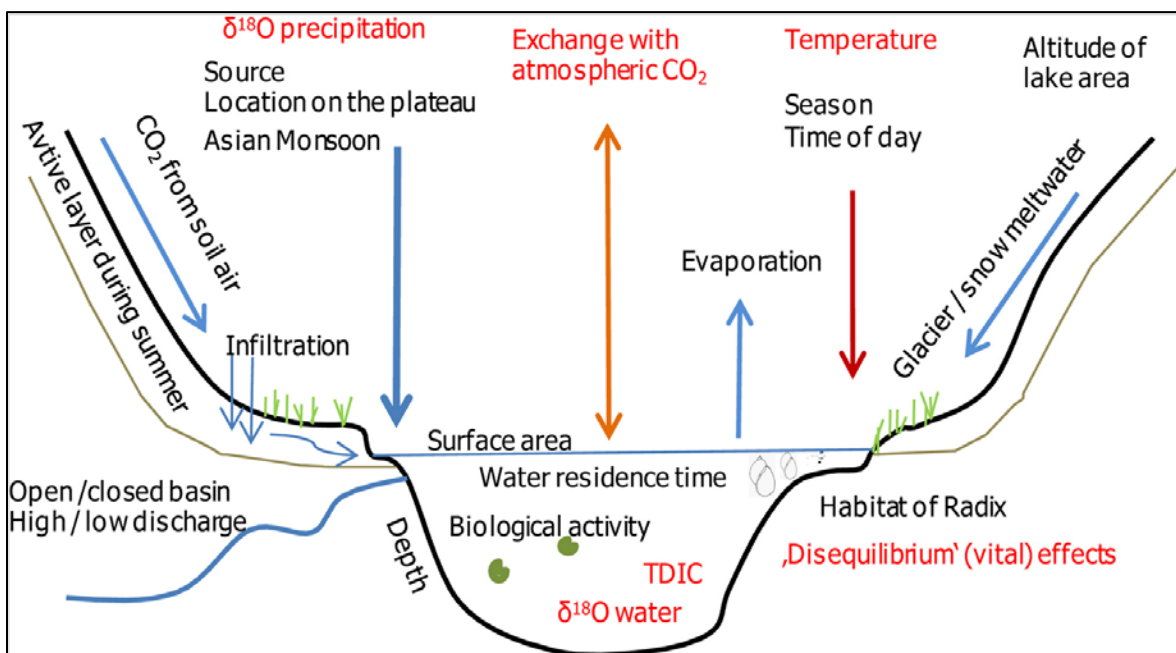
Figure 2: Climate and environmental parameters influencing the chemistry and biology of a lake on the Tibetan Plateau. Changes of these two parameters in turn are reflected in the δ^{18}O and δ^{13}C compositions of the lake water and the *Radix* shells.

Gastropods are widespread in Quaternary lacustrine sediments and are often composed of thermodynamically unstable aragonite. The aragonite can convert to calcite, which effectively "resets" the isotope signals (Leng et al., 1999). Therefore, it is essential to check the shell material before using the shell for isotope analyses. One main advantage of using gastropod shells for palaeoclimate reconstructions is that no so called species-specific "vital effect" is known for most taxa, in comparison to ostracod shells, for example (Leng et al., 1999; White et al., 1999; Leng and Marschall, 2004). "Vital effects" cause a divergence from the equilibrium between isotope compositions of biogenic carbonate and ambient water (Sharp et al., 2007).

1.2.3 Biology and life cycle of the aquatic gastropod Radix

Knowledge of growth period, habitat and life cycle of the gastropods is essential for interpreting the stable isotope data (Leng and Marshall, 2004; Taft et al., 2012, 2013). The pulmonate aquatic gastropod *Radix* (Montfort, 1810; Basommatophora) belongs to the taxonomic family of Lymnaeidae (Rafinesque, 1815). The earliest fossil records of this family are known since the Middle Jurassic (Mordan and Wade, 2008). However, little is known about *Radix* from the TP. *Radix* is a widely distributed invertebrate and is adapted to extreme conditions like high altitude, extended ice cover periods on the water bodies or extreme temperature variations (Röpstorf and Riedel, 2004; Taft et al., 2012). Slow flowing rivers, lakes and back waters are the preferred habitats of this gastropod (Økland, 1990; Glöer, 2002). The life span is assumed to be 1-2 years, but a longer life span cannot be excluded because under cold-water conditions embryogenesis and ontogeny in general can be extremely prolonged (Röpstorf and Riedel, 2004). Shell accretion occurs during all seasons; size increase is much lower during the winter but does not cease (Gaten, 1986). The individuals remain active under the ice cover (Frömming, 1956; Glöer, 2002) and it is assumed that there is no shut down temperature for shell accretion. Further details about nutrition and biological traits are described in Manuscript I, chapter 2. A classification based on morphometric shell attributes turns out to be difficult because shell shape and size not only depend on the particular species but also on environmental conditions (Glöer, 2002). *Radix* from the TP have not been identified at the species level so far, and consequently, the name *Radix sp.* should be used. However, for reading convenience only *Radix* is used in this doctoral thesis.

1.3 Aims and objectives of the thesis

The main goal of this doctoral thesis is to improve the understanding of lake hydrology and dynamics, which depend on climate and environmental changes in modern times and late Quaternary on the TP. The medium for this study is the gastropod genus *Radix*, which could establish itself as a new archive for palaeoclimatic and palaeolimnological studies for the TP and surrounding regions in a sub-seasonal resolution. In this study, modern and past changes of monsoon intensity, patterns and moisture transport pathways are a particular focus. *Radix* is widely distributed on the plateau and adjacent areas and is therefore a suitable organism for regional and inter-regional comparisons. Fossil shells from Lake Karakul in Tajikistan were studied to determine whether the stable isotope signals provide additional detailed information about hydrological and climatic influencing factors such as meltwater flux, which cannot be

unambiguously distinguished by using conventional multi-proxy analyses. This thesis comprises the three following key questions:

- Do sclerochronological $\delta^{18}O$ and $\delta^{13}C$ patterns of modern shells of the gastropod *Radix* from the TP generally mirror modern hydrological and climatic signals? Is this approach therefore a suitable avenue for palaeoenvironmental and palaeoclimatic studies?

- Do sclercochronological $\delta^{18}O$ and $\delta^{13}C$ patterns of modern shells of the gastropod *Radix* collected from seven lakes across the plateau mirror modern hydrological and climatic signals and are the isotope signals dependent on particular lake characteristics (size, open/close, depth, etc.) and regional settings?

- Do sclerochronological and bulk $\delta^{18}O$ and $\delta^{13}C$ values of fossil *Radix* shells mirror palaeoenvironmental and palaeoclimatic conditions and do they offer an additional benefit compared to other archives?

This doctoral thesis comprises three research articles (three chapters) that were written for submission to international peer-reviewed journals. The first manuscript was published in *Quaternary Science Reviews* and the second one was published in *Quaternary International,* while the third manuscript has been submitted to *Journal of Palaeolimnology*. The following chapter 1.4 gives an overview of the three manuscripts.

1.4 Scientific approach and methods

Stable isotope analyses of modern and fossil *Radix* shells for palaeoclimate and palaeoenvironmental reconstructions on the TP and in surrounding regions is a new scientific approach. This doctoral thesis is based on the principle of uniformitarianism as it is often applied in geosciences. It is essential first to understand and characterize modern natural systems and processes before it is possible to understand and assess former processes and climate dynamics. For this reason, the first stage of the study was comprised of extensive field work in order to sample living *Radix* specimens and water samples of different water bodies and habitats from areas with different atmospheric conditions across the TP.

1.4.1 Field work

During field campaigns to the TP in 2008, 2009 and 2010, living *Radix* specimens and ambient water samples were collected from more than 50 water bodies with different characters and settings including lakes, rivers and wetlands.

Figure 3 shows the lakes from which recent *Radix* specimens were collected and the locations which fossil shells come from. Furthermore we measured pH, temperature, oxygen saturation and electrical conductivity of the ambient waters in order to characterize the habitats. Fossil shells were collected at Bangong Co in the western part and Donggi Cona in the north-eastern part of the TP. The fossil shells from Lake Karakul in Tajikistan were collected by Steffen Mischke during a field campaign in 2008.
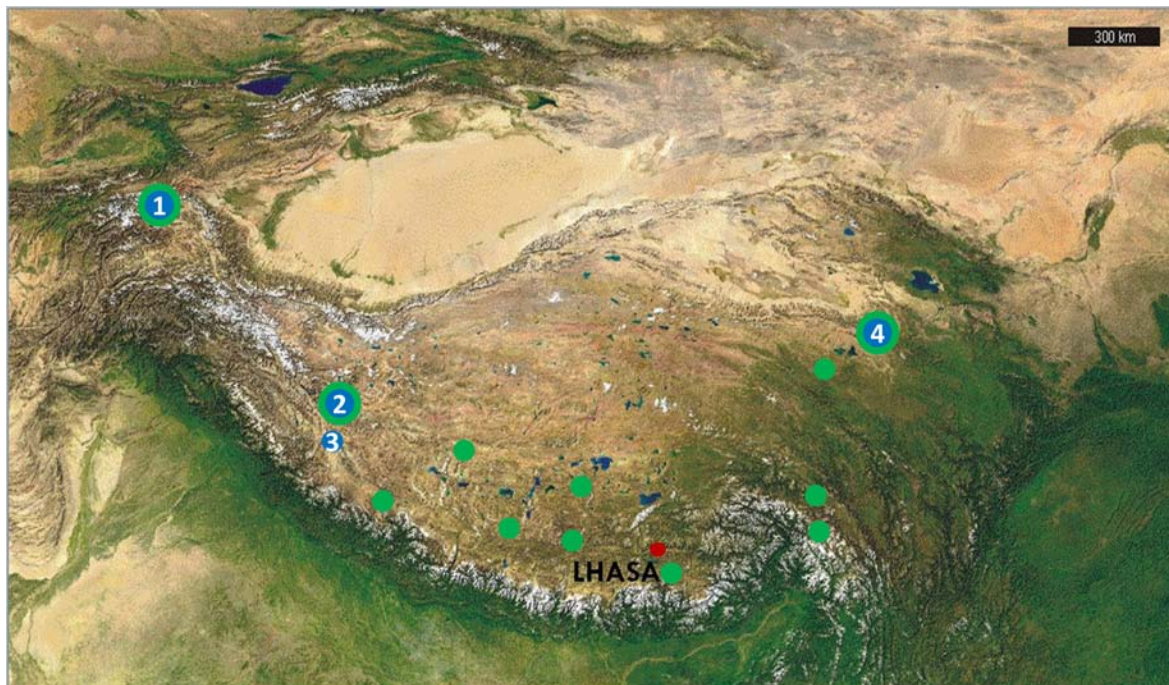
Figure 3: Locations of lakes from which modern *Radix* shells were collected (green points and circles). These lakes are the subject of this doctoral study. Fossil shells (indicated by blue points) were collected from [1] Lake Karakul (Tajikistan), [2] Bangong Co and [3] Zhada Basin in the western part of the TP and [4] Donggi Cona located at the north-eastern margin of the plateau.

1.4.2 Sclerochronology, shell structure and shell preparation

Seasonally to annually resolved, chronologically precisely aligned quantifiable proxy data are required to draw detailed pictures of the past (IPCC, 2007). In order to obtain detailed sub-seasonal information from the isotope compositions of the *Radix* shells about climate and environment on the TP, a sclerochronological approach was selected.

> *"Sclerochronology is the study of physical and chemical variations in the accretionary hard tissues of organisms, and the temporal context in which they formed. Sclerochronology focuses primarily upon growth patterns reflecting annual, monthly, fortnightly, tidal, daily, and sub-daily increments of time entrained by a host of environmental and astronomical pacemakers. Familiar examples include daily banding in reef coral skeletons or annual growth rings in mollusk shells. Sclerochronology is analogous to dendrochronology, the study of annual rings in trees, and equally seeks to deduce organismal life history traits as well as to reconstruct records of environmental and climatic change through space and time."* (Definition by the Organization committee of the 1st International Sclerochronology Conference, St. Petersburg, Florida, USA, in July 2007)

Sclerochronology is a relatively young discipline which has grown rapidly over the last few decades (Wanamaker, 2010). It not only represents a supplement to already established geoscientific methods but has also evolved into a discrete discipline that involves biology, ecology, palaeontology, geology, geography and climatology.

Some shells were investigated by scanning electron microscopy (SEM) to test whether the carbonate material is of calcite or aragonite structure. The chemical composition of these materials is the same ($CaCO_3$) but the crystal structure is different which influences thermodynamic stability and preservation (Leng et al., 1999). Calcite has a trigonal and aragonite an orthorhombic crystal system which is often arranged in cross-lamination (Figure 4). The determination of the shell material is also important because aragonite exhibits a 0.6 ‰ more positive oxygen isotope value and has to be corrected if it is compared to calcite (Abell and Williams, 1989; Leng et al., 1999). For the SEM photos, the shells had to be prepared. First the shells were bisected and the cutting faces were polished. Subsequently, the material was treated in 1% acetic acid for 12 minutes to roughen the cutting faces before the shell parts were rinsed in deionized water for 2 hours. This procedure provided the best visible results in the SEM. The visual investigation confirmed that the shells are of aragonite structure (Figure 4).
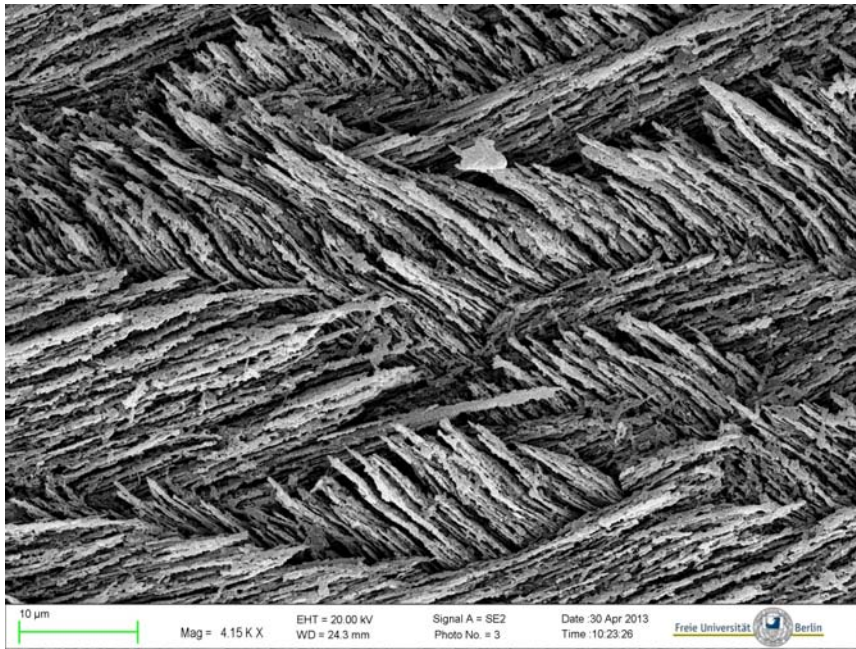
Figure 4: SEM picture illustrating the cross-laminated aragonite structure of a *Radix* shell.

Furthermore the shell structure itself has been studied by SEM in order to test whether the shell is secondarily thickened. If so, each shell section does not mirror a defined time period but a temporally mixed signal in the isotope composition. Significant secondary thickening was mostly excluded. A small zone (Pa 3 = 62.20 μm) of secondary thickening is indicated in Figure 5 however, compared to the broad primary built shell part (Pa 1 = >260 μm), this zone can be neglected for the shell preparation.
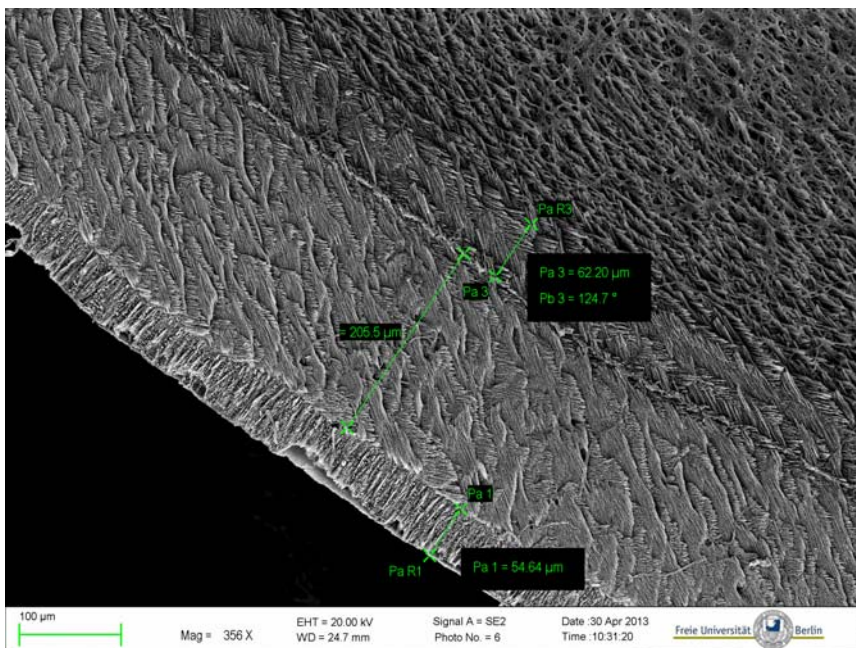
Figure 5: Example of a SEM picture illustrating the shell thickness. Secondary thickening (Pa 3) is not significant for most of the *Radix* shells, but has to be checked before sampling.

For this thesis, the attempt was made to characterize morphometric shell attributes and compare them to particular genetic clades which have been classified by von Oheimb (2011) at the University of Giessen as part of this sub-project. By using the morphometric software *tps morpho-tool* by Rohlf (2007) which is based on digitizing landmarks and outlines, typical shell attributes which are unique for a particular clade were investigated. However, this approach was not realizable because size and shape of the shells seem to be primarily dependent on ecological parameters of the particular habitats and not on particular genetic clades.

Before shell sampling, the shells were cleaned in distilled water with ultrasound for 3-5 minutes before they were treated with 3.5% hydrogen peroxide (H_2O_2) for 24 hours to remove possible residues of the organic periostracum. Shell sampling was then conducted by drilling holes in the shells in equal distances of ca. 1 mm using a dental driller (Figure 6). The holes were drilled in ontogenetic order of the shell increments. The latest shell part (= aperture) was sampled first and the embryonic shell (= protoconch) provided the last sample of a shell (Figure 7).

Figure 6: Dental driller which is used for shell sampling. The rotation speed can be regulated by foot.

Figure 7: The sampling material for stable isotope analyses was obtained by drilling holes along the ontogenetic spiral of growth increments, a=aperture to PRC= protoconch.

For the specimens which were collected alive, meteorological datasets from the particular year could be compared directly by working backwards from the shell aperture.

1.4.3 ^{18}O and ^{13}C analyses

The isotope analyses were conducted using a GasBench II linked to a MAT-253 ThermoFischer Scientific™ isotope ratio mass spectrometer. Borosilicate vials (10 ml) with ca. 200 ± 50 µg sample material were flushed with helium. After that, 3-5 drops of 100% phosphoric acid (H_3PO_4) were added in order to generate a reaction between carbonate and acid. The reaction produces CO_2, which includes the elements oxygen and carbon. A constant temperature of 70°C during the transition of solid carbonate to gaseous CO_2 causes a low fractionation factor α because isotope fractionation decreases with increasing temperature (Sharp, 2007). The reaction of carbonate with H_3PO_4 transports the carbon atoms into a gaseous state (McCrea, 1950):

$$2H^+ + CaCO_3 \rightarrow Ca^{2+} + H_2O + CO_2$$
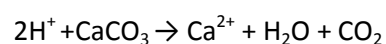
The mixture of helium and CO_2 is automatically transported into the mass spectrometer. The CO_2 molecules are charged positively by ions in the ion source box (Figure 8) and accelerated by an ion accelerator. The stream of molecules is intensified and focused by electric lenses and led through

a magnetic field where the molecules are deflected according to the mass of the individual isotopologues (Sharp, 2007). The Faraday cup collectors are positioned according to the path of those isotopologues (Fig. 8). The molecules pass through them and pick up electrons (Sharp, 2007).
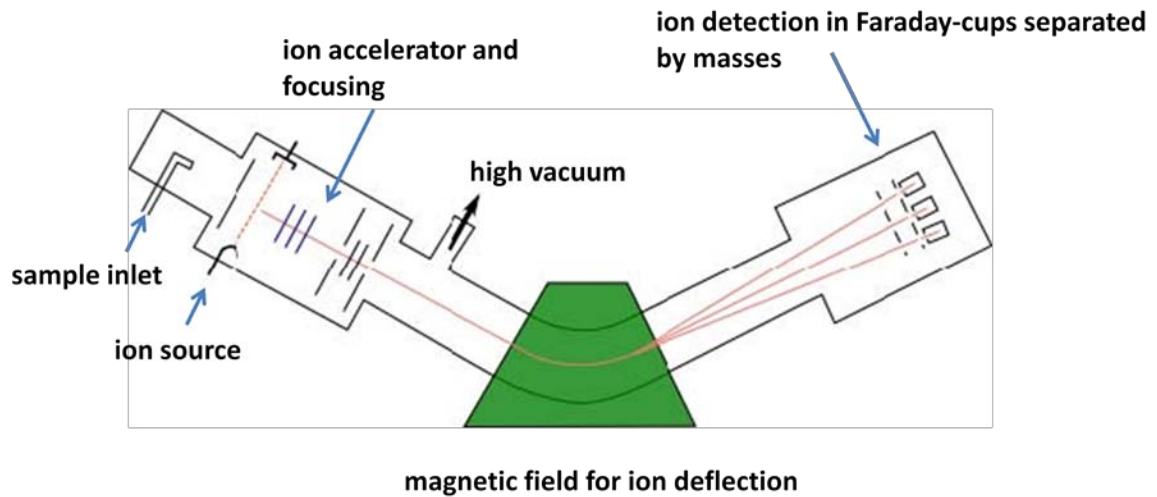
Figure 8: Schematic construction of a mass spectrometer. The complete tube is under high vacuum in order to minimize particle collisions. (Modified after Dyckmans, n.d., Centre for Stable Isotope Research and Analysis, Georg August University Göttingen, Germany).

Three masses with corresponding isotopologues are recorded: Mass 44 ($^{16}O^{12}C^{16}O$), Mass 45 ($^{16}O^{13}C^{16}O$, $^{17}O^{12}C^{16}O$, $^{16}O^{12}C^{17}O$) and Mass 46 ($^{17}O^{13}C^{16}O$, $^{16}O^{13}C^{17}O$, $^{17}O^{12}C^{17}O$, $^{18}O^{12}C^{16}O$, $^{16}O^{12}C^{18}O$). $\delta^{13}C$ is mostly taken over from the ratio 44/45, $\delta^{18}O$ is calculated from the ratio 46/44 (Sharp, 2007). Prior to every measurement of a sample a standard gas is measured. The results from the standard gas provide the individual standard deviation. Standard materials are measured during every analysis and are placed randomly between the carbonate samples so that machine-specific deviations can be detected and verified by data correction. Results are automatically given in δ-values representing the ratio of a heavier isotope (here ^{18}O and ^{13}C) related to the lighter isotope (here ^{16}O and ^{12}C).

1.4.4 Reference standards and data correction

For the comparison of isotope ratios measured by different laboratories, the ratios (here $^{18}O/^{16}O$ and $^{13}C/^{12}C$) are calibrated against internationally accepted reference standards (Sharp, 2007). The isotope values for this thesis were standardized against Cararra marble (CAM) and Kaiserstuhl carbonatite in-house reference material (KKS) which had been calibrated against Vienna-PeeDee

belemnite (V-PDB) internationally accepted reference material NBS-19 and NBS-18. The external error is based on the reproducibility of the in-house reference material Laaser marble (LM). Machine- and technique-specific variations require individual data corrections after every series of measurements. First the "linearity correction" must be conducted to balance variations in the sample weights causing different δ-values. Different initial weights of the reference material LM are measured with the samples. The results of this LM measurement (for both O and C) are plotted against peak area (ion signal intensity) to create a trend line. The trend line equation is used to adjust weight dependent variations. In the next step, all δ-values are multiplied by a constant "stretching factor" so that the measured difference between the standards is the same as the accepted difference (Sharp, 2007). In the last step, "shift correction", a constant is added to all so far corrected δ-values to bring the measured values of the references into agreement with the accepted values (Sharp, 2007). All corrected δ-values of the samples are now on the IAEA scale.

The isotopic analyses for the first and the third manuscript were conducted at the Freie Universität Berlin. Parts of the shell samples for the second manuscript were analysed at the GeoForschungsZentrum Potsdam (GFZ).

1.5 Overview of the manuscripts

This thesis is a cumulative dissertation and therefore consists of three individual manuscripts (Chapters 2 – 4) prepared for publication in international peer-reviewed journals. An overview of all manuscripts is given in Table 1.

Table 1: Overview of manuscripts presented within this dissertation

Chapter	Publication / Main Goal	Journal / Status
2	**"Sub-seasonal oxygen and carbon isotope variations in shells of modern *Radix* sp. (Gastropoda) from the Tibetan Plateau: potential of a new archive for palaeoclimatic studies"** Taft L, Wiechert U, Riedel F, Weynell M, Zhang HC (2012) *Main goal:* *To test whether $\delta^{18}O$ and $\delta^{13}C$ patterns in modern* Radix *shells from the Tibetan Plateau provide information about the modern climate in sub-seasonal resolution and wether the data thus open a promising new avenue of palaeoclimatic and palaeolimnologic research.*	*Quaternary Science Reviews 34: 44-56.* published (2012) http://dx.doi.org/ 10.1016/j.quascirev.201 1.12.006
3	**"Oxygen and carbon isotope patterns archived in shells of the aquatic gastropod *Radix*: Hydrologic and climatic signals across the Tibetan Plateau in sub-monthly resolution"** Taft L, Wiechert U, Zhang HC, Lei GL, Mischke S, Plessen B, Weynell M, Winkler A, Riedel F (2013) *Main goal:* *To test whether the climatic differences across and beyond the Tibetan Plateau are archived in the* Radix *shells and whether they mirror different lake characteristics in a broad spatio-temporal resolution.*	*Quaternary International 290-291: 282-298* published (2013) http://dx.doi.org/ 10.1016/j.quaint.2012.1 0.031
4	**"Oxygen and carbon isotope ratios in *Radix* (Gastropoda) shells indicate changes of glacial meltwater flux and temperature since 4200 cal yr BP at Lake Karakul, eastern Pamirs (Tajikistan)"** Taft L, Mischke S, Wiechert U, Leipe C, Rajabov I, Riedel F *Main goal:* *To test the application to fossil shells and wether it is possible to detect and characterize the influence of meltwater supply in fossil* Radix *shells from Lake Karakul.*	*Journal of Palaeolimnology* submitted (2013)

1.6 Contribution of the author and all co-authors to the individual manuscripts

Linda Taft entirely wrote all manuscripts presented in chapters 2-4 and reviewed the relevant literature. She built the general framework of all analytic steps, collected shell samples from the TP, carried out the major part of the laboratory work for the first manuscript and interpreted all data with support from Prof. Dr. Frank Riedel and Dr. Uwe Wiechert. Prof. Dr. Frank Riedel is also the main supervisor of this thesis and built the general scientific frame for the project; he further did critical reviews and therefore is co-author of all manuscripts. Dr. Uwe Wiechert is the head of a geochemical laboratory at the FU Berlin where major parts of the shell samples were measured. He did critical reviews, participated in the project and is therefore also co-author of all manuscripts.

Jan Evers (FU Berlin) created the regional overview-maps of the first two manuscripts and helped to prepare Figure 11 in manuscript I. Christian Leipe (FU Berlin) created Fig. 30 in manuscript III. All other figures and tables were prepared by Linda Taft.

1.6.1 Manuscript I (Chapter 2)

Marc Weynell (FU Berlin) is co-author of the first manuscript because he analysed the major part of the lake and river water samples from the TP which helped to interpret the *Radix* shell data. He further joined the expedition to the TP in 2008 and helped with shell sampling. *Contribution to the manuscript: 5 %*

Hucai Zhang (Yunnan Normal University, Kunming, China) is the Chinese cooperation-partner in the DFG sub-project. He helped to realize the field trips to the TP and supported my work by collecting samples and providing required meteorological data from the Chinese Meteorological Office and is therefore co-author of the manuscript. *Contribution to the manuscript: 5 %*

1.6.2 Manuscript II (Chapter 3)

Hucai Zhang (Yunnan Normal University, Kunming, China) is the Chinese cooperation-partner in the DFG sub-project. He helped to realize the field trips to the TP and supported my work by collecting samples and providing required meteorological data from the Chinese Meteorological Office and is therefore co-author of the manuscript. *Contribution to the manuscript: 5 %*

GuoLiang Lei (Fujian Normal Univeristy, Fuzhou, China) joined the field campaign to the TP in 2009 and helped to collect *Radix* and water samples. He further provided necessary meteorological data. *Contribution to the manuscript: 5 %*

Steffen Mischke (FU Berlin and University of Potsdam) did the reconnaissance study at Lake Karakul and collected living *Radix* specimens from that location. Furthermore, he helped to improve the manuscript by constructive discussions and critical review. *Contribution to the manuscript: 10 %*

Birgit Plessen (GFZ Potsdam) is the head of the geochemical laboratory at the GeoForschungsZentrum Potsdam and did parts of the analytical work for the manuscript. *Contribution to the manuscript: 5 %*

Marc Weynell (FU Berlin) helped to interpret the *Radix* shell data. He further joined the expedition to the TP in 2008 and helped with shell sampling. *Contribution to the manuscript: 5 %*

Andreas Winkler (FU Berlin) provided the chemical data for the lake waters and wrote the first part of chapter 3.5.1 in manuscript II. He further created the piper plot and interpreted the anion and cation concentrations. *Contribution to the manuscript: 5 %*

1.6.3 Manuscript III (Chapter 4)

Steffen Mischke (FU Berlin and University of Potsdam) did the reconnaissance study at Lake Karakul, provided data from the sediment core, collected living and fossil *Radix* shells from that location and provided the scientific frame for the last manuscript. Furthermore, he helped to improve the manuscript by constructive discussions and critical review. *Contribution to the manuscript: 15 %*

Christian Leipe (FU Berlin) created the DEM map of Lake Karakul and the catchment area. He further helped to improve the manuscript by critical review and constructive discussions. *Contribution to the manuscript: 5 %*

Ilhomjon Rajabov (State Administration for Hydrometeorology of the Committee for Environmental Protection under the Government of the Republic of Tajikistan, Dushanbe, Tajikistan) is the Tajik cooperation-partner and provided necessary data from the meteorological station located at Lake Karakul. *Contribution to the manuscript: 3 %*

2. Sub-seasonal oxygen and carbon isotope variations in shells of modern *Radix* sp. (Gastropoda) from the Tibetan Plateau: potential of a new archive for palaeoclimatic studies

Linda Taft[a*], Uwe Wiechert[a], Frank Riedel[a], Marc Weynell[a], Hucai Zhang[b]

[a]Freie Universität Berlin, Institut für Geologische Wissenschaften, Malteserstr. 74-100, 12249 Berlin, Germany

[b]Yunnan Normal University, Key Laboratory of Plateau Lake Ecology and Global Change, College of Tourism and Geography, Kunming 650092, China

Abstract

Carbon and oxygen isotope ratios have been measured for nine aragonite shells of the gastropod genus Radix *from the lake Bangda Co (30°29'N, 97°04'E, 4450 m a.s.l.) at the south-eastern edge and from two characteristic sites at the lake Kyraing Co (31°09'N, 88°17'E, 4650 m a.s.l.) on the central Tibetan Plateau. Radix shells were sampled for isotope ratio analysis with high spatial resolution along the ontogenetic spiral of growth providing the basis of isotope records with a sub-seasonal time-resolution. $\delta^{18}O$ values of shells from Bangda Co are on average ~ -15.0 ‰ relative to PDB and the pattern exhibits a clear onset and progression of the summer monsoon precipitation indicated by a strong "amount effect". This pattern mirrors the precipitation pattern in the respective year and region as expected for a small (surface area ca. 0.3 km²) and shallow (< 5 m) lake or habitat with short water residence times and little evaporative ^{18}O enrichment of the lake water. In contrast, $\delta^{18}O$ values of Radix shells from Kyaring Co habitat A which is connected to the deep (several tens of metres) and big (surface area ca. 660 km²) lake, average at ~ -13.0 ‰ consistent with a higher evaporation rate and longer water residence time. The latter is supported by more ^{18}O enriched water in this habitat. The $\delta^{18}O$ values of Radix shells from Kyaring Co habitat B are nearly as low as shells from Bangda Co due to the similar habitat characteristic but isotopic patterns of these shells exhibit a weaker "amount effect". In both lake systems $\delta^{13}C$ values of the shells are coupled with oxygen isotopes because a large amount of isotopically light carbon is*

washed from mountain slopes into the lake during the rainy season. Although other processes influence the isotopic patterns, e.g. biological productivity ($\delta^{13}C$) or temperature ($\delta^{18}O$), these influences are minor compared with the monsoon signal or the effect of evaporation in the Radix shell records. The overall weaker amount effect in Radix shells from Kyaring Co habitat B compared with shells from Bangda Co are consistent with a current decreasing monsoon influence from the south-eastern edge towards the central Tibetan Plateau. Thus, fossil shells of the gastropod genus Radix are a valuable archive for reconstructing climatic and environmental changes on the Tibetan Plateau and provide information about former habitat sizes and depths.

2.1 Introduction

2.1.1 Scope

The Tibetan Plateau, with a mean elevation of ca. 5 km over a region of almost 3 million km^2 (Royden et al., 2008), has been shown to modify global climate (e.g. Kutzbach et al., 1989; Raymo and Ruddiman, 1992; Yang and Scuderi, 2010; Yang et al., 2011) and to influence the Asian monsoon intensities (e.g. An et al., 2001; Gupta et al., 2003; Harris, 2006; Molnar et al., 2009; Chen et al., 2010). Understanding the role of the Tibetan Plateau for climate variability is crucial for ca. 2 billion people depending on the monsoon rains. Tectonics and climate dynamics have created thousands of lakes which are scattered on the Tibetan Plateau and which represent the main archives for studying climate variability of the past. Particularly late Quaternary sediments of several dozens of lakes across the plateau have been investigated (e.g. Hövermann and Süssenberger, 1986; Gasse et al., 1991, 1996; Wang et al., 2002; Herzschuh et al., 2005; Morill et al., 2006; Kong et al., 2007; Liu et al., 2007; Daut et al., 2010; Dietze et al., 2010; Liu et al., 2010; Mischke et al., 2010a; Rhode et al., 2010) to infer palaeoclimatic and palaeoenvironmental changes as a prerequisite to model scenarios of future climate dynamics. The temporal resolution of the data is usually centennial or multi-decadal and suitable to outline general moisture and temperature changes. In respect of predictability of future precipitation patterns, however, information on the intra-annual variability of the past is essential but still limited for this region. Dettman et al. (2001) provided stable isotope profiles from bivalve shells and mammal teeth from Himalayan foreland Siwalik Group sediments exhibiting seasonal climate variations from late Middle Miocene to Late Pliocene. Wang et al. (2008) used stable isotope profiles of mammal teeth from Late Pliocene sediments exposed at the northern Tibetan Plateau Kunlun Pass to infer

25

palaeo-environmental changes. Plateau-wide studies, however, have not yet been conducted perhaps due to the lack of suitable archives.

The carbonate (aragonite) shells of the gastropod *Radix* (Montfort, 1810) (Basommatophora, Lymnaeidae) may represent such an archive for environmental signals at the sub-seasonal level. *Radix* belongs to the few aquatic taxa being widely distributed on the plateau and corresponding fossil shells can be found in Neogene and Quaternary fluvio-lacustrine sediments (e.g. Wu et al., 2001; Yue et al., 2003; Wang et al., 2008; Mischke et al., 2010b; own observations).

Shells of freshwater gastropods archive oxygen and carbon isotope signals which have been successfully analysed to infer climatic and environmental conditions (e.g. Linz and Müller, 1981; Abell, 1985; Abell and Williams, 1989; Hailemichael et al., 2002; Jones et al., 2002; Shanahan et al., 2005; Gajurel et al., 2006; Tütken et al., 2006). The oxygen isotope ratios in carbonate shells reflect water composition and temperature during carbonate precipitation. Photosynthesis of aquatic plants, decomposition of biological matter, mineralogical substrate and exchange with atmospheric CO_2 affect the $\delta^{13}C$ composition of the DIC within the lake which provides the basic material for the shells (e.g. Fritz and Poplawski, 1974; Grossman and Ku, 1986; Wu et al., 2002; Gajurel et al., 2006; McConnaughey and Gillikin, 2008). Furthermore metabolic or kinetic vital effects can significantly alter the isotopic composition of biogenic carbonates (Fritz and Poplawski, 1974; Wefer and Berger, 1991; Shanahan et al., 2005). Detailed analyses along growth increments allow the documentation of seasonal variations in $\delta^{18}O$ and $\delta^{13}C$ (Fritz and Poplawski, 1974; Dettman et al., 1999; Jones et al., 2002; Gajurel et al, 2006). The isotopic pattern recorded in a single gastropod shell over a full life-cycle may thus mirror annual hydrological variations which are controlled by distinct climate parameters such as precipitation, evaporation, temperature, humidity, etc.

The major purpose of this study is to address the question whether oxygen and carbon isotope patterns in shells of recent Tibetan Plateau *Radix* record the modern climate in sub-seasonal resolution and whether the data thus open a promising avenue of palaeoclimate research.

2.1.2 Regional Setting

We selected two exhoreic freshwater lakes of different origins which are located on a transect of decreasing monsoon influence from the eastern to the central plateau (Figure 9). At the eastern edge of the plateau we selected Bangda Co, a small, so far unnamed lake located at 30°29'N, 97°04'E (4450 m a.s.l.) and named by us after the nearby Bangda Airport. The lake which formed

after a large mass movement that dammed a small braided river, is located in a wide U-shaped valley, and has a surface area of about 0.3 km² and a strong discharge. Based on the geomorphological setting and its origin the lake is considered comparatively shallow with a maximum water depth of a few metres only. The surrounding mountain ridges rise to about 5100 m a.s.l. and flank the lake at the northern and southern shores. Bangda Co lies within the influence of the Asian monsoons. Total annual precipitation recorded at a meteorological station (31°09'N, 97°10'E, 3306 m a.s.l.) located ca. 70 km north of Bangda Co is 480 mm and the mean annual air temperature is 10.9°C (data from 1958 to 2009, Chinese Central Meteorological Office, 2010). We selected a second meteorological station (33°48'N, 97°08'E, 4415 m a.s.l.) located about 360 km north of Bangda Co at an elevation similar to the lake area. Total annual precipitation there is 510 mm and the mean annual air temperature is -4.5°C (data from 1958 to 2009, Chinese Central Meteorological Office, 2010). Bangda Co is located in the transition zone between seasonally frozen ground (Wang and French, 1995; Jin et al., 2000) and permafrost (personal observations) which is noteworthy in respect of a high surface runoff.

Figure 9: Locality map with geographical position of Bangda Co and Kyaring Co including sampling sites (black dots near the lake shores) and modern atmospheric circulation systems.

On the central Tibetan Plateau we selected Kyaring, Co which has a length of about 60 km, a maximum width of ca. 13 km and is located at 31°09'N, 88°17'E (4650 m a.s.l.). The tectonic origin is related to a strike slip fault located between the Indus-Tsangpo and Bangong-Nujiang suture (Blisniuk et al. 2001; Chengdu Institute of Geology and Mineral Resources, 2004). The minimum

27

width between the north-western basin with a surface area of about 300 km² and the south-eastern basin with a surface area of about 360 km² is 3.8 km. Modern local climate conditions can be deduced from a meteorological station located about 9 km from the south-eastern lake shore at 30°57'N, 88°38'E (4672 m a.s.l.). Total annual precipitation there is 314 mm and the mean annual air temperature is 0.7°C (data from 1958 to 2009, Chinese Central Meteorological Office, 2010). Based on its geomorphological setting the lake is considered significantly deeper than Bangda Co with a maximum water depth of several tens of metres at least. Some surrounding mountain peaks rise to about 5800 m a.s.l. and the lake area is located in a permafrost zone (personal observations).

The ice cover periods of both lakes have not been observed but can roughly be inferred from a study of Beiluhe Basin lakes (Lin et al., 2011) which are located between Bangda Co and Kyaring Co although further north. Using the study by Lin et al. (2011) we suppose that Kyaring Co and Banga Co are completely covered by ice from early November to late April.

2.1.3 Biology of the gastropod Radix

The pulmonate gastropod *Radix* is widely distributed on the Tibetan Plateau living in freshwater and oligohaline to mesohaline systems. These gastropods inhabit preferably calm, shallow waters, e.g. bays, river overflows or backwaters in both lacustrine and riverine environments (Økland, 1990; Glöer, 2002; personal observations). Among gastropods, beside *Radix* only *Gyraulus* (Pulmonta, Planorbidae) could be found in the harsh Tibetan Plateau environments, the diversity of aquatic invertebrates being generally very low. *Radix* species belong to the few continental gastropod taxa which inhabit extreme boreal and arctic environments such as lakes with ice cover periods of more than half a year, e.g. in northern Canada (e.g. Clarke, 1973), northern Norway (Økland, 1990) or Siberia (White et al., 2008). It has been observed in European *Radix* species that individuals remain active under the ice cover of lakes during the winter months (e.g. Frömming, 1956; Glöer, 2002). Frömming (1956) noticed that *Radix* even move directly on the underside of ice. Gaten (1986) observed that *Radix* in Leicester Canal (England) moves in winter from the shallow littoral area to deeper water in order to avoid the ice. The same was observed by Burla (1972) for Lake Zurich (Switzerland). Gaten (1986) measured shell growth during all seasons and found that size increase was much lower in winter but did not cease. Stift et al. (2004) emphasized that palaearctic *Radix auricularia*, which had invaded Lake Baikal usually live in habitats with strong seasonal temperature changes while the cold water temperature in Lake Baikal varies very little. These data suggest that low temperature is not the limiting factor for

growth but nutrition. Primary production is usually much reduced in winter, however, to quite different degrees in different systems. The nutrition of *Radix* consists mainly of chlorophyta, cyanobacteria, diatoms, protozoa and weed (Frömming, 1956; Knecht and Walter, 1977; Gittenberger et al., 1998; personal observations). We conclude that there is no shut-down temperature for shell accretion in *Radix.*

The life span of *Radix* species is approximately one year (Young, 1975; Walter, 1977; Glöer, 2002). Several egg depositions during the warmer months have been observed in European species (e.g. Riedel, 1993; Gittenberger et al., 1998). Shell formation during embryonic ontogeny occurs within the egg capsules which are embedded in a gelatinous mass (Riedel, 1993). Until hatching, the embryo forms a conch of ca. 1.3 whorls which are ca. 0.8 mm in diameter. To this protoconch another ca. 3 whorls are added during later ontogeny (Riedel, 1993). The shell carbonate originates from either metabolic carbon or from the surrounding environment (Shanahan et al., 2005). McConnaughey et al. (1997) concluded that the metabolic source is less than 10 % of the total and that 90 % comes from the DIC (dissolved inorganic carbon) which can be directly used for shell accretion. In respect of $\delta^{18}O$ and $\delta^{13}C$ analyses, it is noteworthy that we could not observe significant secondary thickening of the shell, which means that each shell section represents a clearly defined growth period.

The pH tolerance range of *Radix* is between 5.8 and 9.9; pH values from 7.0-9.6 are preferred (Økland, 1990). The daily radius of movement is dependent on food supply (Knecht and Walter, 1977). This means that the sampling locality is not necessarily the exact place where the specimens spend their whole life.

2.2 Materials and methods

The studied *Radix* specimens were collected during a field trip to the eastern and central part of the Tibetan Plateau from August to October 2008. The specimens from Bangda Co were collected on September 27 and the specimens from Kyaring Co on September 14. The sampled gastropods were preserved in 80% ethanol. At the sampling localities (Figure 10) we determined water temperature, pH value and electrical conductivity. Water samples were taken to Berlin for inorganic chemical and isotopic characterization of the environment of the sampled gastropods.

Figure 10: Sampling sites at Bangda Co and Kyaring Co site A and B.

Our study is linked to investigations at the Justus-Liebig-University in Giessen where the specimens have been genetically analysed. The soft parts of the gastropods were removed from the shells and these were photographed for documentation purposes. Every DNA-sequenced specimen has a 5-digit serial lab number and an additional sample code which enables a clear identification (Table 2). Because Tibetan Plateau *Radix* have not been identified at the species level so far, we use *Radix* sp. The empty shells were conveyed to our group where the following steps were accomplished: All visible organic and inorganic material was removed from the shells using brushes. Subsequently the shells were treated with H_2O_2 to remove dispersed material. Afterwards the shells were rinsed with deionized water in an ultrasonic bath and then dried 24 hours at room temperature. Three shells from Bangda Co and six shells from two distinct localities at Kyaring Co (sites A and B) of similar shell shape and shell thickness were selected (Figure 11).
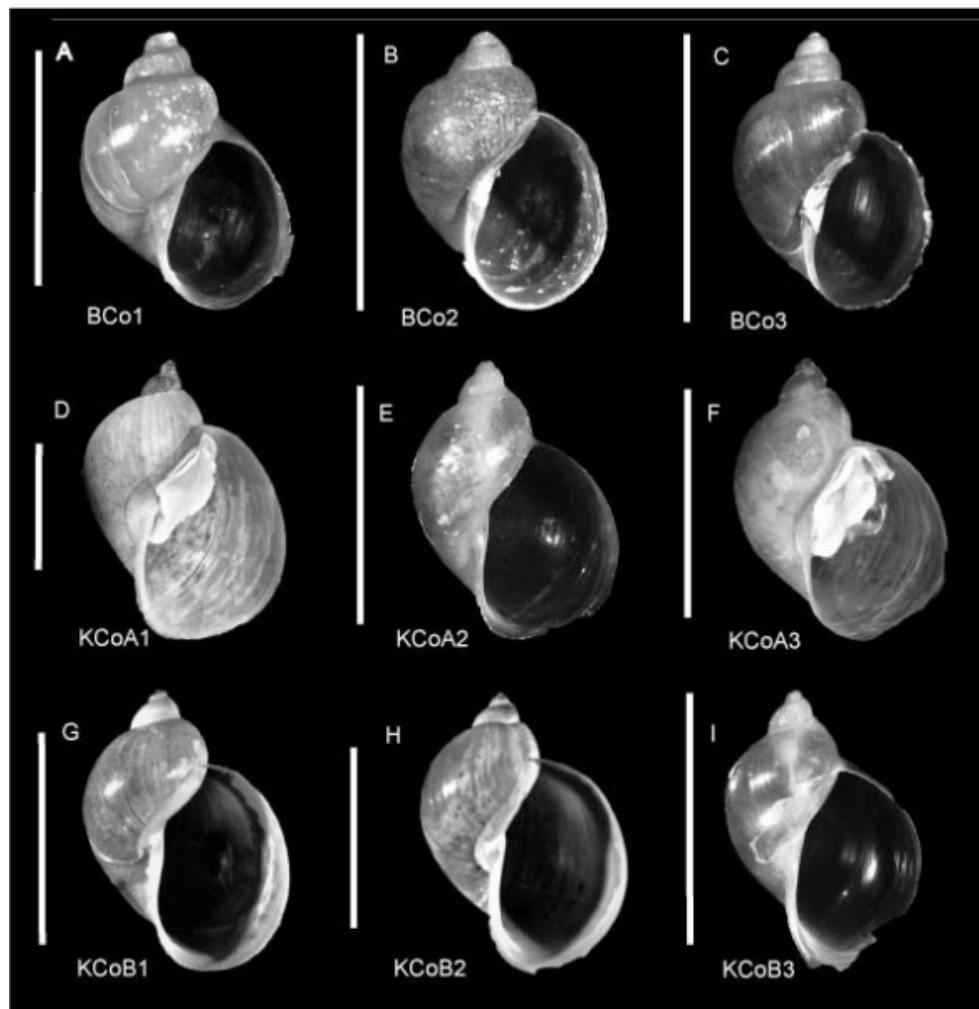
Figure 11: *Radix* **shells (A-I) prior to drill sampling. The scale bar is 1 cm. Shells D and F still contain the soft parts and were photographed by P. von Oheimb (University of Giessen).**

Sub-sampling of the shells was carried out along the ontogenetic spiral of growth increments using dental drillers of 0.1 to 0.5 mm in diameter depending on positions along the shells. To obtain a minimum of 150 µg, 200 ± 50 µg of the samples were taken within a constant distance of ca. 1.0 mm between the drilled holes along the whorls (Figure 12). We obtained a minimum of 13 samples and a maximum of 23 samples per shell (Table 2).

Table 2: Overview of analysed *Radix* shells from Bangda Co and Kyaring Co.

Shell code	DNA lab number	Lake (site) Site water depth	Geographical coordinates	Height / Width in cm	n samples	Figure reference
BCo2	11115	Bangda Co < 0.5 m	30°29'N 97°04'E	1.0 / 0.73	17	Fig. 11B
BCo3	6 (ns)	Bangda Co < 0.5 m	30°29'N 97°04'E	0.95 / 0.67	13	Fig. 11C
KCoA1	10055	Kyaring Co (A) < 0.5 m	30°95'N 88°49'E	2.20 / 1.61	23	Fig. 11D
KCoA2	10054	Kyaring Co (A) < 0.5 m	30°95'N 88°49'E	1.17 / 0.86	22	Fig. 11E
KCoA3	11112	Kyaring Co (A) < 0.5 m	30°95'N 88°49'E	1.25 / 0.95	14	Fig. 11F
KCoB1	11113	Kyaring Co (B) < 0.5 m	31°17'N 88°17'E	1.33 / 0.97	18	Fig. 11G
KCoB2	10058	Kyaring Co (B) < 0.5 m	31°17'N 88°17'E	1.60 / 1.19	16	Fig. 11H
KCoB3	10060	Kyaring Co (B) < 0.5 m	31°17'N 88°17'E	1.14 / 0.71	14	Fig. 11I

The early ontogenetic shell was partly sampled using a different method because of its fragility: Shell parts of ca. 1.0 mm width were manually separated along the ontogenetic spiral of growth by a small knife under a binocular. Afterwards small particles of these stripes were treated in the same way as the other samples. It cannot be excluded that the distances between the particular samples vary marginally. For this reason the samples are labelled in letters and not in scale units. For each locality we adjusted the three diagrams in a way that assumed similar time spans are arranged in one column.
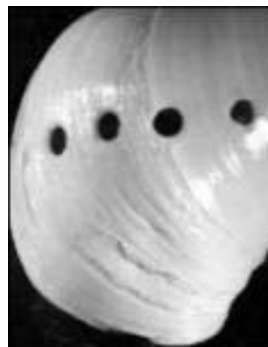
Figure 12: Terminal shell of *Radix* specimen exemplifying sampling method. Diameter of drill holes is 0.3 mm.

The aragonite samples were reacted in 10 ml borosilicate vials with phosphoric acid after flushing with helium. Resulting CO_2 gas was analysed for $\delta^{18}O$ and $\delta^{13}C$ using a GasBench II linked to a MAT-253 THERMO Scientific™ Isotope Ratio Mass Spectrometer. The external error of the measurements is ±0.06 ‰ for $\delta^{18}O$ and ±0.04 ‰ for $\delta^{13}C$ both 2 SD (standard deviations) based on the reproducibility of the in-house reference material Laaser Marble. Measurements were standardized against Cararra Marble (CAM) and Kaiserstuhl carbonatite in-house reference material (KKS) which had been calibrated against Vienna PeeDee Belemnite (V-PDB) international isotope reference material NBS-19 and NBS-18. All results are reported in δ notation relative to V-PDB. For comparing the results with measured meteorological data from the sampling year we used records from the Chinese Central Meteorological Office (2010). We selected the already mentioned three meteorological stations and calculated an average sum of precipitation and a mean annual temperature for the year 2008 (Figure 13). The data were recorded as 10-day average values and consequently three values per month are available. Temperatures are assessed as mean annual temperatures in °C based on 36 averaged values per year.
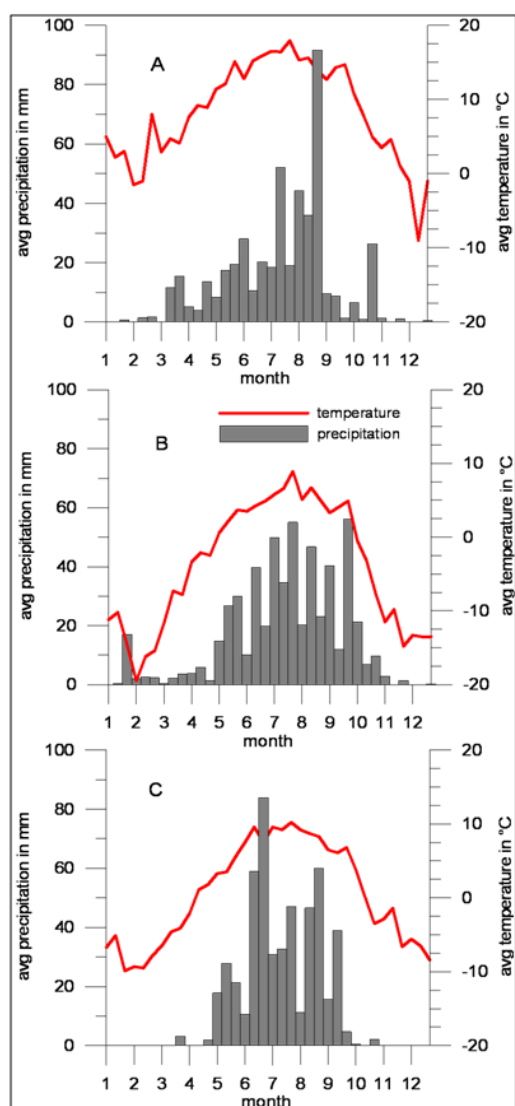
Figure 13: **Precipitation and temperature for the sampling year 2008, recorded by the Chinese Central Meteorological Office (2010): A) ca. 70 km north of Bangda Co at 31°09' N, 97°10'E and 3306 m a.s.l., 474 mm/a; B) ca. 360 km north of Bangda Co at 33°48' N, 97°08' E and 4415 m a.s.l., 562 mm/a; C) ca. 9 km south-east of Kyaring Co at 30°57' N, 88°38' E and 4672 m a.s.l., 314 mm/a.**

33

2.3 Results

2.3.1 Water parameters

The water parameters of Bangda Co and Kyaring Co are displayed in Table 3. Salinity in PSU was

calculated after Hölting and Coldewey (2009) based on electrical conductivity.

Table 3: Lake water parameters measured in the field. The salinity was calculated after Hölting and Caldewey (2009) based on the electrical conductivity. $\delta^{18}O$ and anorganic chemistry was determined at the Free University Berlin.

Locality, Date measured	Water temperature (°C)	Electrical conductivity ($\mu S/cm^{-1}$)	PSU	pH	$\delta^{18}O_{water}$ (‰)	K^+ mg/l	Na^+ mg/l	Mg^{2+} mg/l	Ca^{2+} mg/l	Sr^{2+} mg/l	HCO_3^- mg/l	Cl^- mg/l	NO_3^- mg/l	SO_4^{2-} mg/l
Bangda 27-09-08	15.1	54	0.04	7.9	-18.3	0.6	1.4	1.1	7.9	0.0	48.8	0.3	0.1	3.0
Kyaring Co A 14-09-08	8.3	293	0.21	9.4	-14.2	3.6	15.4	13.6	26.3	0.2	153	3.6	0.5	37.0
Kyaring Co B 14-09-08	13.3	149	0.11	9.3	-16.3	0.7	5.5	2.8	22.5	0.1	91.5	1.0	0.0	13.0

2.3.2 $\delta^{18}O$ and $\delta^{13}C$ in Radix *shells from Bangda Co and Kyaring Co*

For the particular isotope value of each sample see Table 4 (A-I). The isotope patterns of the shells

are described in some detail in the following and are displayed in Figs.Figure 14, Figure 15 and

Figure 16. Every pattern is described ontogenetically from the embryonic shell (protoconch) which

is formed prior to hatching, to the latest shell (aperture). The last sample from the embryonic

shell is displayed at the left ordinate whereas the letter [a] indicates the first sampling point near

the outer edge of the aperture and is displayed at the ordinate on the right.

Table 4: Oxygen and carbon isotope values of samples from Bangda Co (A-C), Kyaring Co site A (D-F) and Kyaring Co site B (G-I).

A

shell code BCo1	δ^{18}O $_{shell}$ (‰)	δ^{13}C $_{shell}$ (‰)
a (aperture)	-15.3	-5,0
b	-15.4	-5.2
c	-15.7	-4.2
d	-15.2	-4.2
e	-14.5	-4.1
f	-14.7	-5.2
g	-13.5	-5.9
h	-12.6	-5.7
i	-12.7	-5.5
j	-15.3	-4.3
k	-15.3	-4.3
l	-14.9	-3.9
m	-14.7	-4.7
n	-14.5	-4.9
o	-14.3	-4.4
p	-14.1	-4,0
q	-14.2	-4.3
r	-14.1	-4.4
s	-14.4	-4.6
t (protoconch)	-14.3	-4.4

B

shell code BCo2	δ^{18}O $_{shell}$ (‰)	δ^{13}C $_{shell}$ (‰)
a (apt)	-15.1	-4.8
b	-15.6	-4.8
c	-15.9	-4.6
d	-16,0	-4.3
e	-15.7	-3.9
f	-14.8	-3.7
g	-14.7	-3.8
h	-15.1	-4.5
i	-14.8	-5.2
j	-13.9	-5.2
k	-13.7	-7.3
l	-13.7	-6.7
m	-13,0	-6.2
n	-12.7	-5.9
o	-14.7	-4.6
p	-15.4	-4.7
q (prc)	-14.8	-4.8

C

shell code BCo3	δ^{18}O $_{shell}$ (‰)	δ^{13}C $_{shell}$ (‰)
a (apt)	-15.5	-3.7
b	-15.9	-4.3
c	-15.9	-4.8
d	-14.8	-3.8
e	-13.9	-3.9
f	-13.6	-4.1
g	-13.3	-3.4
h	-12.9	-3.4
i	-12.3	-4.1
j	-12.3	-4.8
k	-14.4	-4,0
l	-15.6	-3.5
m (prc)	-15.3	-3.9

D

shell code KCoA1	δ^{18}O $_{shell}$ (‰)	δ^{13}C $_{shell}$ (‰)
a (aperture)	-12,0	-5.2
b	-11.9	-5.2
c	-11.7	-5.6
d	-11.9	-5.7
e	-12.2	-5.4
f	-12.8	-5.2
g	-13,0	-5.3
h	-13.1	-5.4
i	-12.8	-5.3
j	-12.2	-5.7
k	-12.3	-6.1
l	-12.5	-6.8
m	-12.8	-7.1
n	-12.4	-7.4
o	-12.6	-7.3
p	-13.2	-7.3

E

shell code KCoA2	δ^{18}O $_{shell}$ (‰)	δ^{13}C $_{shell}$ (‰)
a (apt)	-11.1	-5.7
b	-11.3	-5.6
c	-11.5	-5.6
d	-11.7	-6.4
e	-12.1	-6.6
f	-12.3	-6.5
g	-12.4	-6.5
h	-12.4	-6.6
i	-12.5	-6.8
j	-12.3	-7,0
k	-12.5	-7.2
l	n.d.	n.d.
m	-12.7	-7.2
n	-13.3	-7.2
o	-12.8	-7.2
p	-12.7	-7.1

F

shell code KCoA3	δ^{18}O $_{shell}$ (‰)	δ^{13}C $_{shell}$ (‰)
a (apt)	-11.9	-6,0
b	-12.1	-6.4
c	-12.7	-6.6
d	-12.8	-6.9
e	n.d.	n.d.
f	-13.2	-6.5
g	-12.8	-6.1
h	-12.7	-6.3
i	-12.9	-6.7
j	-13,0	-6.7
k	-12.8	-6.7
l	-13.2	-6.7
m	-12.8	-7.1
n (prc)	-13,0	-6.7

shell code	δ18O shell	δ13C shell	shell code	δ18O shell	δ13C shell	
q	-13.1	-7.3	q	-12.7	-7.2	
r	-13,0	-7.6	r	-12.8	-7.4	
s	-13.3	-7.5	s	-12.6	-7.2	
t	-12.3	-6.9	t	-12.7	-7.2	
u	-9.7	-6.4	u	-12.9	-7.2	
v	-10.3	-6.9	v (prc)	-12.6	-7.3	
w (protoconch)	-10.6	-6.1				

G

shell code KCoB1	$\delta^{18}O$ shell (‰)	$\delta^{13}C$ shell (‰)
a (aperture)	-13.8	-10.7
b	-14.7	-9.8
c	-14.6	-9.9
d	-14.3	-10,0
e	-15,0	-5.1
f	-14.7	-4.9
g	-15,0	-4.3
h	-14.9	-6.6
i	-14.5	-7.4
j	-14.1	-7.8
k	-13.5	-7.8
l	-13.5	-6.2
m	-15.1	-5,0
n	-15.2	-5.4
o	-14.5	-6.4
p	-14.6	-6.1
q	-14.9	-5.5
r (prc)	-14.6	-5.5

H

shell code KCoB2	$\delta^{18}O$ shell (‰)	$\delta^{13}C$ shell (‰)
a (apt)	-13.2	-10,0
b	-13.8	-10.2
c	-15,0	-10.4
d	-15.3	-9.7
e	-14.9	-10.1
f	-15.5	-6.5
g	-15.3	-6.8
h	-15.3	-7.1
i	-14.9	-7.9
j	-14.5	-8,0
k	-14,0	-8.2
l	-13.8	-7.6
m	-14.6	-6,0
n	-15.1	-6.8
o	-15,0	-6.1
p (prc)	-14.7	-6.5

I

shell code KCoB3	$\delta^{18}O$ shell (‰)	$\delta^{13}C$ shell (‰)
a (apt)	-13.1	-11.2
b	-13.2	-11.1
c	-14.1	-11.4
d	-14.7	-11.2
e	-14.9	-11.1
f	-14.5	-11,0
g	-14.3	-10.5
h	-14.6	-9.9
i	-14.6	-9.5
j	-14.9	-8.6
k	-14.8	-8.3
l	-15.2	-8.2
m	-15.1	-8,0
n (prc)	-14.7	-8.3

2.3.3 Shells from Bangda Co

δ^{18}O total values of the three shells (BCo1-3) from Bangda Co range from -12.3 to -16.0 ‰. The absolute δ^{13}C range is from -3.4 to -7.3 ‰.

Figure 14: **Patterns of oxygen and carbon isotope compositions in *Radix* shells from Bangda Co. The greyish lines indicate the onset of monsoon precipitation in June 2008.**

Shell BCo1: 20 samples [a–t]: The protoconch δ^{18}O value [t] is -14.3 ‰, which slightly decreases in the early juvenile [s] but increases again to the initial value in the later juvenile [r-q] before a significant gradual decrease to [k] -15.3 ‰ occurs. A particularly steep increase to -12.6 ‰ [h] represents the highest value in this shell. A subsequent steep decrease to -15.7 ‰ [c] (lowest δ^{18}O value) is interrupted around -14.6 ‰ [e-f]. To the aperture [a] a terminal increase to -15.3 ‰ is observed. The protoconch δ^{13}C value [t] in BCo1 is -4.4 ‰, which slightly decreases in the early juvenile [s] to -4.6 ‰ but subsequently increases to -4.0 ‰ [p]. A rather steep decrease to -4.9 ‰ [n] is followed by a similar steep increase to the highest δ^{13}C value (-3.9 ‰ [l]). In two steps the values decrease to -5.9 ‰ [g] representing the lowest δ^{13}C value in this shell. After a steep increase to -4.1 ‰ [e] little variation follows, before a steep decrease to -5.2 ‰ [b] characterizes the terminal shell. The aperture [a] has a δ^{13}C value of -5.0 ‰.

Shell BCo2: 17 samples [a–q]: The protoconch δ^{18}O value [q] is -14.8 ‰., which decreases in the early juvenile [p], followed by a steep increase to -12.7 ‰ [n] (highest δ^{18}O value) in the later juvenile. The value then decreases in three steps to -16.0 ‰ [d] (lowest δ^{18}O value) with an intermediate increase during [h-g] to -14.7 ‰ [j]. The terminal increase from -16.0 ‰ [d] ends with a δ^{18}O value of -15.1 ‰ at the aperture [a]. The protoconch δ^{13}C value [q] is -4.8 ‰, which slightly increases in the early juvenile prior to a steep decrease to -7.3 ‰ [k] (lowest δ^{13}C value). A two-stepped steep increase to -3.3 ‰ [f] (highest δ^{13}C value) is followed by a terminal decrease with a δ^{13}C value of -4.8 ‰ at the aperture [a].

Shell BCo3: 13 samples [a-m]: The protoconch δ^{18}O value [m] is -15.3 ‰, which decreases in the early juvenile [l], followed by a sharp increase to -12.3 ‰ (highest δ^{18}O value). A short period of little variation is followed by a two-phased decrease to -15.9 ‰ [c]. To the aperture [a] the δ^{18}O value increases to -15.5 ‰. The protoconch δ^{13}C value [m] is -3.9 ‰, which slightly increases in the early juvenile [l] and then decreases to a first minimum of -4.8 ‰ [j]. A subsequent increase to -3.4 ‰ [h] marks the highest value. A two-phased decrease, interrupted by a slight increase during [f-d], leads to a second minimum of -4.8 ‰. A terminal increase results in a value of -3.7 ‰ at the aperture [a].

2.3.4 Shells from Kyaring Co

The δ^{18}O total values of the three shells from Kyaring Co site A (KCoA1-3) range from -9.7 to -13.3 ‰ and the absolute δ^{13}C range is from -5.2 to -7.6 ‰. The δ^{18}O total values of the shells from Kyaring Co site B (KCoB1-3) range from -13.1 to -15.5 ‰ and the absolute δ^{13}C range is from -4.7 to -11.4 ‰.

2.3.4.1. Sampling site A
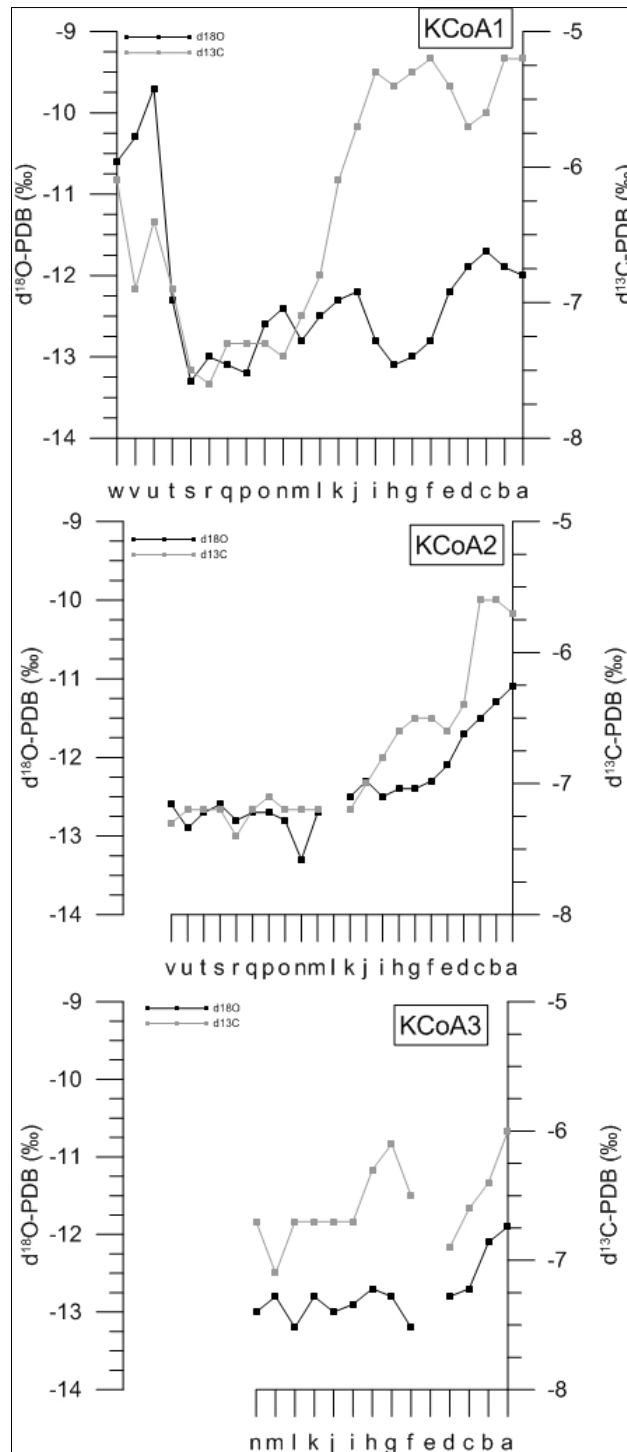
Figure 15: Patterns of oxygen and carbon isotope compositions in *Radix* shells from Kyaring Co site A.

Shell KCoA1: 23 samples [a-w]: The protoconch δ^{18}O value [w] is -10.6 ‰, which increases to -9.7 ‰ in the juvenile (highest δ^{18}O value). A subsequent sharp decrease to -13.3 ‰ [s] (lowest δ^{18}O value) is followed by a three-phased increase to -12.2 ‰ [j]. Another short-lived decrease to -13.1 ‰ [h] is followed by a rather regular increase to -11.7 ‰ [c]. The terminal shell ([b-a]) shows a slight decrease in δ^{18}O. The protoconch δ^{13}C value [w] is -6.1 ‰, which first decreases but then increases in the early juvenile [u-v], followed by a more significant decrease in the later juvenile to -7.6 ‰ [r] (lowest δ^{13}C value), with little variation afterwards until a steep increase to highest values around -5.2 ‰ [i-a]. Slightly lower values were measured for [e-c].

Shell KCoA2: 22 samples [a-v]: The protoconch δ^{18}O value [v] is -12.6 ‰, which slightly decreases in the early juvenile [u] and subsequently varies little in early ontogeny (until [o]). A decrease to the lowest value (-13.3 ‰) is followed by a two-phased increase to the highest value (-11.1 ‰) at the aperture [a]. The protoconch δ^{13}C value [v] is -7.3 ‰. This value varies little during early ontogeny (until [k]) and is followed by a two-phased increase to highest values of -5.6 ‰ during later ontogeny, with a slight decrease at the terminal shell [a].

Shell KCoA3: 14 samples [a-n]: The protoconch δ^{18}O value [n] is -13.0 ‰. The value varies comparatively little during early ontogeny. During later ontogeny the lowest value of -13.2 ‰ [f] is followed by a relatively regular increase to the highest value of -11.9 ‰ at the terminal shell [a]. The protoconch δ^{13}C value [n] is -6.7 ‰. A slight decrease in the early juvenile is followed by a slight increase to the initial value and then by a period with no variation until [i]. A moderate increase from [i-g] to -6.1 ‰ is followed by a decrease to -6.9 ‰. The terminal shell shows a regular increase with the highest value of -6.0 ‰ at the aperture [a].
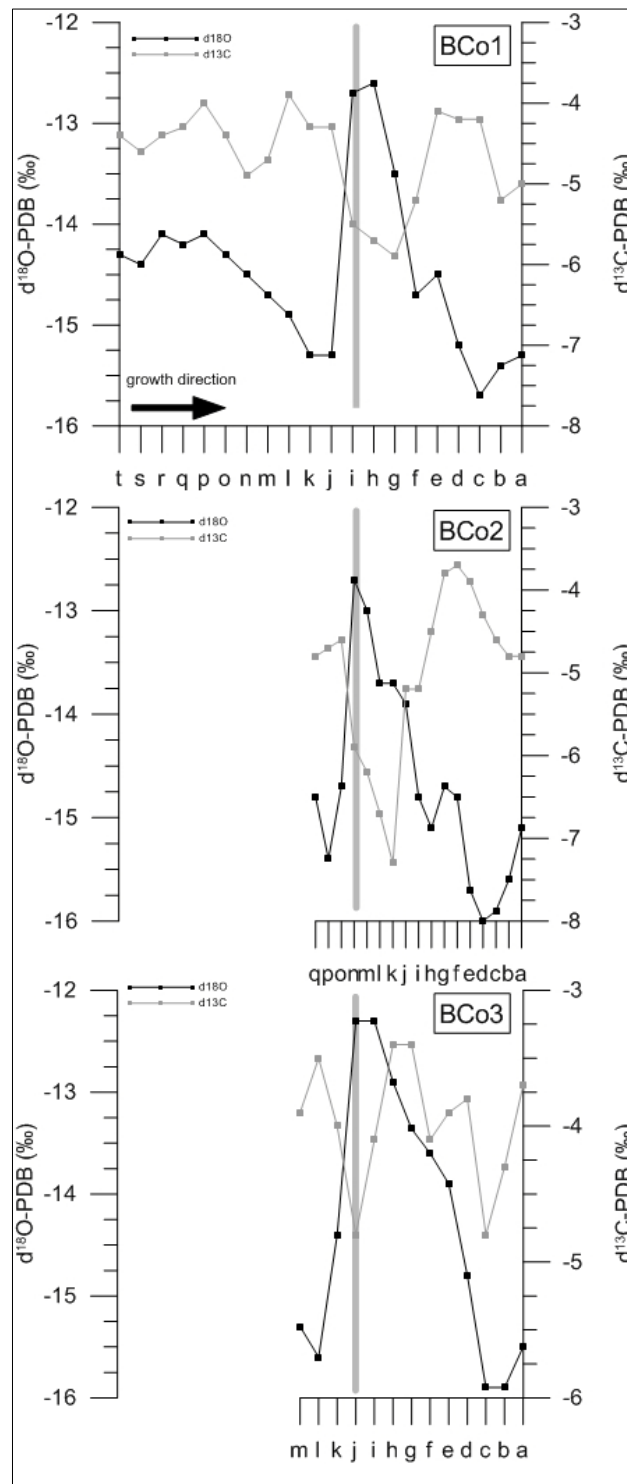
2.3.4.2. Sampling site B
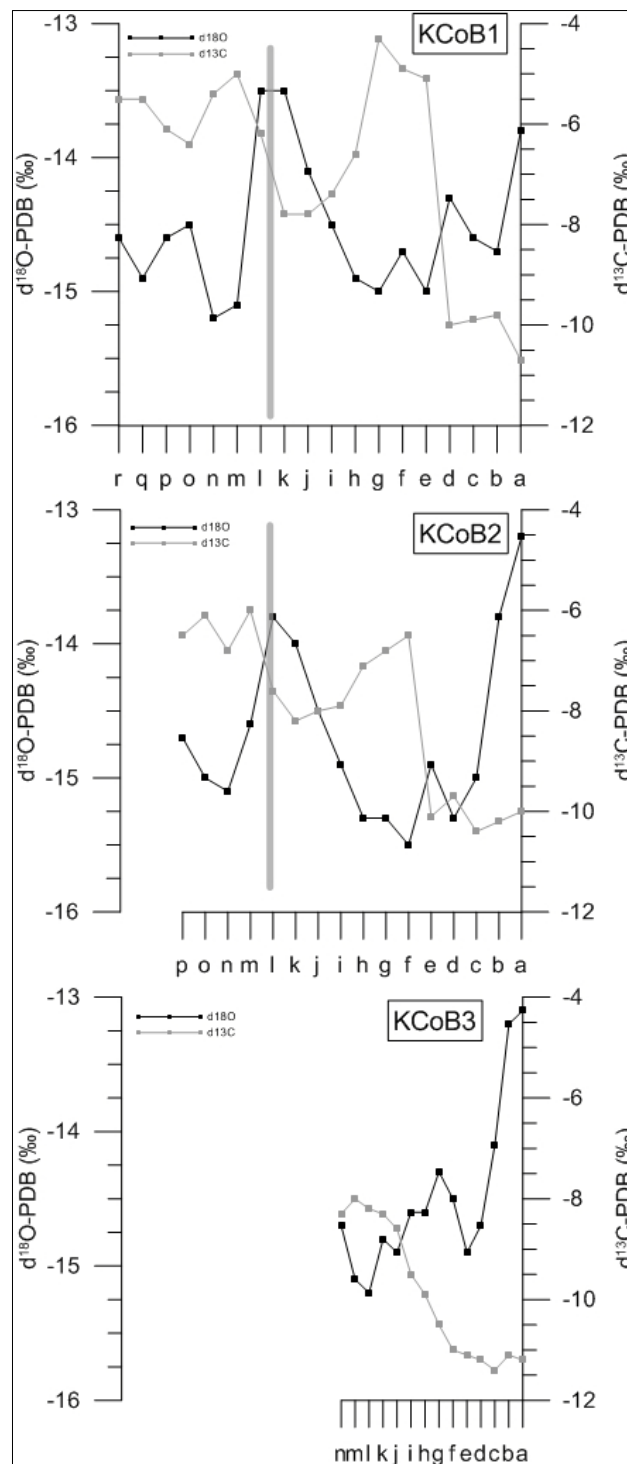
Figure 16: Patterns of oxygen and carbon isotope compositions in *Radix* shells from Kyaring Co site B. The greyish lines indicate the onset of monsoon precipitation in June 2008.

Shell KCoB1: 18 samples [a-r]: The protoconch δ¹⁸O value [r] is -14.6 ‰, which slightly decreases in the early juvenile but then reaches again the initial value. Subsequently the lowest value [n] of -15.2 ‰ is observed from which a steep increase results in the highest values [l-k] of -13.5 ‰.

These are followed by a regular decrease to -15.0 ‰. The late ontogeny is characterized by three stages of increase, terminating at a $\delta^{18}O$ value of -13.8 ‰ at the aperture [a]. The protoconch $\delta^{13}C$ value [r] is -5.5 ‰, a value which decreases to -6.0 ‰ in the early juvenile. During [o-m] the second highest peak (-5.0 ‰) is formed which is followed by a sharp decrease to -7.8 ‰ [k] and a subsequent steep increase to the highest $\delta^{13}C$ value (-4.3 ‰) in this shell. The decrease to the lowest value of -10.7 ‰ at the aperture [a] occurs in four steps, with a particularly sharp decrease from [e-d].

Shell KCoB2: 16 samples [a-p]: The protoconch $\delta^{18}O$ value [p] is -14.7 ‰, which decreases in the early juvenile to -15.1 ‰ prior to a steep increase to -13.8 ‰ during [n-l]. A period of decrease to the lowest value of -15.5 ‰ [f] is followed by a two-phased increase to the highest $\delta^{18}O$ value of -13.2 ‰ at the aperture [a]. The protoconch $\delta^{13}C$ value [p] is -6.5 ‰. It varies from -6.0 (highest value in this shell) to -6.8 ‰ in the early juvenile before it decreases more significantly to -8.2 ‰ [k]. A regular increase to -6.5 ‰ [m] is followed by a sharp decrease to -10.1 ‰ [e]. The terminal shell shows little variation in a range of -9.7 to -10.4 ‰ (lowest $\delta^{13}C$ value).

Shell KCoB3: 14 samples [a-n]: The protoconch $\delta^{18}O$ value [n] is -14.7 ‰. An initial decrease to -15.2 ‰ in the early juvenile is followed by a general increase to the highest value of -13.1 ‰ at the aperture [a]. An intermediate decrease to a value of -14.9 ‰ [e] occurs prior to the terminal steep increase. The protoconch $\delta^{13}C$ value [n] is -8.3 ‰, which varies little during early ontogeny. From [j-c] the value decreases relatively regularly from -8.6 to -11.4 ‰ (lowest value). Terminally a slight increase can be observed.

2.4 Discussion

2.4.1 Bangda Co (eastern Tibetan Plateau)

We focus the discussion on isotope patterns of shell BCo1 which exhibits the longest life span of the three shells (Figure 14). Data from shells BCo2 and BCo3 are used supplementarily to support interpretations.

The remarkable steep increase from -15.3 ‰ [j] to -12.6 ‰ [h] in BCo1 represents the reference point for the interpretation of the Bangda Co shells. Because we had no oxygen isotope data of precipitation from the lake regions, we compared the oxygen isotope patterns in the shells with the weighted annual isotope patterns in precipitation (IAEA/WMO, 2006) recorded for Lhasa (29°39'N, 91°08'E, 3650 m a.s.l.) which is located in a monsoon dominated area (Fig. 8): Lowest δ^{18}O values in precipitation occur during the peak of the monsoon season in August and highest values occur when initial monsoon rains fall in May. Because Lhasa is more than 500 km from Bangda Co, the onset and peak of monsoon rains cannot be synchronized. For contrast see the δ^{18}O composition in precipitation for Yinchuan (38°29'N, 106°13'E, 1111 m a.s.l.) located in Ningxia Autonomous Region in northern central China and beyond monsoon influence. Here the δ^{18}O composition in precipitation follows the annual air temperature. On the basis of the δ^{18}O patterns in the shells (Figure 14), the meteorological records for the sampling year (Figure 13) and the monsoon pattern in precipitation for Lhasa (Figure 17), the onset of monsoon precipitations can be identified in the Bangda Co shells and is dated to June.
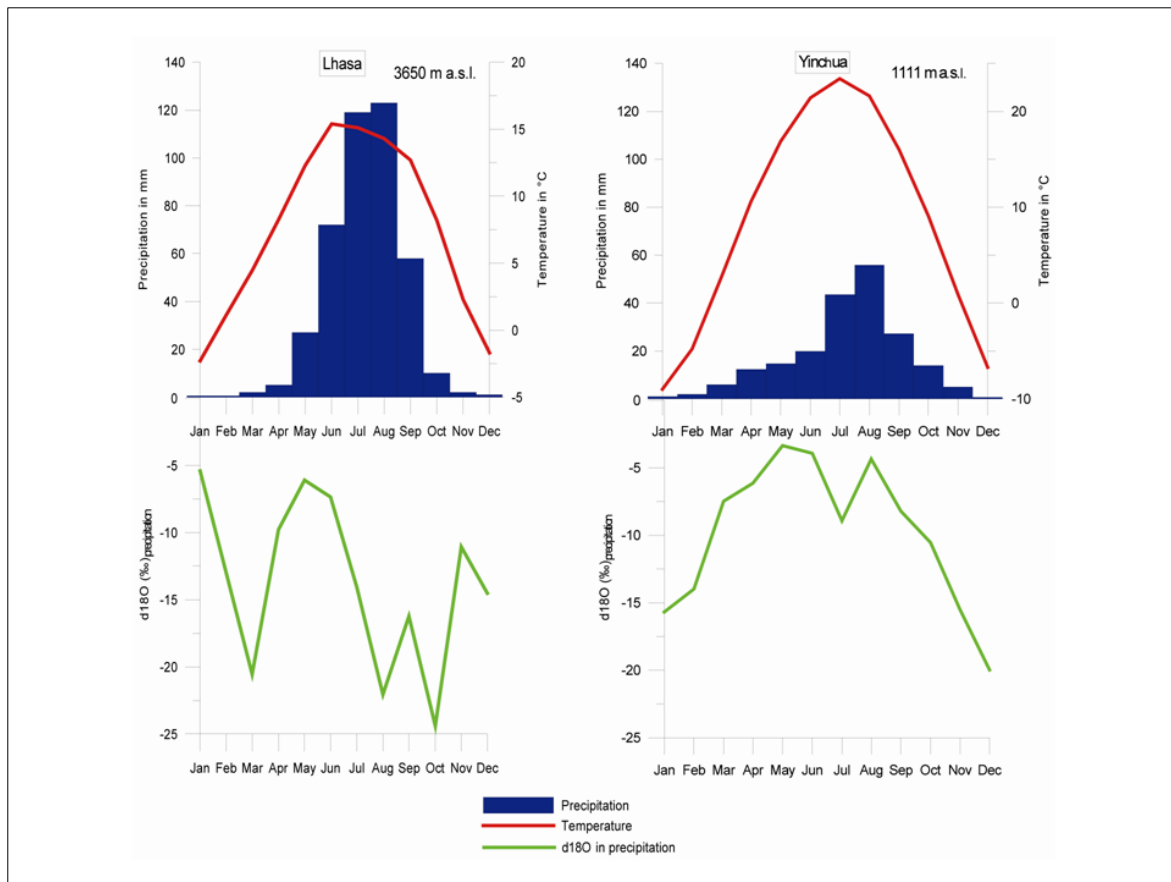
Figure 17: Example of annual oxygen isotope patterns in precipitations which are controlled by temperature (Yinchuan, Ningxia Autonomous Region, 38°29'N, 106°13'E, 1111 m a.s.l.) and by monsoon precipitation (Lhasa, southern Tibetan Plateau, 29°39'N, 91°08'E, 3650 m a.s.l.). Mean annual temperature and precipitation of Lhasa and Yinchuan are based on data from the Chinese Central Meteorological Office (2010). Annual oxygen isotope patterns in precipitation are based on data from the Global Network of Isotopes in Precipitation, GNIP (2006).

The first rains which are related to the monsoon circulation are characterized by isotope values which are heavier than the lake water of Bangda Co which has very low values due to the short residence time and low evaporation. Precipitation from February to May and from September to November (Figure 13) does not result in a significant variation of the δ^{18}O composition in the lake water and therefore in the shells, because these rains have regional sources. After the steep increase of about 2.7 ‰, the oxygen isotopes show a gradual decrease to a minimum value of -15.7 ‰. This pattern represents a typical full monsoon influenced oxygen isotope composition in precipitation which has been reported in several studies (e.g. Leng et al., 1999; Dettmann et al., 2001; Breitenbach et al., 2010). The inverse correlation between precipitation amount and the oxygen isotope composition in the summer monsoon indicates the so called 'amount effect' (Dansgaard, 1964; Lee and Fung, 2007 and references therein; Yu et al., 2008). Most negative values are measured in late August during the peak of monsoon precipitation (Figure 13). The shell section between [c] and [a] represents the time between the peak of monsoon rains and the

44

sampling date in September and represents increasing evaporation. We interpret that the slight decrease in $\delta^{18}O$ from [t] to [s] reflecting the time between hatching and the beginning of ice covering of the lake in November. The relatively stable values between [r] and [p] represent the period when the specimen lived under the ice cover and the lake water was influenced neither by evaporation nor by precipitation. The decrease in $\delta^{18}O$ from -14.1 ‰ [p] to -14.9 ‰ [l] is interpreted to be triggered by decreasing winter temperatures from December to April. Subsequent decreasing values from -14.9 ‰ [l] to -15.3 ‰ [j] are a response to the input of snow and glacier melt waters which are characterized by light $\delta^{18}O$ values. Although snow and ice melting continues during the summer months, this signal is not detectable during the monsoon season due to the strong overprint of the isotope composition in monsoon precipitation. BCo2 and BCo3 hatched most likely in May because they cover the complete monsoon pattern from June to September in their shells but not the winter period. This is in correspondence with smaller shell sizes compared to BCo1 (Figure 11, Table 2).

In all shells the onset of monsoon precipitations corresponds with a steep decrease in $\delta^{13}C$. This negative coupling between $\delta^{18}O$ and $\delta^{13}C$ provides evidence that this reflects a change in the water composition, because a change in temperature or pH would unlikely affect both isotope systems. Most likely decreasing $\delta^{13}C$ values and simultaneously increasing $\delta^{18}O$ values are a result of monsoon precipitation penetrating through unsaturated zones of soils before the water reaches the lake. Although Bangda Co is located in a transition zone between seasonally frozen ground and permafrost, the uppermost active layer contains a lot of micro-organisms, which produce isotopically light CO_2 by respiration and decomposition of organic matter. The CO_2 is accumulated in the pore volume and reaches the lake in a dissolved phase and leads to variations in $\delta^{13}C$. $\delta^{13}C$ changes before and after the monsoon season might be attributed to changes in lake productivity which may be related to seasonal temperature and/or local nutrient variation.

2.4.2 Kyaring Co (central Tibetan Plateau)

We focus the discussion on isotope patterns of shell KCoA1 which has the highest number of whorls, the biggest size among all shells and thus exhibits the longest life span (Figure 15). Data from shells KCoA2 and KCoA3 are used supplementarily to support interpretations.

The steep decrease in $\delta^{18}O$ between [u] and [s] from -9.7 to -13.3 ‰ represents the reference point for the interpretation. The decrease is interpreted as the winter period when the lake surface was covered by ice from November 2007 until April of the sampling year. Based on a study from Gaten (1986) who observed winter growth rates of *Radix* of 0.35 mm per 4 week period, the

shell section between [u] and [s] would represent a period of about 5 months, which coincides with the ice covering on the lake. Most likely the lake water was evaporatively enriched before the surface was covered with ice when this specimen hatched in October 2007. The evaporative enrichment led to more positive oxygen isotope values between -10.6 [w] and -9.7 ‰ [u] between October and November. These values show a tendency towards the typical $\delta^{18}O$ value of lake waters of about -8.0 ‰ in this region (Tian et al., 2008). Ice melting in April indicated by decreasing oxygen isotope values between [r] and [p] is only marginally detectable in the pattern because evaporative enrichment of the lake water starts once the ice cover has disappeared. The evaporation trend is also visible between [p] and [n] when the $\delta^{18}O$ values increase from -13.2 to -12.4 ‰ in May. The typical monsoon pattern is less pronounced in shells from site A at Kyaring Co because the water in the habitat is temporarily mixed with the large water mass of the lake basin which has a long reaction time to meteorological variations. However, a peak of the monsoon season in August is detectable at sample [h] which has a low $\delta^{18}O$ value of -13.1 ‰. A similar pattern, but less pronounced, can be found in KCoA2 and KCoA3. After August, evaporation plays a more and more crucial role in the oxygen isotope composition in the habitat, which leads to increasing values in all three shells. This corresponds to a higher electrical conductivity and a higher SO_4^{2-} content in the lake water in mid-September (Table 3).

The carbon isotope pattern in KCoA1 starts to increase significantly from [n] to [f] initiated by a combination of surface water input and higher biological productivity from May onwards. $\delta^{18}O$ and $\delta^{13}C$ patterns in KCoA2 and KCoA3 differ from those of KCoA1, because of a different micro-habitat. KCoA2 covers the period from April to September; KCoA3 hatched in May. The comparatively parallel developing of $\delta^{18}O$ and $\delta^{13}C$ in both shells indicates that the water in the habitat is consistently mixed with the lake water.

In summary, the isotope patterns of shells from Kyaring Co site A indicate a habitat which is influenced by temperature and evaporation during the pre- and post-monsoon period. Only from the onset of monsoon rains in June to the peak of the rainy season in August are the isotope compositions in the shells mainly influenced by precipitation.

For Kyaring Co sampling site B we focus the discussion on isotope patterns of shell KCoB1 which exhibits the longest life span of the three shells (Figure 16). Data from shells KCoB2 and KCoB3 are used supplementarily to support interpretations.

The noticeable steep increase of $\delta^{18}O$ from -15.1 ‰ [m] to -13.1 ‰ [l], and the following steep decrease to -15.0 ‰ [g] in KCoB1 have been the reference point for the interpretation of the isotope patterns at site B. Compared with the precipitation data from the meteorological station

(Figure 13) and the isotope values in precipitation for Lhasa (Figure 17), this pattern reflects the onset and progression of monsoon precipitation. The steep increase mirrors the onset in June, and the lowest value [g] represents the peak of the monsoon precipitation in August. The specimen which built shell KCoB1 hatched in April, when the ice cover on the lake started to disappear. The decrease of $\delta^{18}O$ from -14.5 ‰ [o] to -15.2 ‰ [n] reflects the input from isotopically lighter snow and glacier melt water in May once the ice cover on the lake surface had disappeared. This corresponds with the fact that the sampling site B at Kyaring Co is very close to steep sloping mountains. The increasing trend after the monsoon peak to -13.8 ‰ [a], which reflects the increasing influence of evaporation in this habitat in late August and early September, is interrupted by a slight decrease from -14.3 ‰ [d] to -14.7 ‰ [b]. When the carbon isotope pattern is additionally integrated in the interpretation, this slight decrease in $\delta^{18}O$ can be explained as follows: The steep decrease in $\delta^{13}C$ values accompanied by an increase in $\delta^{18}O$ after the peak of the monsoon season in August in KCoB1 and KCoB2 [e-d; f-e] may reflect a storm event in which isotopically heavier lake water was mixed into the somewhat sheltered habitat. After this storm event, the oxygen isotope composition in the habitat water again tended towards more negative values, which might be caused by new rain events at the beginning of September (Figure 13). Decreasing $\delta^{13}C$ values [m-c] are also noticeable in KCoB3 but the trend is rather gradual. This is most likely because of a different micro-habitat of the particular specimen. The successive decrease of $\delta^{13}C$ accompanied by an increase of the oxygen isotope values in KCoB3 is rather a result of evaporation and the oxidation/respiration of organic matter. In summary, KCoB1 exhibits the period from April to September; KCoB2 hatched in May and KCoB3 hatched during the monsoon season in July.

Mean $\delta^{18}O$ values of shells from site A are about 2 ‰ higher than shells from site B. These differences must be related to distinct habitats because both sites at Kyaring Co are clearly under monsoon influence. The *Radix* specimens from site A are from a habitat which is connected to the main lake basin whereas site B represents a habitat which is partly and temporarily separated from the open lake (Figure 10). The $\delta^{18}O$ compositions of KCoB1 and KCoB2 are similar to shells from Bangda Co and show distinct patterns with a steep increase followed by a rather gradual decrease, which we interpret as primarily controlled by monsoon precipitation. Note the strong negative coupling between $\delta^{18}O$ and $\delta^{13}C$ during the monsoon rains, providing evidence for meteorological and/or environmental changes which are not mainly controlled by temperature changes.

2.4.3 Comparison of Bangda Co and Kyaring Co

The catchments of both lakes are reached by summer monsoon precipitation (Tian et al., 2001; Liu et al., 2010) which is clearly recorded by the isotopes in modern *Radix* shells from Bangda Co and Kyaring Co sampling site B, as discussed in earlier chapters. The $\delta^{18}O$ signature of the lake water sample collected at Bangda Co (-18.3 ‰) is close to the average of many rivers (~ -18.0 ‰) in this region, as reported by Tian et al. (2008). The $\delta^{18}O$ of water from site A (-14.2 ‰) and B (-16.3 ‰) at Kyaring Co falls between river waters (ca. -18.0 ‰) and lake waters (~ -8.0 ‰) in this area (Tian et al., 2008). Big lakes with long water residence times such as Kyaring Co lose a lot of water by evaporation, which is evident from less variable and on average higher $\delta^{18}O$ values in shells from site A. Although this habitat reacts slowly to water influx and therefore *Radix* shells from this site cannot provide as much information on seasonal variations as shells from the other habitats, long-term climatic changes may be detectable and a clear distinction of the habitat is extractable from these shells.

Evidence for a significant difference between Bangda Co and Kyaring Co site B on the one hand and site A on the other hand is also the mean $\delta^{18}O$ shell value. Whereas shells from Bangda Co and Kyaring Co site B have similar oxygen isotope mean values of around -14.5 ‰, shells from Kyaring Co site A exhibit mean values about 2 ‰ higher, around -12.5 ‰. The discharge is lower and water residence time longer than at site B which is also supported by the higher salinity, the higher $\delta^{18}O$ value of the water (-14.2 ‰) and a higher ion concentration (Table 3). When the shallow, sheltered sample area B at Kyaring Co obtains $\delta^{18}O$ depleted rain during the peak and late monsoon period and water from hill slopes, the composition of the lake water changes rapidly. A comparable habitat exists at Bangda Co. *Radix* shells from site B at Kyaring Co have low mean carbon isotope compositions. This is consistent with a strong input of light carbon, most likely from slope water input from the high mountains near the lake. However, shells from both sampling sites are far from having a typical lake water composition as described by Tian et al. (2008) due to the strong influence of the oxygen isotope composition in precipitation.

We do not know whether carbon has been precipitated in equilibrium or is altered by vital effects (e.g. Fritz and Poplawski, 1974; Wefer and Berger, 1991; Shanahan et al., 2005) because the isotopic composition of dissolved inorganic carbon (DIC) in both lakes is unknown. It would be interesting to quantify the vital effect in the isotope compositions of the shells, but that would not change the interpretation of the results because vital effects would affect all samples to the same degree and the isotopic patterns would not change.

It is assumed that the growth rate of *Radix* increases significantly from April to September and that relatively small shell sections represent, in comparison to the winter months, less time. However, the specimens which cover a longer time period exhibit a larger size.

2.5 Conclusions

Oxygen and carbon isotopes in shells of the modern freshwater gastropod *Radix* provide valuable information on various parameters characterizing regional climate and lake environments. The oxygen isotope compositions in the shells are mainly dominated by precipitation and riverine inflows when water residence times in *Radix* habitats are short such as those at Bangda Co or sampling site B at Kyaring Co. Compared with meteorological data recorded during the life span of the animals, the isotope patterns within the shells provide an archive with sub-seasonal resolution.

Shells from site A at Kyaring Co exhibit less isotopic variation, which is consistent with a longer residence time of water and carbon in this habitat. The isotopically heavier oxygen in habitat A compared with habitat B is consistent with a larger portion of water evaporated at site A. This is confirmed by a high cation and anion concentration in water samples of habitat A.

Isotopically light carbon in the shells is coupled with monsoon precipitations. Before and after the monsoon season biological activity and respiration of organic matter compete with each other, but carbon isotope ratios are typically higher than during the monsoon season.

When the meaning of distinct isotopic values and patterns in shells of modern *Radix* are understood the method can be applied to fossil shells for reconstructing climate and lake environments on the Tibetan Plateau of the past.

3. Oxygen and carbon isotope patterns archived in shells of the aquatic gastropod *Radix*: Hydrologic and climatic signals across the Tibetan Plateau in sub-monthly resolution

Linda Taft[a], Uwe Wiechert[a], Hucai Zhang[b], Guoliang Lei[c], Steffen Mischke[a,d], Birgit Plessen[e], Marc Weynell[a], Andreas Winkler[a], Frank Riedel[a]

[a]Free University Berlin, Institute of Geological Sciences, Palaeontology, Building D, Malteserstr. 74-100, 12249 Berlin, Germany

[b]Yunnan Normal University, Key Laboratory of Plateau Lake Ecology and Global Change, College of Tourism and Geography, Kunming 650092, China

[c]Fujian Normal University and Fujian Key Laboratory of Subtropical Resources and Environment, Institute of Geography, Fuzhou 350007, China

[d]University of Potsdam, Institute of Earth and Environmental Science, Karl-Liebknecht-Str. 24-25, 14476 Potsdam, Germany

[e]Helmholtz-Zentrum Potsdam, Deutsches GeoForschungsZentrum (GFZ), Telegrafenberg C 327, 14473 Potsdam, Germany

Abstract

The Tibetan Plateau (TP), including its surrounding mountain ranges, represents the largest store of ice outside the polar regions. It hosts numerous lakes as well as the head waters of major Asian rivers, on which billions of people depend, and it is particularly sensitive to climate change. The moisture transport to the TP is controlled by the Indian and Pacific monsoon and the Westerlies. Understanding the evolution of the interaction of these circulation systems requires studies on climate archives in different spatial and temporal contexts. The objective of this study is to learn more about the interannual variability of precipitation patterns across the TP and how different hydrologic systems react to different climatic factors.

Aragonite shells of the aquatic gastropod Radix, which is widely distributed in the region, may represent suitable archives for inferring hydrologic and climatic signals in particularly high resolution. Therefore, sclerochronological studies of $\delta^{18}O$ and $\delta^{13}C$ ratios in Radix shells from seven lakes were conducted, each representing a different hydrologic and climatic setting, on a transect from the Pamirs across the TP.

The shell patterns exhibit an increasing influence of precipitation and a decreasing influence of evaporation on the isotope compositions from west to east. $\delta^{18}O$ values of shells from lakes on the eastern and central TP (Donggi Cona, Yamdrok Yumco, Tarab Co) mirror monsoon signals, indicated by more negative values and higher variabilities compared to the more western lakes (Karakul, Bangong/Nyak, Manasarovar). In Yadang Co, located on the central southern TP, the monsoon rains did not reach the lake in the sampling year, although it is located in a region which is usually affected by monsoon circulation. The $\delta^{18}O$ values are used to differentiate the annual hydrological cycle into ice cover period, melt water period, precipitation period and evaporation period. $\delta^{13}C$ compositions in the shells particularly depend on specific habitats, which vary in biological productivity and in carbon sources. $\delta^{18}O$ and $\delta^{13}C$ patterns show a positive covariance in shells originating from large closed basins. The results show that Radix shells mirror general climatic differences between the seven lake regions. These differences reflect both regional and local climate signals in sub-seasonal resolution, without noticeable dependence on the particular lake system.

3.1 Introduction

3.1.1 Scope

The scientific and public interest in understanding and predicting the complex spatio-temporal variability of the Asian monsoons is especially high because these atmospheric circulation systems and linked teleconnections affect more than half of humanity worldwide (Benn and Owen, 1998; Cook et al., 2010). Of particular interest are long term changes of the system, and extreme events such as droughts which have occurred e.g. in India in 2000 and 2007 (Krishnan et al., 2003; Sinha et al., 2011) and in southwestern China in 2010 (Stone, 2010), or flooding events which were recorded in the Indian Himalayas, Pakistan and western Tibet in 2010 (Webster et al., 2011; Gautam, 2012). The Tibetan Plateau (TP), including its surrounding mountain ranges (Pamirs, Hindu Kush, Tien Shan, Himalayas, Karakoram), has been considered to control the Asian monsoons because the large and highly elevated and sparsely vegetated area receives strong

insolation during the Northern Hemisphere summer (Clemens et al., 1991; Prell and Kutzbach, 1992; Ye and Wu, 1998; Fleitmann et al., 2003, 2007; Kong et al., 2007; Lee et al., 2009; Sato, 2009; An et al., 2011). Modern observations of the climate, however, identify the Himalayas, rather than the TP, as the dominant thermal forcing in the region of the Indian Summer Monsoon (Boos and Kuang, 2010). Irrespective of the ongoing discussion about major forcing and driving mechanisms, the highly elevated region has an enormous water storage capacity. The TP represents Earth´s largest store of ice outside the polar regions (Qiu, 2008). Approximately 1600 lakes larger than 1 km^2 are scattered across the TP spanning ca. 50,900 km^2 (Zheng, 1997). Billions of people depend on water from the Indus, Brahmaputra, Mekong, Yangtze and Yellow rivers which all have their head waters on the TP (Xu et al., 2008; Hua, 2009; Immerzeel et al., 2010; Piao et al., 2010). The ECHAM5 climate model, however, predicts severe freshwater resource shortages in China for the period AD 2071 to 2100 (Harding, 2012). The water resources of the TP are sensitive to climate change, and changes in temperature and precipitation are expected to seriously affect melt characteristics (Cui and Graf, 2009; Immerzeel et al., 2010). During recent decades, most of the glaciers have retreated (Qiu, 2008; Pang et al., 2010), but significant regional differences occur (Yao et al., 2006).

Understanding moisture transport onto the TP not only in modern times but also during the past is crucial for understanding the development of this ice and water storage. Numerous publications have focused on the interplay of the Asian monsoons with the Westerly circulation and with ENSO, many discussing moisture transport and availability on the TP, considering different spatio-temporal resolutions (e.g. Gasse et al., 1991; Fan et al., 1996; An et al., 2000; Anderson et al., 2002; Brown et al., 2003; Yang et al., 2003; Wang, P.X., et al., 2005; Wang, Y.J., et al., 2005; Bookhagen and Burbank, 2006; Herzschuh, 2006; Xu et al., 2007; Mischke et al., 2008; Qian et al., 2009; Zhang and Mischke, 2009; Mischke and Zhang, 2010; Wang et al., 2010; An et al., 2011; Cook et al., 2011; von Oheimb et al., 2011; Wischnewski et al., 2011; Taft et al., 2012). Studying past climate variability in particular with high temporal resolution archives has helped to infer precipitation and temperature patterns of the past and compare them with the documented historical and modern situation (Yang, Y.D. et al., 2007; Liang et al., 2008; Qian et al., 2009; Yu et al., 2009; Fan et al., 2010). Speleothems which can have seasonal resolutions (Wang et al., 2001; Dykoski et al., 2005; Johnson et al., 2006; Overpeck and Cole, 2008; Tan et al., 2009; Cai et al., 2010), ice cores which also have seasonal resolutions (Thompson et al., 1989, 2000; Yang, B. et al., 2007) and tree rings which have annual resolutions (Feng et al., 1999; Bräuning and Mantwill, 2004; Liu et al., 2009; Qin et al., 2011) are such archives which are used in the study region. Such studies have demonstrated considerable interannual variability of precipitation patterns, with regard to the timing of monsoonal rains or snowfall controlled by the Westerlies and the range of

the moisture transport (Li and Yanai, 1996; Gadgil, 2003; Yu et al., 2009; Cook et al., 2010). Learning about the palaeo-seasonality across the TP, however, appears to be possible only from a few regions. Speleothems have not been described in detail from the TP. Trees are scarce at such high altitudes and information from tree rings is usually restricted to the last millennium (Bräuning, 2001). Ice cores have been studied from a few regions of the TP representing essential archives for high resolution climate studies across the TP (Thompson et al., 1997; Thompson, 2000; Thompson et al., 2006; Kang et al., 2010; Zheng et al., 2010). Recently, Taft et al. (2012) have demonstrated that another archive can be used to infer information about the precipitation period during the monsoon season and melt water pulses of the pre-monsoon period etc. Sclerochronological analysis of stable oxygen and carbon isotope ratios in the aragonitic shells of the aquatic gastropod *Radix* (Montfort, 1810) provided hydrological and climatic information at sub-seasonal resolution (Taft et al., 2012). A major advantage of the climate archive *Radix* is that its populations are widely distributed in lakes and rivers across the TP (von Oheimb et al., 2011). The fossil record of *Radix* on the TP reaches back to the Miocene (Wu et al., 2001; Wang et al., 2008), potentially opening a long time window for understanding moisture pathway dynamics of the Asian monsoons and the Westerlies. Before fossil shells can be used to infer climate variations of the past, however, additional fundamental research on the new archive is necessary. This paper presents a study of $\delta^{18}O$ and $\delta^{13}C$ patterns in modern *Radix* shells from six lakes of the TP and from one lake of the Pamirs, each representing a different climatic setting, either in relation to the Asian monsoons or to the Westerlies. The aim is to test whether the climatic differences across and beyond the TP are archived in the shells and whether *Radix* shells mirror different lake characteristics in a broad spatio-temporal resolution.

The wide distribution of *Radix* in modern lakes and rivers as well as in Holocene fluvio-lacustrine sediments across Eurasia may open new possibilities for understanding human-environment interactions of the past. The sub-monthly resolution of palaeoclimate signals archived in *Radix* shells can be applied to infer the spatio-temporal variation of palaeo-seasonality which has influenced the livelihood of people and may even have triggered cultural shifts.

3.1.2 $\delta^{18}O$ and $\delta^{13}C$ values in carbonate shells of aquatic gastropods

Shells of continental aquatic gastropods archive oxygen and carbon isotope signals of the ambient water and have been successfully studied to infer environmental and climatic conditions (e.g. Linz and Müller, 1981; Abell, 1985; Abell and Williams, 1989; Hailemichael et al., 2002; Jones et al., 2002; Shanahan et al., 2005; Gajurel et al., 2006; Tütken et al., 2006; Taft et al., 2012). Detailed

analyses along growth increments allow the documentation of seasonal variations in $\delta^{18}O$ and $\delta^{13}C$ values (Fritz and Poplawski, 1974; Dettman et al., 1999; Jones et al., 2002; Gajurel et al., 2006; Taft et al., 2012). In general, the oxygen isotope ratios in the shells reflect the isotopic composition and temperature in the lake water during carbonate precipitation. The $\delta^{18}O$ pattern recorded in a single *Radix* shell over a full life cycle, which lasts approximately one year, mirrors annual hydrological variations which are controlled by distinct climate parameters such as precipitation, evaporation, temperature, humidity, and distinct lake system parameters such as size, depth, water residence time, and water composition of inflows (Taft et al., 2012). Shells originating from monsoon-influenced exorheic lakes exhibit a characteristic monsoonal isotope pattern which is marked by a negative correlation between $\delta^{18}O$ and the amount of rainfall mirroring the "amount effect" in precipitation (Pang et al., 2005; Lee and Fung, 2007; Cai et al., 2010; Liu et al., 2010; Taft et al., 2012).

The carbon in the shell originates from either metabolic carbon or from the surrounding environment (Shanahan et al., 2005). McConnaughey et al. (1997) concluded that carbon in aquatic gastropod shells is made of less than 10 % metabolic carbon and more than 90 % dissolved inorganic carbon (DIC). The $\delta^{13}C$ composition of DIC in a lake is controlled by photosynthesis, decomposition of organic matter, mineralogical substrate, the isotopic composition of inflowing waters, soil carbon and exchange with atmospheric CO_2 (Li et al., 2012). Increasing biological activity during spring and summer leads to more positive $\delta^{13}C$ ratios in the lake water, indicating CO_2 removal by photosynthesis (Henderson et al., 2003; Li et al., 2012). The carbon isotope composition in the lake water and the gastropod shells can thus represent seasonal changes of primary production within the lake. Calcareous rocks in the surroundings of lakes influence the saturation with aragonite, calcite, dolomite and gypsum in the habitat waters which also control the isotopic signature of the DIC. Although the $\delta^{13}C$ composition of DIC cannot be used as a direct indicator for evaporation, strong evaporation increases the lake water salinity, which results in higher $\delta^{13}C$ values through the loss of ^{12}C-enriched CO_2 to the atmosphere in arid areas and closed lakes (Li and Ku, 1997; Henderson et al., 2003; Li et al., 2012).

3.2 Regional setting

On a transect from the Pamirs to the eastern edge of the TP, seven lakes were selected, located at altitudes between ca. 3930 and 5060 m a.s.l. and differing in size, origin, hydrology, and location with respect to the atmospheric circulation (Figure 18 A,B and Table 5). For comparison, data from Bangda Co (30°29'N, 97°04'E, 4450 m a.s.l.) and Kyaring Co (31°09'N, 88°17'E, 4650 m a.s.l.) (Taft et al., 2012) are displayed in Figure 18 A, B and listed in Table 5.
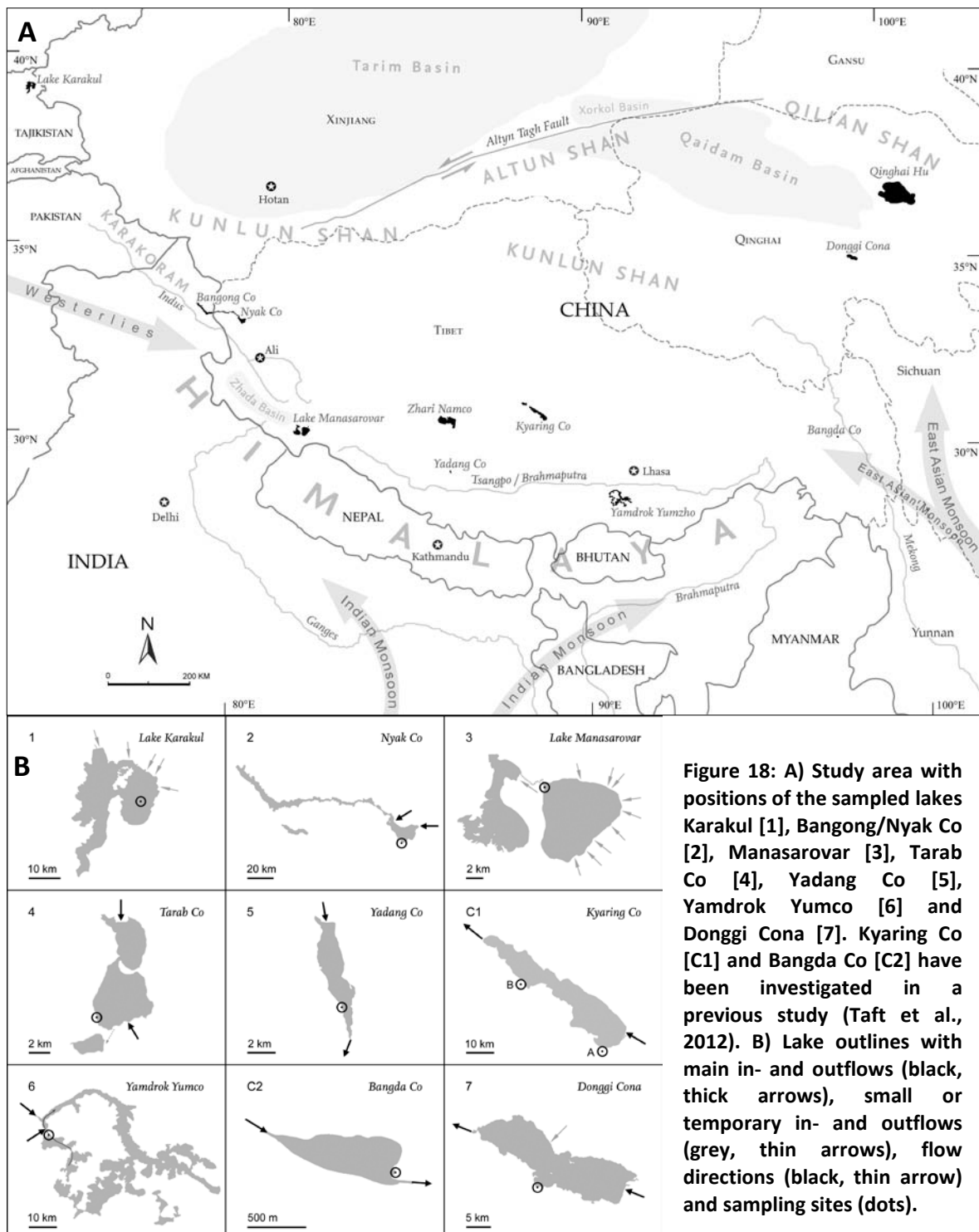
Figure 18: A) Study area with positions of the sampled lakes Karakul [1], Bangong/Nyak Co [2], Manasarovar [3], Tarab Co [4], Yadang Co [5], Yamdrok Yumco [6] and Donggi Cona [7]. Kyaring Co [C1] and Bangda Co [C2] have been investigated in a previous study (Taft et al., 2012). B) Lake outlines with main in- and outflows (black, thick arrows), small or temporary in- and outflows (grey, thin arrows), flow directions (black, thin arrow) and sampling sites (dots).

Lake Karakul in the Pamirs in Tajikistan (39°00'N, 73°30'E, 3928 m a.s.l.) is an endorheic brackish-water lake in a tectonic graben basin, although an origin as a meteorite impact structure has also been proposed (Gurov et al., 1993; Arrowsmith and Strecker, 1999; Robinson et al., 2007). It is located in an area which is influenced by the Westerly wind system and not by the monsoons. Precipitation is generally scarce, 82 mm per year (Mischke et al., 2010b), due to the mountain ranges to the west, which block the Westerly moisture penetration into the lake catchment (Komatsu et al., 2010). With a mean annual temperature of about -4°C, the climate is characterized as cold semi-arid, BSk in the Köppen-Geiger climate classification (Peel et al., 2007). The meteorological data are recorded at a station on the eastern lake shore. From the end of November until the end of May, the lake is covered with ice up to 1 m thick (Mischke et al., 2010b). The main inflows are located on the northern shore of the lake. *Radix* gastropods and water samples were collected from the central part of the eastern basin (Figure 18B) at a water depth of 19.1 m (Table 5).

Nyak Co (33°33'N, 79°55'E, 4250 m a.s.l.) is a freshwater to oligosaline lake, originated from tectonic faulting, and comprises the eastern basin of Bangong Co, the largest lake system of western Tibet (Fontes et al., 1996). Meteorological data are recorded at a station in Ali (also referred to as Shiquanhe, 30°32'N, 80°05'E, 4285 m a.s.l.), ca. 100 km south of the lake. Today, the area is mainly influenced by the Westerlies (Zhang et al., 2011) and convective rainfalls (Fontes et al., 1996), with mean annual precipitation of 70 mm (data from 1961 until 2009; Chinese Central Meteorological Office, 2010). However, exceptional strong and spatially extended monsoon rainfalls sometimes penetrate into this region because of its position close to the normal maximum northward extent of the Indian Summer Monsoon (Gasse et al., 1991; Fontes et al., 1996; Wu et al., 2006; Tian et al., 2007). The mean annual air temperature is 0.6°C (data from 1961 until 2009; Chinese Central Meteorological Office, 2010) and the climate is characterized as cold-dry, BWk (Peel et al., 2007). The ice cover period on the surface of the lake is unknown, and therefore a time span from November to April has been estimated on the basis of a study of Lin et al. (2011) who observed alpine tundra lakes in Beiluhe Basin, central TP. Wang and French (1995) note that the lake is located in a permafrost region. The main inflows are located at the northeastern shore. The gastropod and water samples were taken from the easternmost shore of the lake (Figure 18B) at a water depth of 0.5 m (Table 5).

Lake Manasarovar (30°45'N, 81°22'E, 4595 m a.s.l.), also referred to as Mapam Yumco (Murphy and Burgess, 2006; Murphy et al., 2010), is a freshwater lake located between the Himalaya Mountains and the Gangdisi Mountains in the southwestern part of the TP. The lake has an ephemeral outlet to its adjacent lake Langa Co, which is located 8 km westwards. Lake

Manasarovar originated from tectonic faulting (Murphy and Burgess, 2006; Yao et al., 2009) and lies within a zone of sporadic plateau permafrost (Wang and French, 1995). The main inflows are located in the north and northeastern region of the lake. The lake water has a long residence time and thus is characterized by intensive evaporation (Yao et al., 2009). The mean annual precipitation is 125 mm and the mean annual temperature is 3.6°C at Pulan County, approximately 40 km southwest of the lake (Yao et al., 2009). The climate is characterized as Dwb-climate in the Köppen-Geiger climate classification (Peel et al., 2007). An ice cover period can be assumed for November to April (Lin et al., 2011). The region is influenced by precipitation from varying sources, but rainfall is concentrated in August (Yao et al., 2009). Samples were taken from the northwest lake shore (Figure 18B) at a water depth of 0.5 m (Table 5).

Tarab Co (32°26'N, 83°12'E, 4450 m a.s.l.) is a small endorheic lake located on the central TP in a semi-arid region, Dwb-climate (Peel et al., 2007), where high mountains surrounding this area block moisture transport from the west and the south (Tian et al., 2007). Meteorological data are recorded at a station in Gaize (32°18'N, 84°03'E, 4430 m a.s.l.), 80 km east of the lake. Most of the sparse rainfall is concentrated in July and August (data from 1952 until 2009, Chinese Central Meteorological Office, 2010) provided by a small number of storm events which transport moisture originating from the Indian Monsoon onto the TP (Tian et al., 2007) The mean annual precipitation is 173 mm and the mean annual temperature is -7.5°C (data from 1952 until 2009, Chinese Central Meteorological Office, 2010). An ice cover period from November to April can roughly be inferred after Lin et al. (2011). The lake has two main inflows, from the north and southeast and is located in a zone with widespread plateau permafrost (Wang and French, 1995). Many beach ridges, primarily at the eastern part of the basin, are evidence of former higher lake levels. *Radix* and water samples were collected in the southern part of the lake (Figure 18B) at a water depth of 0.1 m (Table 5).

Yadang Co (29°39'N, 85°44'E, 5060 m a.s.l.) is located in the southern part of the central TP which is mainly influenced by monsoon rainfalls, concentrated in July and August. The climate is characterized as BWk (Peel et al., 2007). The exorheic lake is located north of the Yarlung Tsangpo (Brahmaputra) River valley, one of the pathways of the Indian Monsoon moisture onto the TP (Tian et al., 2007). The mean annual precipitation recorded from a station 200 km east of Yadang Co (in Lhatse, 29°04'N, 87°38'E, 4030 m a.s.l.) is 277 mm and the mean annual temperature is -3.7°C (data from 1959 until 2009, Chinese Central Meteorological Office, 2010). The main inflow is located on the northern shore of the lake, which lies within a zone of widespread permafrost (Wang and French, 1995). After Lin et al. (2011), the ice cover period is assumed to be from

November to April. The samples were taken in the central western part of the lake (Figure 18B) at a water depth of 0.3 m (Table 5).

Yamdrok Yumco (29°02'N, 90°25'E, altitude of terminal basin 4437 m a.s.l.) is a lake system located on the southern TP, south of the Yarlung Tsangpo (Brahmaputra) Valley at the northern edge of the Himalayan Mountains. The lake system consists of several exorheic interconnected lakes which terminate in a large closed basin (see Figure 18B). The catchment area is drained by several rivers, which are located in the east, southeast and west (Tian et al., 2008). About 90% of the annual rain falls from June to September due to the influence of the Indian Summer Monsoon (Tian et al., 2008). Mean annual precipitation is 378 mm and the average annual temperature is 3.3°C at Langkazi meteorological station located at 28°58'N, 90°24'E and 4460 m a.s.l. on the western shore of the terminal lake basin (data from 1991-2007, Chinese Central Meteorological Office, 2010). The climate is characterized as cold-dry, Dwb (Peel et al., 2007). The lake is covered with ice from November until March (Tian et al., 2008) and is located within a zone of alpine permafrost (Jin et al., 2000). Liu (1995) reported that the annual lake level variation is within 0.6 meters and calculated a lake level fall of 0.6 meters for the last 100 years. Yamdrok Yumco is an important place for migrating and wintering waterfowl (Lang et al., 2007). The samples come from the western part of the terminal basin (Figure 18B) and were collected at a water depth of 0.3 m (Table 5).

Donggi Cona (35°15'N, 98°30'E, 4090 m a.s.l.) is an exorheic freshwater-lake which is located in a pull-apart basin at the northeastern margin of the TP (Van der Woerd et al., 2002; Dietze et al., 2010; Mischke et al., 2010a). Mean annual precipitation at Madoi, approximately 50 km southwest of the lake (34°55'N, 98°13'E, 4272 m a.s.l.), is 304 mm and the mean annual air temperature is -4.1°C (data from 1959 until 2009, Chinese Central Meteorological Office, 2010); the climate is characterized as BWk (Peel et al., 2007). The lake is covered with ice from November to April (Mischke et al., 2010a). The area is located close to the maximum western limit of the East Asian Monsoon trajectories (Zhang et al., 2011) and lies within a zone of discontinuous permafrost (Dietze et al., 2010). Ancient shorelines and erosional terraces document fluctuations in the hydrological balance in the past (Dietze et al., 2010; Mischke et al., 2010a). The main inflows come from the north and east (Dietze et al., 2010). *Radix* specimens and water samples were collected at the centre of the southern shore (Figure 18B) at a water depth of 0.3 m (Table 5).

Table 5: Characterizing parameters of studied lakes and *Radix* sampling localities. Data for Kyaring Co and Bangda Co are presented in Taft et al. (2012).

	Lake Karakul	Nyak Co	Lake Manasarovar	Tarab Co	Yadang Co	Kyaring Co	Yamdrok Yumco	Bangda Co	Donggi Cona
	[1]	[2]	[3]	[4]	[5]	[C1]	[6]	[C2]	[7]
Locality	39°00'N, 73°30'E	33°33'N, 79°55'E	30°45'N, 81°22'E	32°26'N, 83°12'E	29°39'N, 85°44'E	31°10'N, 88°10'E	29°02'N, 90°25'E	30°29'N, 97°04'E	35°15'N, 98°30'E
altitude (m a.s.l.)	3928[a]	4250	4595	4450	5060	4650	4437	4450	4090
Surface area (km²)	380[b]	225	412[d]	28	12	660	621[e]	0.3	229[f]
System	endorheic	endorheic	semi-endorheic	endorheic	exorheic	exorheic	semi-endorheic	exorheic	exorheic
Origin	tectonic	tectonic	tectonic[g]	fluvial?	fluvial?	tectonic	tectonic	dammed river lake	tectonic
Max. depth (m)	238[b] (western sub-basin)	~ 40[c]	n.d.	n.d.	n.d.	n.d.	55[e]	n.d.	92[f]
Dominant atmosph. system	W + regional	W +AM	AM + regional	AM	regional	AM	AM	AM	AM
Date of sampling	July 5, 2008	Sept 24, 2009	Sept 19, 2009	Oct 02, 2010	Oct 02, 2009	Sept 14, 2008	Sept 08, 2008	Sept 27, 2008	Oct 05, 2008
Trophic level	oligotrophic	oligo-mesotrophic	oligotrophic	oligotrophic	oligotrophic	oligotrophic	oligo-mesotrophic	oligotrophic	oligotrophic
Water depth at sampling point (m)	19.1	0.5	0.5	0.1	0.3	0.3	0.3	0.3	0.3
water temperature (°C)	9.7 - 13.2[a]	12.4[1]	11.9[1]	9.1[1]	4.5[1]	13.3[1]	17.6[1]	15.1[1]	19.8[1]

[1] Water data refers to *Radix* sampling localities

[a] Mischke et al. (2010b)

[b] Komatsu et al. (2010)

[c] Dortch et al. (2011)

[d] Yao et al. (2009)

[e] Tian et al. (2008)

[f] Dietze et al. (2010)

[g] Yao et al. (2009)

W = Westerlies

AM = Asian Monsoons

3.3 Ecological and biological traits of the gastropod *Radix*

The diversity of aquatic invertebrates in the harsh TP environments is generally very low. However, the pulmonate gastropod *Radix* (Figure 19) is widely distributed on the TP, living in freshwater and oligohaline to mesohaline water bodies and belongs to the few continental gastropod taxa which inhabit extreme boreal and arctic environments (Clarke, 1973; Økland, 1990; White et al., 2008). The intrageneric diversity of *Radix* on the TP and its surrounding regions has been analyzed by von Oheimb et al. (2011).

Figure 19: Shell of *Radix*, example from Lake Manasarovar.

The preferred habitats are calm, shallow waters in both lacustrine and riverine environments (Økland, 1990; Glöer, 2002). The life span of *Radix* species is approximately one year (Young, 1975; Walter, 1977; Glöer, 2002). Taft et al. (2012, and references therein) compiled further information about the biology and the life cycle of *Radix.*

The individuals either remain active under the ice cover of lakes during the winter months (e.g. Frömming, 1956; Glöer, 2002) or move from the shallow littoral area to deeper water (Burla, 1972; Gaten, 1986). The shell growth does not cease during the winter but is much slower. Gaten (1986) observed a winter growth rate of 0.35 mm per month. There is no shut-down temperature for accretion of shell carbonate and, concerning the isotope values, there is no significant secondary thickening of the shell, which means that there is no temporal mix-signal. Thus, each shell section represents a clearly defined growth period.

3.4 Materials and methods

3.4.1 Sampling

Living *Radix* specimens from the TP were collected near the shores of the lakes in shallow water (< 0.5 m) during three field trips (August - October 2008, 2009 and September - October 2010) to the eastern, central and western part of the TP (von Oheimb et al., 2011) (Figure 18A, B). Living specimens from Lake Karakul were collected in July 2008 at a water depth of 19.1 m with a Hydro-Bios-Ekman mud grab (Mischke et al., 2010b).

The gastropods were preserved in 80% ethanol in the field. At the sampling localities, the temperature, pH value and specific conductivity of the habitat water were determined using a Hach® HQ 40d multiparameter instrument. The inorganic chemical composition of the ambient water was analyzed at the Free University of Berlin. The water chemistry was processed with AquaChem 5.1.

This study is linked to investigations at the Justus-Liebig-University in Giessen where genetic studies of *Radix* specimens have been conducted by von Oheimb et al. (2011), who described different clades but did not indicate species names. The term *Radix* sp. is therefore used. Specimens from the lakes Yamdrok Yumco, Manasarovar, Yadang Co and Nyak Co belong to Clade 2 and specimens from Tarab Co and Donggi Cona belong to Clade 9 (von Oheimb et al., 2011). *Radix* specimens from Lake Karakul have been identified as *Radix auricularia* (Linnaeus, 1758).

Shells of genetically analyzed specimens (for example see Figure 19) were sent to Berlin where they were cleaned, prepared and sampled for isotopic measurements (see Taft et al., 2012). The sampling was carried out at a constant distance of 1 mm between the samples and along the ontogenetic spiral of growth increments using a dental drill, starting with the latest shell part at the aperture. Depending on shell size and total number of whorls, 14 to 31 samples per shell were obtained (Table 6).

Table 6: Overview of analyzed *Radix* shells

Shell code	DNA lab number	Lake (site)	Height / Width in cm	n whorls	n samples
Kar1	11551	Lake Karakul	1.22 / 0.75	4.1	15
Kar2	11552	Lake Karakul	1.37 / 0.84	4.6	18
NyCo1	12047	Nyak Co	1.57 / 0.97	3.7	24
NyCo2	12068	Nyak Co	1.43 / 1.11	3.95	23
Manas1	12062	Lake Manasarovar	1.46 / 0.95	4.15	26
Manas2	not completed	Lake Manasarovar	1.52 / 1.06	3.8	24
TaCo1	15126	Tarab Co	0.9 / 0.6	4.0	16
TaCo2	15127	Tarab Co	1.08 / 0.73	4.3	20
YaCo1	not completed	Yadang Co	2.19 / 2.09	2.8	31
YaCo2	not completed	Yadang Co	1.97 / 1.7	3.25	25
YaYu1	11111	Yamdrok Yumco	1.97 / 1.54	4.1	26
YaYu2	10051	Yamdrok Yumco	1.84 / 1.06	3.75	18
DoCo1	10069	Donggi Cona	1.03 / 0.91	4.0	15
DoCo2	10070	Donggi Cona	0.97 / 0.64	3.8	14

3.4.2 Isotopic analysis

Carbonate samples Kar1, Kar2, YaYu2, DoCo1 and DoCo2 (Table 6) were isotopically analyzed in the laboratory at the Free University in Berlin, using a GasBench II linked to a MAT-253 ThermoFisher Scientific™ Isotope Ratio Mass Spectrometer. The external error of the measurements is ±0.06 ‰ for $\delta^{18}O$ and ±0.04 ‰ for $\delta^{13}C$ both 2 SD (standard deviations) based on the reproducibility of the in-house reference material Laaser Marble. The measurements were standardized against Cararra Marble (CAM) and Kaiserstuhl carbonatite in-house reference material (KKS) which had been calibrated against Vienna PeeDee Belemnite (V-PDB) international isotope reference material NBS-19 and NBS-18. The other samples were analyzed at the GFZ (GeoForschungsZentrum) Potsdam, using a Gas Bench II linked to a DELTAplusXL ThermoFisher Scientific™ Isotope Ratio Mass Spectrometer. Replicate analysis of reference material NBS19 reported relative to the Vienna PeeDee Belemnite standard (V-PDB) yielded standard errors of ±0.06 ‰ for $\delta^{18}O$ and ±0.04 ‰ for $\delta^{13}C$ both given in 2 SD. All results are reported in δ notation relative to V-PDB.

The lake water samples were isotopically analyzed in the laboratory at the Free University in Berlin, using a GasBench II linked to a MAT-253 ThermoFisher Scientific™ Isotope Ratio Mass Spectrometer. The external error of the measurements is ±0.012 ‰ for $\delta^{18}O$ and ±2.5 ‰ for δD both 2 SD based on the reproducibility of the in-house reference material Feth-2. Measurements were standardized against Talo Dome (TD) and Alboran Seewater (ASW) in-house standards which had been calibrated against Vienna Standard Mean Ocean Water (V-SMOW) and Vienna Standard Light Antarctic Precipitation (V-SLAP). All results for the water samples are reported in δ notation relative to V-SMOW.

3.4.3 Meteorological data

Meteorological data of the sampling years from the Chinese Central Meteorological Office (2010) were used for comparing the isotope patterns in the shells with meteorological conditions. In cases where meteorological stations are not located in the lake drainage system, data from the nearest stations were used. Temperature and precipitation data were recorded as 10-day average values for stations on the TP. For Lake Karakul, only monthly average values were available (Figure 20).
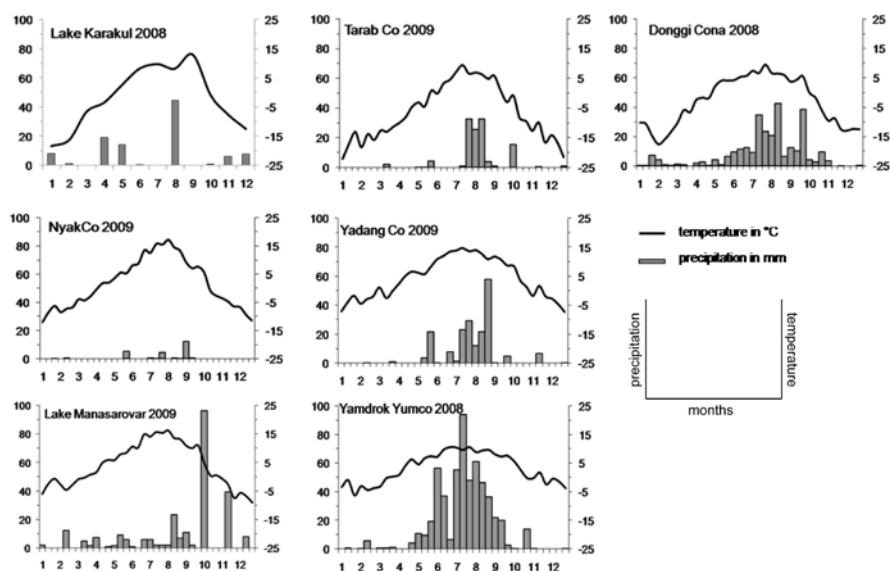
Figure 20: Meteorological data for the lakes obtained from nearest weather stations. The data correspond to the particular sampling year and are expressed in 10-day average values. The meteorological data for Lake Karakul represent monthly average values.

3.5 Results and discussion

3.5.1 Water properties

The lake water properties are compiled in Figure 21 and Figure 22.

Most of the samples have a dominance of Mg and/or Na, except the waters from Yadang Co and Yamdrok Yumco which are Ca dominated. Lake Karakul is the only lake without HCO_3^- as a dominant species, due to the high salinization. A unique property of most waters is the supersaturation of dolomite, calcite and aragonite. Gypsum is always undersaturated even in the brackish Lake Karakul.
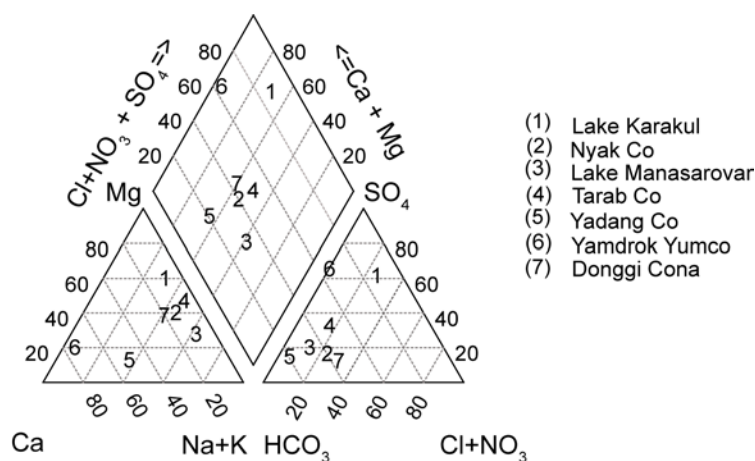
Figure 21: Piper Plot of major anions and cations for the lake waters.

The only two lakes with undersaturation of carbonate are those with a low specific conductivity of 140 µS·cm^{-1} (Yadang Co, for all carbonates) and 430 µS·cm^{-1} (Tarab Co, for aragonite only) and more importantly with the lowest pH of all samples (Table 7). Considering that rainfall in equilibrium with normal partial pressure of CO_2 (without components of acid rain) has a pH of about 5.6, these waters had the shortest contact time with the rocks or contact with the least soluble rocks. They are not buffered enough to have carbonate oversaturation.

Table 7: Chemical properties of the studied lakes.

Locality	Electrical conductivity (µS/cm^{-1})	PSU	pH	K$^+$ mg/l	Na$^+$ mg/l	Mg^{2+} mg/l	Ca^{2+} mg/l	Sr^{2+} mg/l	HCO$_3^-$ mg/l	Cl$^-$ mg/l	NO$_3^-$ mg/l	SO$_4^{2-}$ mg/l
Karakul	10300	7.5	9.2	160	1014	1211.5	165	0.3	830	1297	0.0	4520
Nyak Co	913	0.7	8.8	9	103	53	30	0.3	330	93	0.0	79
Lake Manasarovar	688	0.5	10.4	63	112	36	16	0.3	336	44	0.0	87
Tarab Co	430	0.3	8.4	29	315	165	7	0	671	180	0.2	420
Yadang Co	142	0.1	7.4	2	12.5	2	17	0.1	77	4	0.2	13
Yamdrok Yumco	353	0.3	9.0	2	4	10	56	0.5	79	0.5	0.0	127
Donggi Cona	711	0.5	8.9	5	66.5	36	28	0.4	268	90	0.0	57

Based on the high δ^{18}O and δD values of the lake waters (Figure 22), it is clearly visible that Lake Karakul, Nyak Co and Lake Manasarovar have the character of large closed water bodies with a relatively long water residence time. These lakes are located in arid regions and are strongly influenced by evaporation, which leads to a relative enrichment of δ^{18}O in the lake waters. The values for the lake water of Donggi Cona range around this group as well, but this lake has an outflow. Donggi Cona is a large and deep water body and the water has a relatively long residence time. The large surface of the lake is also highly influenced by evaporation. The low values for Yadang Co, Kyaring Co and Bangda Co indicate open lakes with a high discharge and a relatively short water residence time. These lakes are located in regions which are influenced by monsoon precipitation and glacier and melt water run-off. Although Kyaring Co for example has also a large surface, the isotope values suggest little influence of evaporation (Taft et al., 2012). Alternatively, it is overprinted by the isotopic signal of precipitation. The δ^{18}O and δD values for the lake water of Yamdrok Yumco are between these two groups. Most likely the complex character of this lake (see Regional Setting) causes this ambiguous signal. The lake is a closed water body but the exorheic sub-basins have the character of open lakes.

In summary, based on the δ^{18}O and δD values of the lake waters, one can distinguish between the lakes located in the more arid western part and the lakes located in the eastern part of the TP. Furthermore, the isotope values allow the classification of open and closed basins.
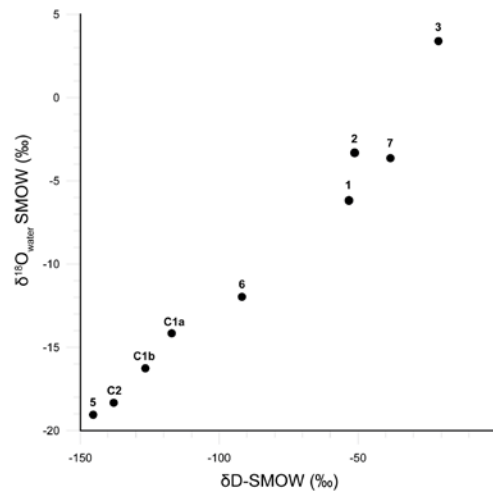
Figure 22: δ^{18}O and δD of the lake waters: [1] Lake Karakul, [2] Nyak Co, [3] Lake Manasarovar, [5] Yadang Co, [6] Yamdrok Yumco, [7] Donggi Cona, [C1] Kyaring Co, [C2] Bangda Co. Data for Tarab Co could not be detected. Further details in Weynell et al. (in prep.)

3.5.2 δ^{18}O and δ^{13}C patterns of Radix shells

The approximate life spans result from the date at the latest shell section [a] which is exactly known and the hatching date at the embryonic shell section (protoconch) which is estimated based on seasonal meteorological changes and ice cover periods which are mirrored in the isotope patterns of the shell carbonate.

3.5.2.1 Lake Karakul

The isotopic patterns of two *Radix* shells are displayed in Figure 23.

Shell Kar1: The range of δ^{18}O values is from -1.60 to -0.45 ‰ and the average value is -1.23 ‰. The slight increase of δ^{18}O values from -1.50 ‰ [c] to -0.45 ‰ [a] indicates the evaporation in June when no rainfall occurred and the solar radiation is high. Although evaporation starts directly when the ice cover on the lake disappears in May, this effect is not visible in the δ^{18}O shell pattern between [g] and [c] which mirrors the time period between May and June. This may be due to the fact that melt water from the surrounding glaciers, which have lower oxygen isotope values than the lake water, dominate the pattern during this phase. From [k] to [h] the δ^{18}O values are the lowest (-1.36 to -1.60 ‰). This period may reflect the time when the lake surface was covered by ice up to 1 m thick from the end of November until May (Mischke et al., 2010b). The shell section between [k] and [h] mirrors a longer time period than does the shell part from [g] to [a]. This is due to decelerated shell growth during the winter months compared to the warmer season

67

(Gaten, 1986; Taft et al., 2012). Most likely, slightly decreasing values from [o] to [n] from -0.67 to -1.18 ‰ mark the difference between an encapsulated embryo and a hatchling.

$\delta^{13}C$ values ranges from -1.76 to -0.65 ‰ and the average value is -1.23 ‰. The little variation of 1.11 ‰ is an indicator that the amount and isotopic composition of HCO_3^- which the specimen used for shell accretion remained constant throughout the life cycle (Leng et al., 1999). The carbon isotope pattern is very similar to the oxygen pattern in most parts of the shell. Because the vegetation in the catchment is restricted to some cold- and drought-tolerant plants and soil formation is reduced, the $\delta^{13}C$ range of the lake water and therefore in the *Radix* shell mainly reflects lake productivity by phytoplankton and authigenic carbonate formation. Thus, the slight increase of $\delta^{13}C$ from -1.76 ‰ [g] to -0.65 ‰ [a] indicates increasing lake productivity, which implies preferential uptake of ^{12}C by phytoplankton, between May and July. Small variations in $\delta^{13}C$ between -1.26 ‰ [n] and -0.98 ‰ [l] cannot be attributed to particular parameters. The life span of this specimen is from ~ October 2007 before the lake was covered by ice to 5th July 2008. Hence, the age of Kar1 was around nine months when it was collected.
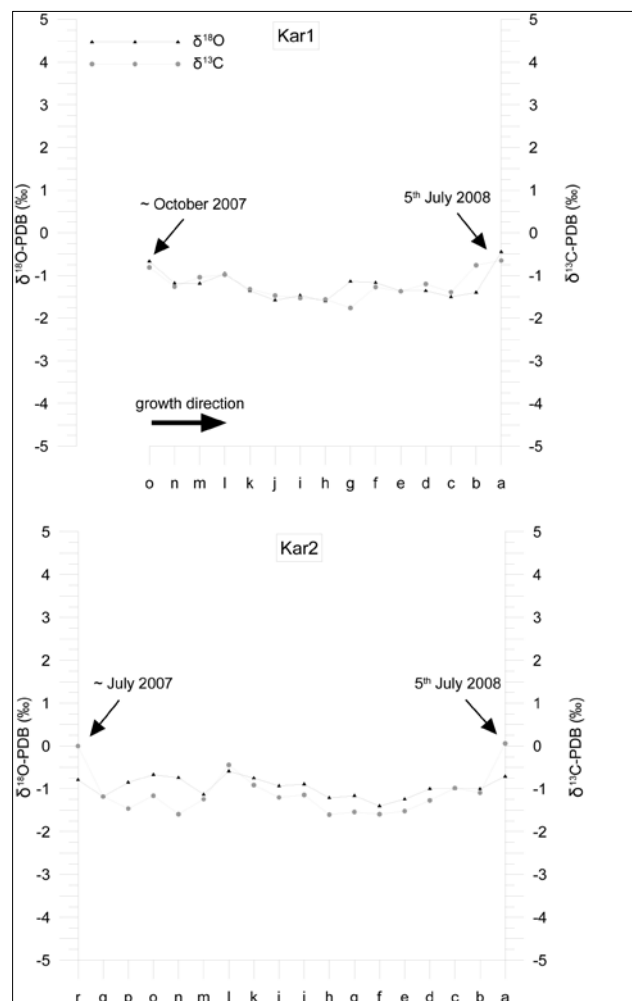
Figure 23: $\delta^{18}O$ and $\delta^{13}C$ shell patterns of two *Radix* specimens from Lake Karakul.

Shell Kar2: The δ^{18}O range is from -1.40 ‰ to -0.59 ‰ and thus in a very similar range as the values of Kar1. The average oxygen isotope value is -0.96 ‰. The pattern covers a longer time span because shell Kar2 has more whorls than Kar1 (Table 6) and the values at the protoconch [r] are comparable to those of the aperture [a] indicating that a complete annual hydrological cycle is archived.

The δ^{13}C values of shell Kar2 also show very little variation and range between -1.60 ‰ [h] and 0.06 ‰ [a]. The average value is -1.10 ‰. The slight increase from -1.52 ‰ [e] to 0.06 ‰ [a] probably shows increasing lake productivity between May and July when the ice cover on the lake had disappeared. The carbon isotope values from the protoconch [r] to sample [n] reflect the time between hatching in July 2007 and ice covering of the lake in November 2007. The life span is defined to be approximately one year from ~ July 2007 to 5th July 2008.

In summary, the patterns show only very little isotope variations during the life span of the gastropods which indicates that the specimens lived in a habitat with relatively constant conditions. The *Radix* specimens were sampled from a water depth of 19 m where more constant conditions prevail than in shallow water habitats. The patterns represent thus a characteristic "lake pattern" and mirror long-term conditions rather than short-term (sub-seasonal) changes contrary to the other lakes with sample depths of 0.1-0.5 m. Hence, these data sets are hardly comparable but present suitable information about climatic trends.

The δ^{18}O "lake-pattern" is not primarily controlled by precipitation or temperature, but by evaporation (high absolute values). Also the relatively high δ^{18}O$_{water}$ value of -4.0 ‰ and the absent outflow point to a system which is rather influenced by evaporation. The lake is large enough and well enough mixed to average out the short-term variations (Leng and Marshall, 2004). High Na, HCO$_3$ and Cl contents in the lake water also indicate high evaporation. The high similarity between δ^{18}O and δ^{13}C values in both shells depends on the buffering effect of total CO$_2$ on the δ^{13}C composition of the lake water, vapour exchange, enhanced evaporation and productivity and can be an indicator for a closed brackish-saline lake (Talbot, 1990; Li and Ku, 1997; Leng and Marshall, 2004).

3.5.2.2 Nyak Co

The isotopic patterns of two *Radix* shells are displayed in Figure 24.

Shell NyCo1: The range of δ^{18}O is from -2.81 to -1.39 ‰ and the average value is -2.18 ‰. The lake water in the *Radix* habitat had a value of -4.34 ‰ at the sampling date which means that it is

strongly enriched in[18]O by evaporation. The small variation of 1.42 ‰ during the life span of this specimen indicates a habitat with comparatively constant conditions. The shell pattern phase from [n] to [j] probably reflects the period when the lake was covered by ice between November and April.

The range of δ^{13}C in NyCo1 is from -4.97 to -0.63 ‰ and the average value is -2.35 ‰. Continuously increasing carbon isotope values from -4.97 ‰ [k] to -0.76 ‰ [a] mirror most likely increasing lake productivity from April to September. Based on the assumption that the habitat is completely covered by ice from November on, the δ^{13}C value at [r] reflects the water composition at the beginning of October 2008. Consequently, specimen NyCo1 had lived for more than one year and hatched around July 2008, when the isotope composition in the shell was similar to shell section [d] to [c].
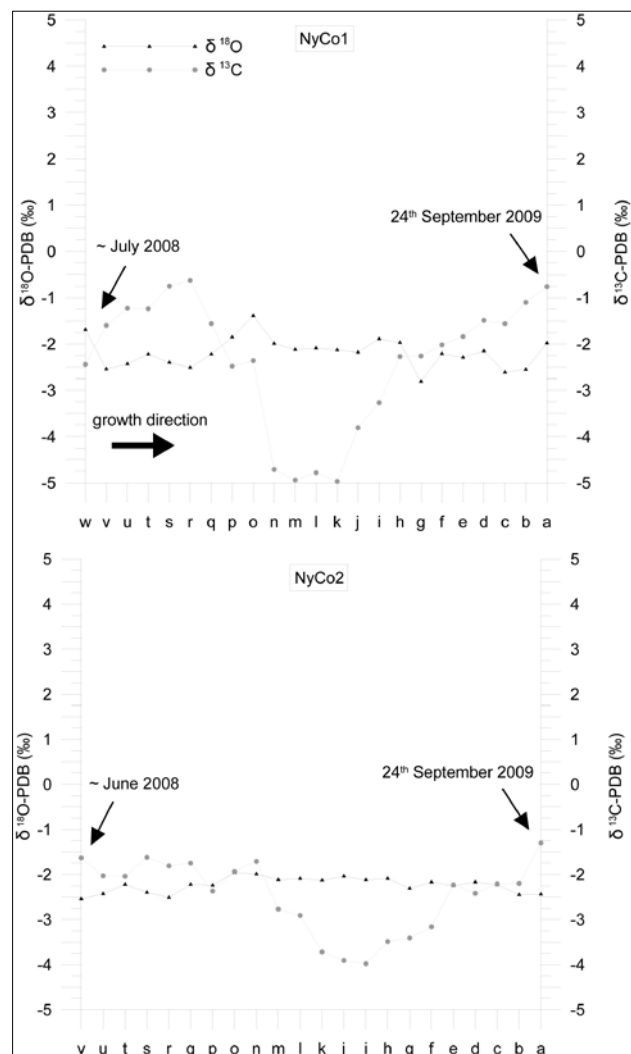
Figure 24: δ^{18}O and δ^{13}C shell patterns of two *Radix* specimens from Nyak Co.

Shell NyCo2: The range of δ^{18}O is from -2.54 to -1.96 ‰, the average value is -2.23 ‰ and hence in the same range as the values of shell NyCo1. The absolute variability is even lower and within

70

0.59 ‰. This means that the habitat water conditions were constant during the whole life span of this specimen.

The range of $\delta^{13}C$ is from -3.98 to -1.30 ‰ and the average value is -2.48 ‰. The variability is lower than in shell NyCo1. The striking signal in this pattern is the decrease from -1.71 ‰ [n] to -3.98 ‰ [i] and the following gradual increase to -1.30 ‰ [a] which marks the same period as the $\delta^{13}C$ signal [r] to [a] in the shell pattern from NyCo1. This section probably represents again the phase of reduced lake productivity between the end of October 2008 and April 2009 and the following period with increasing productivity until September 2009. The life span is from ~ June 2008 to 24th September 2009.

The fact that the variability in both isotope compositions is lower compared to NyCo1 indicates slight differences between the habitats. In summary, both $\delta^{18}O$ shell patterns show only very little seasonal variation, which is characteristic of a lake with a long water residence time, probably several decades. Only the $\delta^{13}C$ patterns indicate a seasonal defined change in photosynthesis by aquatic organisms caused by the preferential uptake of the lighter isotope ^{12}C, leaving the TDIC (total dissolved inorganic carbon) relatively enriched in ^{13}C during the period without ice covering. The shell pattern phase from [n] to [j] in NyCo1 which presents the ice cover period from November to April is marked by constant $\delta^{18}O$ values and synchronously decreasing $\delta^{13}C$ values due to the reduction in biological productivity.

3.5.2.3 Lake Manasarovar

The isotopic patterns of two *Radix* shells are displayed in Figure 25.

Shell Manas1: The range of the oxygen isotope values is from -1.80 to 0.71 ‰ and the average value is -0.70 ‰. From the latest shell section [a] to sample [e], the values vary only between -1.42 and -1.68 ‰. From [f] to [s], the pattern is plateau-like with a clear trend towards lighter values in a range between 0.71 and -0.80 ‰. Subsequently the values decrease again to -1.34 ‰ [t] and remain constant to the protoconch [z] which has a value of -1.31 ‰. Concerning the shell size, the number of whorls (Table 6) and the isotope values at the aperture [a] and the protoconch [z], we assume a life span of ca. one year of this specimen. Therefore, decreasing values from 0.71 ‰ [g] to -1.42 ‰ [a] reflect the period between August 2009 and the sampling date. The decrease might be caused by an interaction of melt water input from the glaciers located to the south, precipitation and river waters, which all exhibit more negative $\delta^{18}O$ values than the lake water which has a $\delta^{18}O_{SMOW}$ value of 3.39 ‰. Precipitation concentrates in August

with an average $\delta^{18}O_{SMOW}$ value of -14.42 ‰ and the rivers have an average value of -14.95$_{SMOW}$ ‰ during this time (Yao et al., 2009). Slightly increasing values from -0.80 ‰ [o] to 0.70 ‰ [g] indicate the time from the end of May until the end of July when the isotope composition of the lake water is mainly controlled by evaporation due to increasing temperatures and solar radiation. After the ice cover disappeared in late April, the pattern shows a slight decrease from -0.39 ‰ [q] to -0.80 ‰ [o] which probably corresponds to an increase in temperature of about 1.5°C after the equation of Dettman et al. (1999). The short shell section between [s] and [q] was most likely built during the winter period from November until April, when shell accretion decelerated. Decreasing temperatures between October and November caused increasing $\delta^{18}O$ values from -1.77 ‰ [v] to 0.06 ‰ [s]. From the protoconch [z] to sample [v], the pattern mirrors the period from late August to the end of September 2008.

The range of $\delta^{13}C$ in shell Manas1 is from -3.50 to 3.11 ‰ and the average value is -0.56 ‰. This pattern exhibits a large variability indicating a) sub-seasonal changes in carbon input, and b) varying portions of different carbon sources. Highest values in August and September 2009 from 1.62 ‰ [e] to 3.11 ‰ [a] mirror the highest annual biological productivity in the lake. Lowest values were measured in the shell section between [j] and [g] which range between -3.50 and -3.14‰. This indicates an input of dissolved inorganic allochthonous carbon into the habitat of this specimen in June and July, transported by glacial melt waters. Possibly the drop from -1.19 ‰ [o] to -3.45 ‰ [n] is also caused by melt waters which transport a first inflow of dissolved inorganic carbon into the lake. Decreasing $\delta^{13}C$ values from 1.38 ‰ [u] to -1.53 ‰ [q] mirror decreasing lake productivity, caused by decreasing temperatures and the onset of ice cover on the lake. Between the protoconch [z] and section [u], the pattern varies between 1.72 and 1.38 ‰. This specimen lived ca. one year, from the end of August 2008 to 19th September 2009.
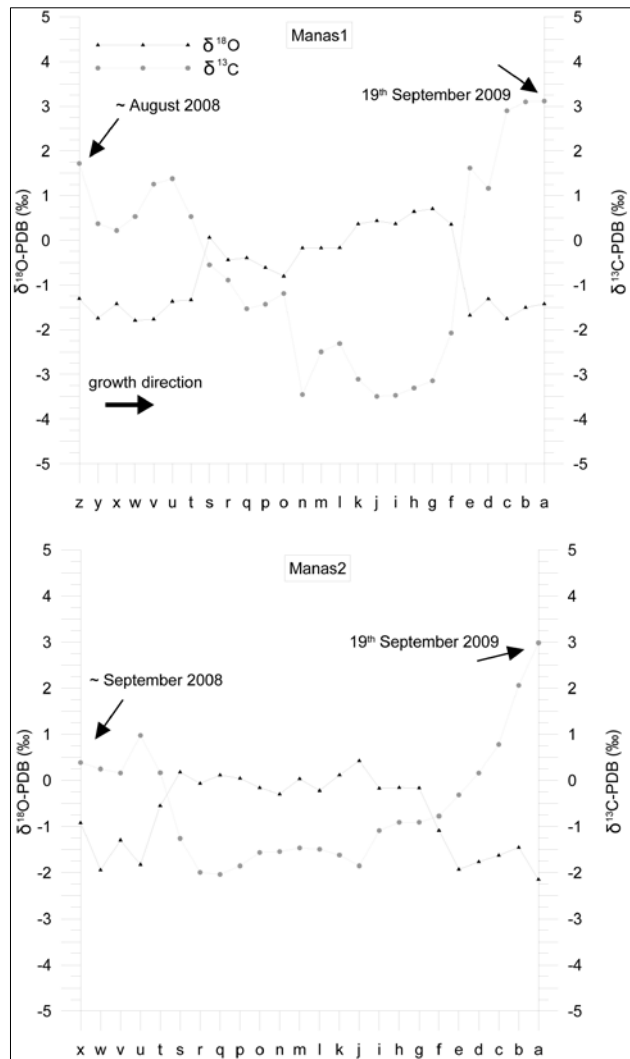
Figure 25: δ^{18}O and δ^{13}C shell patterns of two *Radix* specimens from Lake Manasarovar.

Shell Manas2: The δ^{18}O values vary between -2.15 and 0.42 ‰ and the average value is -0.70 ‰. The pattern of the values is very similar to that of shell Manas1, indicating that these specimens spent their lives in similar habitats. Due to the smaller shell size of Manas2, the lower number of whorls and the slightly different isotope values at the protoconch, this specimen hatched somewhat later than specimen Manas1. The hatching date was ca. September 2008, before the lake surface was covered by ice.

δ^{13}C in shell Manas2 varies between -2.04 and 2.98 ‰ and the average value is -0.53 ‰. Similar to shell Manas1, most negative values occur between [r] and [p] from -1.99 to -1.85 ‰ and reflect the period when the lake surface was ice covered. From [j] to [a] the values increase continuously from -1.85 to 2.98 ‰ which mirrors an increase in biological productivity. Although the oxygen isotope patterns indicate the same habitat of the two gastropods, the micro-habitats seem to

diverge due to the slightly different $\delta^{13}C$ pattern. The life span is approximately one year, from September 2008 to September 19th 2009.

In summary, the high $\delta^{18}O$ values of the shell patterns indicate high evaporation rates and a long residence time of the lake water, which is also supported by a $\delta^{18}O_{water}$ value of 3.23 ‰ and a δD value of -21‰ . The noticeable evaporative characteristic of Lake Manasarovar has already been confirmed by Yao et al. (2009). They reported an average $\delta^{18}O$ value of the lake water of -5.52 ‰ and an average δD value of -60.04 ‰ in August 2004 and 2005. Based on the variability of the shell patterns, the habitat water reflects both sub-seasonal changes which are in particular triggered by glacial melt water input, ice cover and biological productivity, and evaporation. Most positive $\delta^{13}C$ values in both shell patterns indicate high biological lake productivity during the warmest months from July to September. The isotope shell patterns show a clear signal of a closed basin, although Lake Manasarovar is a temporarily morphologic exorheic basin due to its ephemeral outlet to its adjacent lake Langa (Figure 18B). The shell patterns suggest that this outlet was not active during the life spans of the gastropods.

3.5.2.4 Tarab Co

The isotopic patterns of two *Radix* shells are displayed in Figure 26.

Shell TaCo1: The range of $\delta^{18}O$ is from -13.43 to -11.52 ‰ and the average value is -12.39 ‰. Most negative values occur between -13.34 ‰ [g] and -13.43 ‰ [f] and mirror the precipitation maximum in late August which is isotopically influenced by moisture from the Indian Summer Monsoon onto the TP (Tian et al., 2007). The depletion of the oxygen isotope values is caused by a weak "amount effect" during the peak of precipitation which has been the subject of numerous studies (e.g. Dansgaard, 1964; Araguás-Araguás et al., 1998; Lee and Fung, 2007 and references therein; Yu et al., 2008). From sample [e] to [a] the values increase continuously from -12.97 to -11.63 ‰ due to the interaction of decreasing temperatures and an evaporation trend which is no longer overprinted from the precipitation signal between the beginning of September and the sampling date on 2nd October. Specimen TaCo1 hatched during the first summer precipitation events when the $\delta^{18}O$ signal was still more positive.

$\delta^{13}C$ values in TaCo1 vary between -12.71 and -11.65 ‰, with an average value of -12.27 ‰. The variability in this pattern is low and characterizes a habitat in which the biological lake productivity varies only slightly, at least from July until October. Between August and September, the values show a slight increase whereas the oxygen isotope values decrease. This can be caused

by isotopically light CO_2 from the soil air which is transported in a dissolved phase by water from the surrounding hill slopes into the habitat during stronger rainfalls. The life span is from ca. the end of June to 2nd October 2010.
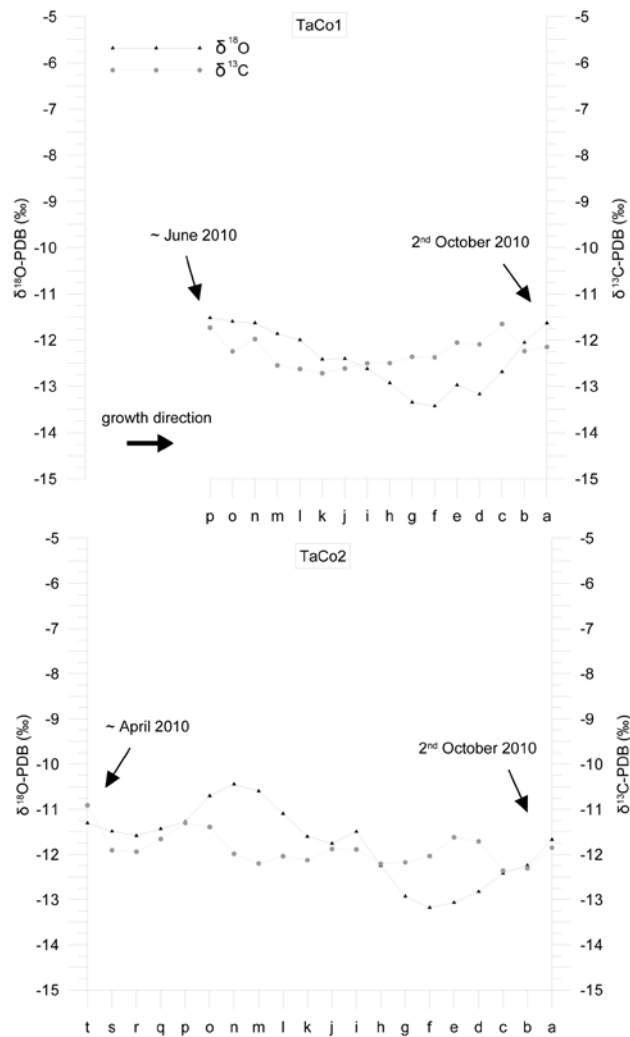
Figure 26: $\delta^{18}O$ and $\delta^{13}C$ shell patterns of two *Radix* specimens from Tarab Co.

Shell TaCo2: We measured $\delta^{18}O$ values from -13.18 to -10.44 ‰. The average value is -11.77 ‰. The shell section from sample [n] to [a] is very similar to the same section in TaCo1 and thus very likely covers the same time interval from July to October. From [t] to [n] the values increase from -11.31‰ to -10.44 ‰ reflecting the period from April (hatching) to July. The slight increase of the values might be caused by the onset of evaporation after the ice had disappeared from the lake surface.

$\delta^{13}C$ values in TaCo2 vary between -12.36 and -10.91‰, with an average of -11.88 ‰. The variability is slightly larger than in TaCo1 due to the longer life span of TaCo2, but also does not show large variations. The life span is from ~ April to 2nd October 2010.

The isotope patterns of *Radix* shells from Tarab Co indicate a water body which is mainly influenced by the isotope composition of precipitation, at least from April to October. The low δ^{18}O values in both shells suggest a short water residence time and high run-off. A weak, but visible, "amount effect" combined with negative δ^{18}O shell values indicates that the isotope composition of precipitation in the Tarab Co area is affected by long-distance transport instead of local water recycling processes. The general low δ^{13}C values point to a different source of organic carbon compared to other lakes.

3.5.2.5 Yadang Co

The isotopic patterns of two *Radix* shells are displayed in Figure 27.

Shell YaCo1: δ^{18}O values vary between -15.85 and -13.05 ‰ and the average value is -14.62 ‰. From [d] to [a], the pattern decreases from -13.38 to -15.35 ‰ and reaches the previous lower level. From [p] onwards the values increase from -15.40 to -13.05 ‰ [g] and reach the highest value of this pattern. The values from [z6] to [s] vary only between -15.85 and -14.79 ‰ and mirror probably the period from April to June. Thus this specimen hatched after the ice cover had disappeared. There is no winter signal in the pattern and the noticeable sequence between [p] and [a] does not replicate in an earlier section of the shell. This suggests a life span of about six months, although the highest number of samples was obtained from shell YaCo1. The shell was very large (Table 6) but the number of whorls (< 3) was low compared to shells from other lakes, indicating a shorter life span of this specimen and favourable nutrient conditions for shell growth in the habitat.

The δ^{13}C values vary between -8.89 and -6.10 ‰ with an average of -7.16 ‰. The decrease from -6.21 ‰ [n] to -8.89 ‰ [f] and the subsequently increasing values to -6.98 ‰ [a] correspond to the δ^{18}O sequence with increasing values, which is interpreted as influenced by precipitation in July and August. The negative coupling of δ^{13}C and δ^{18}O values indicates precipitation caused by isotopically lighter CO_2 produced by microorganisms. This depletion probably results from respiration and decomposition of organic matter in the uppermost soil layer. The CO_2 reaches the lake water in a dissolved phase as runoff from the hill slopes in the west during stronger rainfalls, which leads to more negative δ^{13}C shell values (Taft et al., 2012). From the protoconch [z6] to [n], the values remain rather constant between -6.98 and -6.21‰. Variations seem to be attributable to short-term changes in the isotope composition of the habitat. For example, decreasing values from -6.39 ‰ [z1] to -7.75 ‰ [x] can be caused by a decreased biological productivity or input of

CO_2 into the lake caused by an intense rainfall event in May. This specimen lived from ~ April to 2nd October 2009.
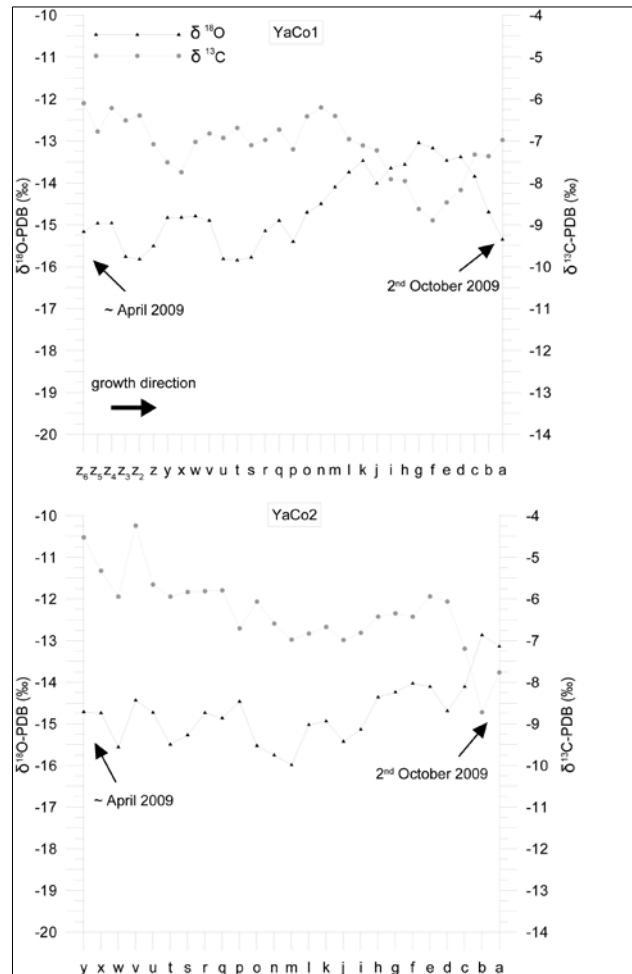
Figure 27: δ^{18}O and δ^{13}C shell patterns of two *Radix* specimens from Yadang Co.

Shell YaCo2: δ^{18}O values range between -15.99 and -12.87 ‰. The average value is -14.73 ‰. The oxygen isotope pattern is characterized by short-term variations of values in the shell section between [y] and [j] which vary between -14.44 ‰ [v] and -15.99 ‰ [m]. Noticeable is the subsequent gradual increase from -15.99 ‰ [m] to -12.87 ‰ [b] which reflects moisture from a regional source between June and August, but the pattern is less pronounced compared to YaCo1 indicating that the specimens spent their lives in different micro-habitats. The specimens were collected within a radius of a few meters but it cannot be excluded that one specimen spent its life in a habitat where, for example, the exchange with the main water body is different which can lead to various patterns. However, the general trend and the absolute values are similar.

The δ^{13}C values in shell YaCo2 vary between -8.72 and -4.24 ‰ and the average value is -6.30 ‰. The variability is higher than in YaCo1 which is a further indicator that the specimens did not

77

spend their lives in the same habitat. Decreasing $\delta^{13}C$ values and synchronously increasing $\delta^{18}O$ values which reflect the precipitation peak in late August in shell YaCo1 are also visible in shell YaCo2 but only in the latest shell section between [d] and [a]. Slightly increasing values from -6.98 ‰ [m] to -5.94 ‰ [e] mirror a trend to an increasing biological productivity in the habitat between June and August. The life span is from ~ April to 2nd October 2009.

YaCo1 and YaCo2 exhibit isotope patterns which are not clearly attributable to distinct meteorological or environmental parameters. Because Yadang Co is a lake with high discharge and, probably, a rather short water residence time and is located near the Yarlung Tsangpo (Brahmaputra River) Valley which is one of the pathways of the Indian Summer Monsoon moisture onto the TP, the isotope composition in the water and the shells should clearly reflect the precipitation. A "monsoon pattern" characterized by decreasing $\delta^{18}O$ values during the peak of rainfalls in late August caused by the "amount effect" would be expected. Instead, the pattern shows a clear trend to more positive values during the rainy season. Perhaps due to the northward location and the higher altitude of the lake (5060 m a.s.l.) compared to the Yarlung Tsangpo Valley (ca. 4400 m a.s.l. at this longitude), the monsoonal precipitation did not reach the lake in 2009 which is supported by the India Meteorological Department (2012) reporting a weaker monsoon in 2009 compared to the average normal amount and distribution. The values between -14.71‰ [o] and -13.38 ‰ [d] probably indicate a regional source of moisture originating from the lake district located to the north. If monsoon moisture had reached the lake in 2009, this should be mirrored in the isotope shell patterns due to the lake system characteristic.

As in the shell patterns of Tarab Co, the $\delta^{13}C$ values are more negative compared to other lakes which indicate a different source of organic carbon into the lake.

3.5.2.6 Yamdrok Yumco

The isotopic patterns of two *Radix* shells are displayed in Figure 27. Shell YaYu1: $\delta^{18}O$ values vary between -10.85 and -8.82 ‰ and the average value is -9.92 ‰. From [v] to [j] the values show a slight increasing trend from -10.30 to -8.92 ‰ which mirrors increasing evaporation between May and July. Subsequently the $\delta^{18}O$ composition tends to more negative values to -10.84 ‰ [a] which is a precipitation signal between July and September. Although this signal is not very pronounced and steeply increasing values during the initial monsoon rains are lacking compared to strongly monsoon-influenced lakes (Taft et al., 2012), it is assumed that monsoon rains led to this slight depletion in $\delta^{18}O$ values because it was recorded that the monsoon rainfalls reached the lake in

78

2008 (Chinese Central Meteorological Office, 2010). The shells were collected from the closed terminal lake basin which has a long water residence and reaction time, and thus the shell patterns show a different signal compared to other monsoon-influenced localities.

The range of $\delta^{13}C$ in YaYu1 is from -4.01 to -0.52 ‰ with an average of -2.89 ‰. In most sections the $\delta^{13}C$ pattern is very similar to the $\delta^{18}O$ pattern indicating a closed system and a long water residence time (Li and Ku, 1997). Increasing values from -3.66 ‰ [t] to -0.63 ‰ [j] reflect increasing biological productivity and evaporation in the lake from April to June. During the peak of monsoon precipitation in July, the $\delta^{13}C$ values decrease to -4.01‰ due to the increased input of isotopically light soil CO_2 or due to distinct biological activities in the habitat. The life span is from ~ October 2007 to 8th September 2008.
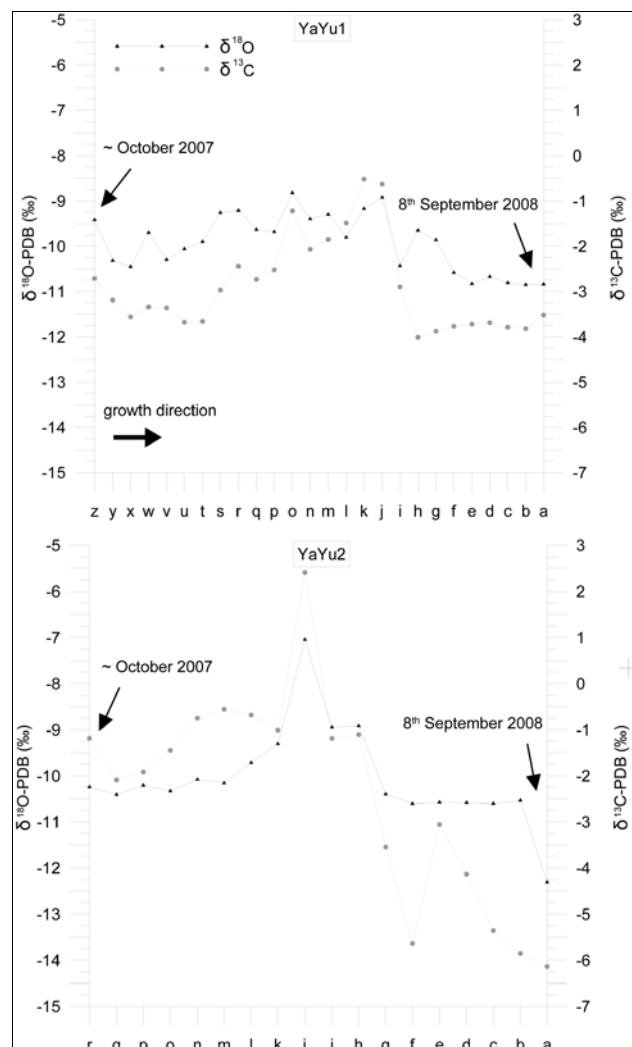
Figure 28: $\delta^{18}O$ and $\delta^{13}C$ shell patterns of two *Radix* specimens from Yamdrok Yumco.

Shell YaYu2: $\delta^{18}O$ values range between -12.3 and -7.04 ‰ and the average value is -10.05 ‰. The $\delta^{18}O$ peak at -7.04 ‰ [j] in the shell pattern is the reference point for our interpretation and discussion. This peak coincides with the first monsoon precipitation at the end of May 2008, recorded at Langkazi Meteorological Station (Figure 20). Subsequently decreasing $\delta^{18}O$ values from -7.04 to -10.60 ‰ [f] mirror the period from the end of May until July when monsoon rains had reached the maximum in the sampling year. This pattern reflects the "amount effect" in precipitation which is reflected in the shell patterns and leads to more negative $\delta^{18}O$ values during the peak of monsoon rains. From [f] to [b] the pattern is stable, which might be caused by high precipitation rates and relatively stable air temperatures around 10°C between mid-July and mid-August. The sharp decrease in $\delta^{18}O$ values from -10.53 ‰ [b] to -12.30 ‰ [a] in the latest shell section marks the increasing influence of river inflow and the decreasing influence of precipitation on the isotope composition in the lake water and therefore also in the snail shell. From the end of May until August the isotope composition in the shell is mainly controlled by the isotope composition of precipitation and only to a minor portion by temperature, evaporation and river/melt water inflow. The increasing trend in $\delta^{18}O$ values from -10.15 [m] to -9.30 ‰ [k] mirrors increasing evaporation after the ice cover on the lake surface disappeared in April. The unvarying pattern from [r] to [m] from -10.24 to -10.15 ‰ indicates the ice cover period of the habitat when neither temperature variations nor the sparse precipitation in February (Figure 20) had affected the stable isotope composition of the lake water. Probably, the *Radix* specimen which built shell YaYu2, hatched shortly before the lake was covered by ice in late October 2007. Burla (1972) and Gaten (1986) observed that *Radix* moves in winter from the shallow littoral area to deeper water in order to avoid the ice, which would result in relatively unvarying isotope compositions because of more constant conditions in the deeper lake. Although Yamdrok Yumco is also fed by glacial melt waters (Tian et al., 2008), the specific melt water signal could not be detected in the oxygen isotope pattern. Probably, this signal is overprinted by evaporation and precipitation signals or the contribution of melt water is too low in comparison to the lake water volume.

The range of $\delta^{13}C$ in YaYu2 is between -6.14 and 2.41 ‰ and the average value is -2.40 ‰. The numerical variability in this shell is thus comparatively high. In most parts of the pattern the $\delta^{13}C$ values run parallel to the $\delta^{18}O$ pattern, but from [f] to [b] the carbon isotope values show a steep increase from -5.64 ‰ [f] to -3.06 ‰ [e] followed by a decrease to -5.85 ‰ [b] whereas the oxygen isotope values remain constant. Because shell growth decelerated during the winter season, the shell section between [q] and [m] reflects a longer period than other parts of the same length formed during spring and summer. Therefore, the shell section [r] to [q] mirrors the period before the lake was completely covered by ice, and the increasing $\delta^{13}C$ values in shell part

[q] to [m], from -2.09 to -0.56 ‰, suggest slightly increasing biological productivity in the lake under the ice cover from February until April. The parallel trend of $\delta^{18}O$ and $\delta^{13}C$ values from [k] to [g] reflects the period from May to July. Because the carbon isotope composition in the lake water strongly depends on the particular habitat, small variations of carbon sources can lead to rapid changes in the shell pattern, such as in shell section [h] to [c]. This specimen lived from ca. late October 2007 to 8th September 2008.

The shell patterns from Yamdrok Yumco diverge from each other, which indicates differences in habitats of the gastropods. The $\delta^{18}O$ composition in shell YaYu2 shows a more pronounced precipitation signal caused by the Indian Summer Monsoon precipitation. In YaYu1, this signal is only a slight gradual decrease instead of a steep decrease. Based on these observations, it is likely that the *Radix* specimen of shell YaYu1 lived in a somewhat deeper part of the sampling area where the conditions remained more stable during the year. The $\delta^{13}C$ pattern of shell YaYu1 shows more pronounced seasonal changes in biological productivity in the habitat. $\delta^{18}O$ and $\delta^{13}C$ of shell YaYu2 recorded both sub-seasonal habitat variations.

In summary, the oxygen and carbon isotope pattern of both shells mirror a large closed lake basin with a long water residence time due to the covariance in most shell sections (Talbot, 1990; Li and Ku, 1997; Leng and Marshall, 2004). The values in shell YaYu1 exhibit only slight variations and a less pronounced precipitation signal than expected due to the terminal lake character. Shell YaYu2, which was probably mainly built in a different micro-habitat shows a pronounced monsoon precipitation signal and exhibits a large variability in the isotope values, similar to what is observed from a small exorheic lake with high discharge (Taft et al., 2012). The data suggest that, although the terminal lake is a large endorheic basin, it is significantly influenced by the upstream exorheic lakes which mirror short-time climatic and/or environmental changes. The low average oxygen isotope values of the shells indicate that the lake is mainly influenced by precipitation from distant moisture sources.

3.5.2.7 Donggi Cona

The isotopic patterns of two *Radix* shells are displayed in Figure 29.

Shell DoCo1: $\delta^{18}O$ values range between -9.84 ‰ and -7.59 ‰ and the mean value is -9.33 ‰. The $\delta^{18}O$ pattern exhibits one steep increase from -9.08 ‰ [k] to -7.59 ‰ [j] and a subsequent steep decrease to -9.77 ‰ [g]. This pattern is characteristic of a shell which was built in a habitat in which the water composition is significantly influenced by precipitation during the rainy season

(Taft et al., 2012). The first more intense rainfall started in mid-July 2008 (Figure 20), mirrored by an increase of the $\delta^{18}O$ value at sample [j]. The following continuing decreasing trend in the shell pattern is characterized by an inverse correlation between precipitation amount and the oxygen isotope composition. This pattern indicates monsoon precipitation and is characteristic of shallow habitats, which have a short water residence and reaction time. During the monsoon season, the precipitation signal overprints the evaporation signal. Furthermore, when rainfalls continue, the air gets more humid and evaporation decreases. Relatively constant values distinguish the embryonic and juvenile shell part between [o] and [m] with values between -9.47 and -9.67 ‰. Because *Radix* specimens do not hatch while a lake is covered by ice and the winter period is not reflected in the pattern, specimen DoCo1 hatched after the ice had disappeared in late April or early May.

$\delta^{13}C$ values in DoCo1 range between -7.16 ‰ and 0.84 ‰ and the mean value is -2.08 ‰. The variability of 8.00 ‰ is very high compared to $\delta^{18}O$. The amount and composition of the TDIC (total dissolved inorganic carbon) utilized in the shell carbonate varied a lot during the life span.

During the onset of monsoon rains, the $\delta^{13}C$ values decrease steeply from -0.75 ‰ [m] to -7.16 ‰ [j]. The same pattern could be observed in a monsoon-influenced small exorheic lake, Bangda Co, at the southeastern margin of the TP (Taft et al., 2012).

Decreasing $\delta^{13}C$ values and simultaneously increasing $\delta^{18}O$ values can be a result of rain water penetrating through unsaturated zones of soils before the water reaches the lake. Variabilities in lake productivity before and after the monsoon season may be related to local nutrient variations. However, the mean $\delta^{13}C$ value of DoCo1 is high, indicating high lake productivity during the whole shell growth period. This specimen lived from ~ late April to 5th October 2008.
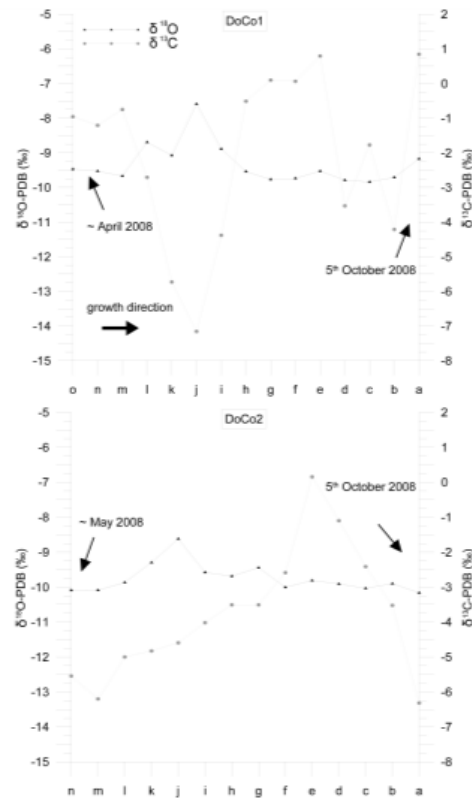
Figure 29: δ¹⁸O and δ¹³C shell patterns of two *Radix* specimens from Donggi Cona.

Shell DoCo2: The $\delta^{18}O$ pattern varies between -10.16 and -8.62 ‰. The average value is -9.75 ‰. Between [i] and the aperture [a] the values remain relatively constant between -9.58 and -10.16 ‰. From [l] to [j] the pattern shows a peak from -9.87 to -8.62 ‰ similar to DoCo1 but less pronounced. The shell section from [n] to [l] represents the period between late May and June.

$\delta^{13}C$ values in DoCo2 range between -6.32 and 0.15 ‰ with an average value of -3.78 ‰. The absolute variability is 6.47 ‰ and thus lower than in DoCo1 but still high. From [m] to [e] the values increase from -6.20 to 0.15 ‰ and subsequently decrease steeply to -5.54 ‰ [a]. At sample [e] the peak in $\delta^{13}C$ is very similar to that in DoCo1. The more negative values in DoCo2 during the peak of the monsoon rains are also similar to those in DoCo1, but less pronounced. The life span is from ca. May to 5th October 2008.

Donggi Cona is located close to the modern limit of the East Asian Monsoon (Zhang et al., 2011) which means that the interannual variation of monsoon precipitation is particularly high. The $\delta^{18}O$ patterns of the shells indicate that precipitation in the sampling year is characterized by long-distance transport and is not of local origin.

3.5.2.8 Summary and comparison of all lakes

$\delta^{18}O$ and $\delta^{13}C$ patterns in shells of *Radix* provide valuable information characterizing lake systems and large-scale as well as regional climate conditions. The oxygen isotope compositions in shells from the seven lakes show very different patterns depending on lake hydrology (open/closed, size, water residence time, depth) and locality within the atmospheric circulation (source of precipitation, Westerly or monsoon dominated). The carbon isotope compositions are particularly dependent on specific habitats, which vary in terms of biological productivity and in respect of carbon sources. $\delta^{18}O$ and $\delta^{13}C$ values show a positive covariance for shells originating from large closed basins.

On the transect from Lake Karakul in the Pamirs to Donggi Cona at the eastern margin of the TP, the shell patterns show an increasing influence of precipitation and a decreasing influence of evaporation on the isotope compositions. A precipitation pattern controlled by the monsoon circulation is visible in shells from Yamdrok Yumco, Tarab Co and Donggi Cona, although the lake systems differ strongly in terms of size, discharge and hydrology. The values are significantly more negative, and the shell patterns exhibit a higher seasonal variability compared to the western lakes, which provides evidence that the lake waters mirror short-term sub-seasonal changes. The $\delta^{18}O$ shell patterns from Nyak Co and Lake Manasarovar, which are located in arid regions on the western TP, are predominantly controlled by evaporation, indicated by relatively high values and mirror rather long residence times of the lake waters. The $\delta^{13}C$ shell patterns of Tarab Co and Yadang Co exhibit more negative values compared to the other lakes which indicate a different source of organic carbon. Unlike the other lakes, the specimens from Lake Karakul were collected at a depth of 19 m. Thus it is not surprising that the isotopic shell patterns are more stable than all other patterns because the influence of precipitation, temperature changes or glacial melt water is low. Nevertheless, the shell patterns of Lake Karakul mirror the arid climate, the closed lake system, the long water residence time and the evaporative influence by relatively high oxygen isotope values, which is also supported by the water analysis.

Even interannual meteorological variabilities can be shown, for example in the case of Yadang Co on the southern TP. The isotope shell patterns indicate that the monsoon rains did not reach the lake in 2009, although it is located in a region which is usually affected by the modern monsoon.

3.6 Conclusions

In comparison to other climate archives from the TP, the isotope patterns from the archive *Radix* mirror general climatic differences and trends as well as interannual and even sub-seasonal changes on a plateau-wide scale.

The shell patterns exhibit an increasing influence of precipitation and a decreasing influence of evaporation on the isotope compositions from west to east. $\delta^{18}O$ values of shells from lakes on the eastern and central TP (Donggi Cona, Yamdrok Yumco, Tarab Co) mirror monsoon signals, indicated by more negative values and higher variabilities compared to the more western lakes (Karakul, Bangong/Nyak, Manasarovar).

General climatic differences of the lake regions due to the different regional settings are clearly mirrored in the isotope patterns of the *Radix* shells, without noticeable dependence on the particular lake system.

Supplementary data

Numerical isotope values for each shell sample and numerical values of hydrogeochemical analyses are available in the PANGAEA data information system, www.pangaea.de, doi: 10.1594/PANGAEA.777838.

4. Oxygen and carbon isotope ratios in *Radix* (Gastropoda) shells indicate changes of glacial meltwater flux and temperature since 4200 cal yr BP at Lake Karakul, eastern Pamirs (Tajikistan)

Linda Taft[a], Steffen Mischke[a,b], Uwe Wiechert[a], Christian Leipe[a], Ilhomjon Rajabov[c], Frank Riedel[a]

[a]Free University Berlin, Institute of Geological Sciences, Palaeontology, Building D, Malteserstr. 74-100, 12249 Berlin, Germany

[b]Institute of Earth and Environmental Science, Universität Potsdam, Karl-Liebknecht-Str. 24-25, 14476 Potsdam-Golm, Germany

cState Administration for Hydrometeorology of the Committee for Environmental Protection under the Government of the Republic of Tajikistan, 47 Shevchenko St., Dushanbe 734025, Tajikistan

Abstract

We report $\delta^{18}O$ and $\delta^{13}C$ ratios of 21 fossil Radix *(aquatic gastropod) shells from a sediment core taken in the eastern basin of Lake Karakul, Tajikistan (38.86-39.16°N, 73.26-73.56°E, 3928 m above sea level) which covers the last 4200 cal yr BP. The lake is surrounded by many palaeoshorelines evidencing former lake level changes, most likely triggered by changes in meltwater flux. This hypothesis was tested by interpreting the isotope ratios of Radix shells compared to $\delta^{18}O$ of Ostracoda and authigenic aragonite. The mean $\delta^{18}O$ Radix and Ostracoda values fall along the same general negative long-term trend indicating decreasing air temperatures, probably influenced by decreasing solar summer insolation. The sclerochronological $\delta^{18}O$ and $\delta^{13}C$ patterns in* Radix *shells provide seasonal climatic and/or hydrological information which are discussed in context with previously proposed climatic changes in the last 4200 cal yr BP. The period ~4200-3000 cal yr BP was characterized by cooling, stepwise decreasing lake level and, most likely, glacier advance in the catchment. Subsequently the climate remained cold and the lake system became increasingly unstable characterized by fluctuating lake levels and climate conditions. From ~1800 cal yr BP the sclerochronological patterns provide evidence for increasing melt water flux and transport of allochthonous carbon into the lake, most likely due to glacier retreat. The period around 1500 cal yr BP was characterized by strong warming, increasing*

meltwater flux, glacier retreat and an increasing lake level. Warm conditions continue until ~500 cal yr BP probably representing the Medieval Warm Period. A short relatively cold (dry?) period and a lower lake level are assumed for ~ 350 cal yr BP, maybe indicating the Little Ice Age. Since ca. 350 cal yr BP the lake level has been increasing due to warmer conditions. Our results show that the lake system is quite complex and that changes were triggered by changing meltwater fluxes and temperature. The similarity between Radix *and ostracod δ^{18}O ratios demonstrates that both archives provide significant information.*

4.1 Introduction

The dynamics of mountain glaciers are among the most visible indications of the effects of climatic changes (Solomina et al. 2004; IPCC Report 2007) and it has been observed that many glaciers all over the world melt in response to warmer air temperatures since 150 years (World Glacier Monitoring Service 2012). However, timing and extent of glacial responses are highly variable and depend on size, location and climate regime (Bolch 2007). In most areas of Central Asia the glaciers retreat since the termination of the Little Ice Age (LIA; Solomina et al. 2004; Khromova et al. 2006; Bolch 2007; Kutuzov and Shahgedanova 2009). On the other hand, more than 50% of observed glaciers in the Karakoram region are advancing or stable since the last decade (Scherler et al. 2011). As long as glaciers are large, one visible response of glacial retreat is the meltwater discharge which can cause rising water levels in glacier-fed lakes (Sorrel et al. 2006; Komatsu et al. 2010; Osipov and Khlystov 2010). Glacier and meltwater fluctuations in modern and historical times can be monitored by remote sensing, morphologic studies and mass-balancing or evaluated from written records (Solomina et al. 2004; Khromova et al. 2006; Narama et al. 2010). Variations which occurred further back in time can only be modeled (Sarikaya et al. 2009; Goehring 2012) or reconstructed by using proxy data indicating glacier stages, temperature fluctuations or freshwater supply (Ricketts et al. 2001; Owen et al. 2002; Seong et al. 2007, 2009). Lakes represent important systems in this context because they archive a number of suitable proxies in their sediments (Wünnemann et al. 2006; Mischke and Zhang 2010; Vasskog et al. 2012).

Of special interest are lakes located in regions which are particularly sensitive to environmental and climatic changes. One example is Lake Karakul located in the eastern Pamir Mountains of Tajikistan (Figure 30). Palaeoshorelines up to 205 m above the modern lake level evidence lake dynamics which are related to Pleistocene climate fluctuations (Komatsu 2009; Komatsu et al.

2010). Mischke et al. (2010) analyzed a 104 cm long sediment core, covering the last 4200 cal yr BP, studying geochemical, granulometrical and palynological properties and concluded, that the data indicate mainly temperature-driven changes in meltwater supply due to the presence of glaciers in the catchment area and the aridity of the region. However, the qualitative characterization of meltwater supply and other processes which influence lake level changes could not be provided.

$\delta^{18}O$ and $\delta^{13}C$ signals from fossil ostracod shells have been used for the palaeolimnological reconstruction (Mischke et al. 2010). As ostracods shed and build their valves several times during ontogeny, sclerochronological analyses which could cover the annual hydrological cycle from which the meltwater signal can be inferred, are not practical. Mischke et al. (2010) interpreted the ostracod isotope data with certain limitation because palaeoecological inferences seemed not to be represented by the studied, probably endemic taxon.

Taft et al. (2012, 2013) have demonstrated that sclerochronological $\delta^{18}O$ and $\delta^{13}C$ patterns in aragonite shells of the aquatic gastropod *Radix* mirror seasonal variations in modern lakes across the Tibetan Plateau. Ice cover, meltwater, precipitation and evaporation periods can be differentiated. The method has also been applied to modern shells of Lake Karakul (Taft et al. 2013).

In the here presented study, we adopt the method to fossil *Radix* shells from late Holocene sediments of Lake Karakul and evaluate whether late Holocene meltwater input rates can be inferred from the shells and related to temperature changes and glacier fluctuations in the catchment area. We further consider whether the shell data can be related to the geochemical results of Mischke et al. (2010) to improve our understanding of the hydrological system.

4.2 Study area

Karakul (38.86-39.16°N, 73.26-73.56°E, 3928 m above sea level) is an endorheic brackish-water lake in the eastern Pamirs in Tajikistan, (Figure 30) which are part of the extensive high mountain system of Central Asia, comprising the Pamir-Karakoram-Hindu-Kush ranges. The lake consists of a relatively shallow eastern sub-basin with a maximum water depth of ca. 20 m and a deep western sub-basin with a water depth of 242 m (Molchanov 1929). The surface area of the lake is ca. 380 km² (Komatsu et al. 2010), which is covered by ice of up to ca. 1 m thickness from the end of November until the end of May (Mischke et al. 2010). The lake is located in a tectonic graben

basin (Melack 1983; Hammer 1986; Gopal and Ghosh 2009) but an origin as meteor impact structure was discussed in the past

(Gurov et al. 1993; Safarov 2006). The highest mountain peaks in the catchment area are above 6000 m asl and many of the surrounding mountains are covered by snow and ice, which are the most important sources of the lake water (Ni et al. 2004). The main seasonally active inflow is located at the northern shore of the lake (Figure 30). Three water samples from the eastern basin have $\delta^{18}O$ values ranging from -3.8 to -3.5 ‰ relative to V-SMOW and inflowing streams, which transport predominantly glacial meltwater, have values ranging from -18.0 to -14.0 ‰ (Mischke et al. 2010). The comparatively higher $\delta^{18}O$ value of the lake water mirrors the long residence time and the strong influence of the insolation which results in low air humidity and a high evaporation rate for the lake surface.

Lake Karakul is located in an area dominated by the Westerly wind system but due to the high mountain ranges to the west, blocking the Westerly moisture penetration into the lake catchment (Komatsu et al. 2010), the annual precipitation is only 82 mm with slightly higher precipitation between March and July and least precipitation during the winter months (Mischke et al. 2010). Meteorological data have been recorded at the station located on the eastern lake shore (39.01°N, 75.36°E, 3930 m asl) since 1934 with a break between 1995 and 2004. With a mean annual temperature of about -4°C, the climate is characterized as cold semi-arid, BSk in the Köppen-Geiger climate classification (Peel et al. 2007).

Komatsu (2009) and Komatsu et al. (2010) studied the palaeoshorelines and reconstructed a lake history for the Mid- to Late Pleistocene based on remote sensing data, field mapping and tentative chronology. They classified four groups of shorelines indicating higher or constant lake levels which are correlated to the glacial maxima of MIS 8, 6, 4 and 2. Geomorphic glacial landforms show that Pleistocene glaciers came close to the modern eastern, northern and southern lake shore (Komatsu et al. 2010; Mischke et al. 2010). Relatively little is known about the Holocene glacial history of the Lake Karakul region. On the base of dendrochronological data, colder conditions were concluded for 1897-1916 indicating a glacier advance in the drainage area of Lake Karakul (Ni et al. 2004). For 1925-1980, it is assumed that the glacier area in the lake catchment has decreased (Ni et al. 2004), probably in response to global warming. Based on historical surveys and remote sensing, Khromova et al. (2006) detected a glacier decrease between 1978-2001 in the eastern Pamir region. However, detailed glacial studies in the catchment of Lake Karakul have not been conducted yet.
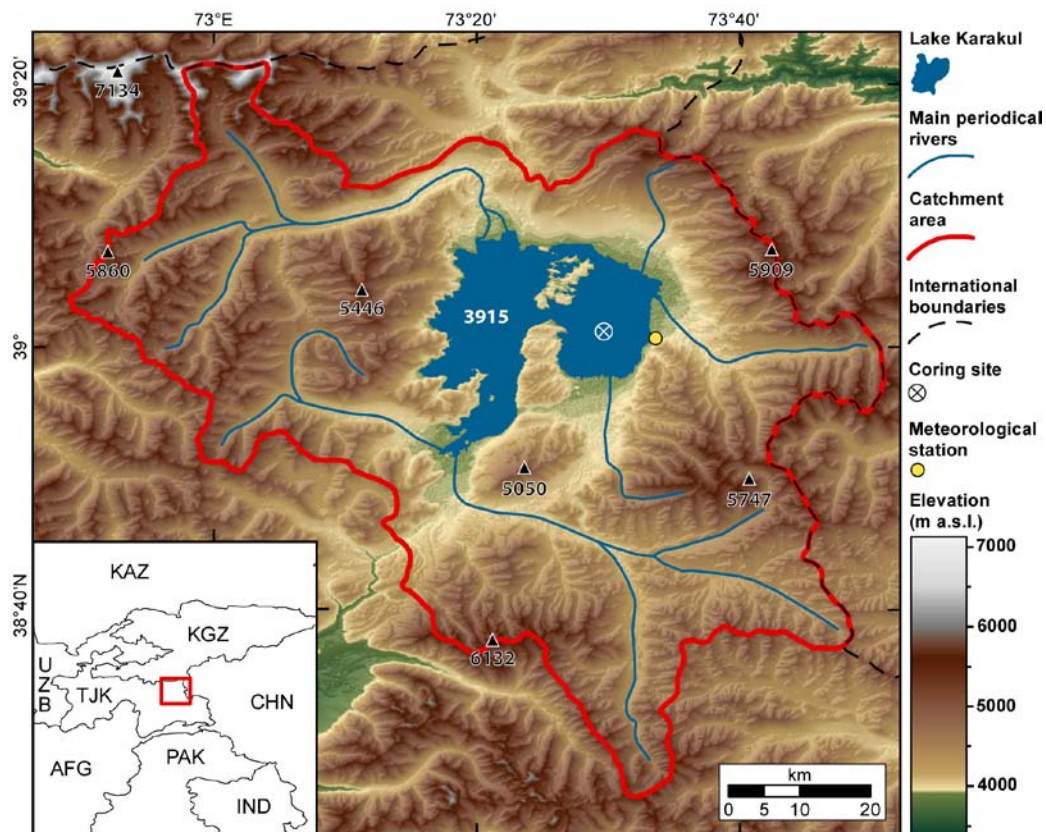
Figure 30: Lake Karakul with core location and periodical inflows. The catchment area of Lake Karakul measures 4464 km² and was calculated in ArcGIS v10.0 (ESRI, 2011) with the use of HydroSHEDS v1.0 data (Lehner and Döll 2004; Lehner et al. 2006) in the projected coordinate reference system Pulkovo 1942/3-degree Gauss-Kruger CM 72E (EPSG: 2599).

4.3 Material and methods

4.3.1 Shell sampling and preparation

21 *Radix* (Figure 31) shells (17 complete shells and four large fragments) were collected from 21 sediment layers from a core of 104 cm length (Figure 32), which was obtained from 19.1 m water depth in the center of the eastern sub-basin of Lake Karakul (Figure 30). The core covers the last 4200 cal yr BP (Mischke et al. 2010). Modern *Radix* specimens from Lake Karakul represent the species *Radix auricularia* (Linnaeus 1758; von Oheimb et al. 2011). Fossil shells from the core show the same shell morphology and thus are assigned to the same species. Details about biology, shell growth, life cycle, nutrition, etc. are presented by Taft et al. (2012, 2013).

The shells were cleaned manually and in an ultrasonic bath from coarse mud. Subsequently, they were treated with H_2O_2 for 24 hours to remove remaining organic matter before they were dried for 24 hours at room temperature. The shells were sampled for stable isotope samples in a constant distance of 1mm along the ontogenetic spiral of growth increments using a dental driller. Depending on shell size and total number of whorls, we obtained 7 to 25 sub-samples per shell. The sub-samples were labeled in alphabetical order beginning with [a] which represents the latest shell part. The four shell fragments (from core layers 10 cm; 30 cm; 61 cm and 101 cm) were homogenized and isotopically analyzed as powdered bulk samples.

Figure 19: Example of a well-preserved fossil Radix shell from Lake Karakul.
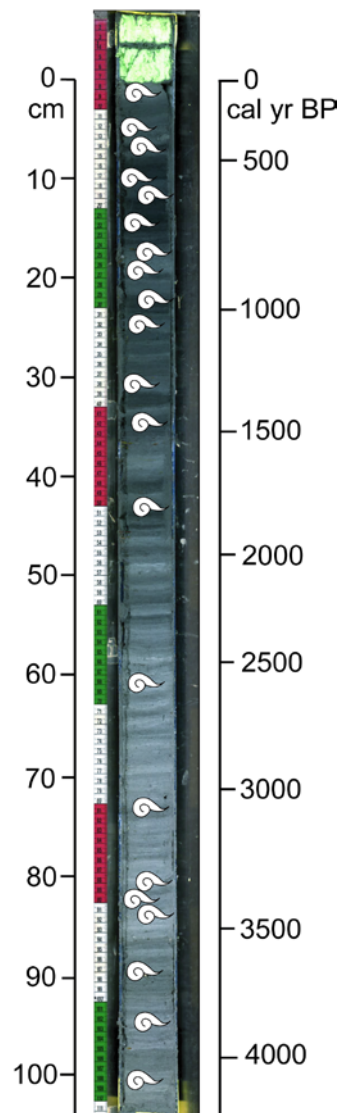
Figure 20: Sediment core of 104 cm length taken from the eastern sub-basin of Lake Karakul (Mischke et al. 2010) with positions of fossil *Radix* shells.

4.3.2 Stable isotope analysis

The aragonite shell samples were isotopically analyzed at the Freie Universität Berlin using a GasBench II linked to a MAT-253 ThermoFisher Scientific™ isotope ratio mass spectrometer. The external error of the measurements is ±0.06‰ for $\delta^{18}O$ and ±0.04‰ for $\delta^{13}C$ both 1 SD (standard deviations) based on the reproducibility of the in-house reference material Laaser marble. The

measurements were standardized against Carrara Marble (CAM) and Kaiserstuhl carbonatite in-house reference material (KKS) which had been calibrated against Vienna PeeDee Belemnite (V-PDB) international isotope reference material using NBS-18 and NBS-19. All results are reported in δ notation relative to V-PDB (Table 8, Figure 33 and Figure 34C, D).

4.4 Results

4.4.1 Mean $\delta^{18}O$ and $\delta^{13}C$ shell values

Mean $\delta^{18}O$ shell values cover a range from -1.43 to 0.86 ‰. The highest values occur at 95 cm (0.86 ‰), 83 cm (0.22 ‰) and 15 cm (0.36 ‰) core depth (Table 8 and Figure 34C). The values are low at 43 cm (-1.12 ‰) and from 6 cm core depth to the top (from -1.43 to -0.93 ‰). From the deepest part of the core to the top, a trend to more negative values is visible (Figure 34C). This general trend is interrupted by excursions to more positive values (at 95, 83, 61, 35, 30, 15 and 10 cm core depth). The shifts at 95 cm (0.86 ‰), 83 cm (0.22 ‰) and 15 cm (0.36 ‰) core depth are most pronounced.

Mean $\delta^{13}C$ shell values cover a range from -1.53 to 1.70 ‰. The highest values occur at 81 cm (1.53 ‰), 30 cm (1.11 ‰) and 10 cm (1.70 ‰) core depth (Table 1). The values are relatively low at 83 cm (-0.98 ‰), 25 cm (-1.53 ‰) and 1 cm (-0.87 ‰) core depth.

Table 8: Individual mean and absolute δ^{18}O and δ^{13}C values for each shell sub-sample. Sub-sample [a] represents the latest shell part, respectively. Shells from 10, 30, 61 and 101 cm core depths were isotopically measured as bulk samples. Maxima and minima values are marked in bold.

core depths cm	1		5		6		10		11		15		18		19		23		25		30		35		43		61		73		81		83		84		89		95		101	
sub-samples	δ^{18}O	δ^{13}C	δ^{18}O	δ^{13}C	δ^{18}O	δ^{13}C	δ^{18}O	δ^{13}C	δ^{18}O	δ^{13}C	δ^{18}O	δ^{13}C	δ^{18}O	δ^{13}C	δ^{18}O	δ^{13}C	δ^{18}O	δ^{13}C	δ^{18}O	δ^{13}C	δ^{18}O	δ^{13}C	δ^{18}O	δ^{13}C	δ^{18}O	δ^{13}C	δ^{18}O	δ^{13}C	δ^{18}O	δ^{13}C	δ^{18}O	δ^{13}C	δ^{18}O	δ^{13}C	δ^{18}O	δ^{13}C	δ^{18}O	δ^{13}C	δ^{18}O	δ^{13}C	δ^{18}O	δ^{13}C
ø	-0.18	-0.87	-1.37	-0.36	-1.43	0.70	-0.30	1.70	-0.76	0.96	0.36	0.62	-0.75	-0.25	-0.77	0.71	-0.31	0.57	-0.64	-1.53	-0.04	1.11	-0.13	-0.04	-0.96	-0.26	-0.28	0.67	-0.75	-0.33	-0.55	1.53	0.23	-1.18	-0.39	0.63	-0.19	-0.47	0.86	0.70	-0.49	0.59
a	**-0.18**	**0.37**	-0.97	-0.77	-1.56	0.91			**-0.15**	**0.00**	0.26	0.82	-0.94	0.32	**-0.21**	**1.22**	**0.11**	0.89	**0.00**	**0.21**			0.36	0.01	**-0.13**	**0.73**			-0.03	0.27	**-0.85**	1.09	n.d.	n.d.	0.20	0.90	-0.27	-0.09	0.82	0.56		
b	-0.55	-0.84	-1.68	-0.69	-1.20	**1.07**			-0.16	1.00	**0.84**	0.56	-0.73	0.07	-0.22	1.07	-0.27	0.68	-0.54	-0.29			-0.01	-0.12	1.37	0.07			-0.67	0.69	-0.82	1.86	0.50	1.03	0.17	0.96	-0.18	-0.18	0.99	0.56		
c	-0.26	-0.38	-1.68	0.44	-1.45	1.03			-0.40	1.01	0.41	**0.45**	-1.01	-0.60	-0.91	0.73	-0.42	0.76	-0.65	-0.31			-0.45	-0.35	-0.95	0.16			-2.01	-1.38	-0.82	**0.57**	0.52	**1.30**	-0.22	0.95	**-0.56**	**-0.46**	**1.42**	1.08		
d	-0.86	-0.69	-1.79	0.15	**-1.63**	0.62			-0.54	1.13	**-0.09**	0.53	-0.62	0.24	-0.93	0.41	**-0.70**	0.66	-0.66	-0.27			-0.46	-0.13	-0.34	-0.11			-0.84	-0.66	-0.71	1.56	0.30	-0.79	**-0.82**	**1.03**	-0.01	0.03	0.98	0.71		
e	-1.07	-0.65	**-1.87**	**0.44**	-1.17	0.60			-0.29	0.74	0.15	0.56	-0.68	0.59	-0.96	0.56	-0.69	0.78	-0.28	-0.17			-0.25	0.05	-0.60	-0.09			-0.78	-0.20	-0.04	1.21	0.74	0.81	-0.73	0.88	-0.19	**0.21**	0.62	0.76		
f	-1.23	-0.17	-1.51	0.31	-1.58	**-0.02**			**-1.30**	1.07	0.31	0.73	-0.53	0.64	-0.95	0.75	-0.43	0.87	-0.26	0.09			-0.31	-0.03	-0.64	-0.35			-0.82	-0.84	-0.82	**2.61**	0.52	-0.19	-0.40	0.90	-0.19	0.10	**0.52**	1.01		
g	-0.99	-0.26	-1.74	-0.01					-1.25	1.05	0.61	0.71	-0.49	0.55	-0.83	0.62	-0.40	0.65	-0.42	-0.85			-0.11	0.23	-0.60	-0.19			-0.57	-0.65	-0.27	1.52	0.43	-0.62	-0.30	0.62	0.00	-0.06	0.67	0.94		
h	-1.16	-0.29	-1.22	-0.02					-1.20	0.68			-0.34	0.50	-0.93	0.54	-0.25	**1.07**	-0.75	-1.75			0.04	0.37	**-1.71**	-0.26			-0.38	-0.02	-0.40	1.29	0.26	-1.97	0.18	0.63	-0.13	-0.75	n.d.	n.d.		
i	-1.11	-1.36	-1.28	-0.32					-0.84	0.57			-0.69	**0.91**	-0.58	1.15	-0.20	0.57	-0.97	-2.19			0.34	0.71	-0.91	0.19			-0.77	-0.47	-0.23	2.06	n.d.	n.d.	-0.63	0.31	**0.04**	-1.28	0.94	0.84		
j	-0.89	-1.49	-1.18	-0.29					-0.77	1.40			-1.02	-0.23	-0.35	0.80	-0.46	0.13	-1.07	-2.81			**0.37**	0.56	-1.00	-0.17			-0.65	-0.04			0.78	1.19	-0.79	0.40	-0.39	**-1.48**	1.42	1.28		
k	-0.28	0.22	-1.16	-0.32					-0.90	1.31			-1.05	-0.97	-0.45	0.51	-0.44	**-0.04**	-1.01	-2.29			0.35	0.66	-2.07	-0.39							n.d.	n.d.	-0.45	0.17	-0.14	-1.17	1.25	0.83		
l	-1.05	-0.52	**-0.71**	0.05					-1.14	1.07			-1.03	-0.88	-0.69	0.61	-0.16	0.39	**-1.15**	-3.17			0.16	**0.77**	-1.09	0.01			-0.32	-2.89	-0.80	**-0.24**							0.76	0.54		
m	-1.19	-2.18	-1.54	-0.79					-1.15	1.05			-0.73	0.47	-0.92	0.50	0.10	-0.02	-0.83	-1.78			0.23	0.16	-0.69	0.12							-0.15	-2.69	-0.30	0.84			0.59	0.45		
n	-1.17	-0.25	-1.47	-0.40					-0.83	0.90			**-1.06**	**-1.23**	**-1.18**	0.49	-0.42	0.61	-0.94	**-3.29**			-0.27	-0.02	-0.94	-0.30							-0.25	-3.01	-0.36	0.46			0.54	0.39		
o	-1.24	**-2.41**	n.d.	n.d.					-0.43	**1.45**			-0.72	-1.12	-0.98	0.86	-0.08	0.58	-0.93	-2.88			-0.19	-0.18	-0.82	-0.93							-0.05	**-3.13**	-0.66	0.63			0.54	**0.07**		
p	-1.29	-2.33	-1.44	-0.89									**-0.29**	-1.05	-1.16	0.60			-0.71	-2.20			-0.30	0.00	-0.43	0.04							-0.01	-3.10					0.56	0.12		
q	-0.81	-0.84	-1.40	**-1.09**									-0.88	-0.87					-0.60	-1.62			**-0.56**	-0.51	-1.51	**-2.02**							-0.01	-2.38					0.77	0.17		
r	-1.09	-1.55	-1.22	-0.81									-0.70	-1.16					-0.96	-2.21			-0.56	-0.44	-1.48	-1.12							n.d.	n.d.					n.d.	n.d.		
s	**-1.29**	-0.99	-1.06	-0.73									-0.68	-1.02					-0.73	-2.15			-0.27	-0.49	n.d.	n.d.							n.d.	n.d.					1.09	0.71		
t			-1.14	-0.60															-0.75	-2.47			-0.26	-0.41															1.40	0.84		
u			-1.27	-0.38															-0.13	-1.36			-0.14	-0.61															0.71	0.59		
v			-1.38	-0.76															-0.21	-1.00			-0.32	-0.41															0.59	0.42		
w																			-0.28	-0.51			-0.39	**-0.69**															0.76	0.87		
x																																							0.94	0.97		
y																																							0.82	**1.37**		

4.4.2 Sclerochronological $\delta^{18}O$ and $\delta^{13}C$ variations

$\delta^{18}O$ intra-shell values of all samples cover a range from -2.07 to 1.42 ‰. $\delta^{13}C$ values are in a larger range from -3.29 to 2.61 ‰. The individual mean and absolute values for each sub-sample are presented in Table 8 and the sclerochronological patterns are shown in Figure 33.

Sub-samples from 73 and 43 cm core depth exhibit the highest $\delta^{18}O$ variability (> 1.90 ‰) of all samples. Sub-samples 25 and 6 cm core depth feature the lowest variability (< 0.51 ‰). Sub-samples from 83 and 25 cm core depth show the highest $\delta^{13}C$ variability (4.43 and 3.5 ‰) and sub-sample from 15 cm core depth exhibits the lowest variability (0.37 ‰).

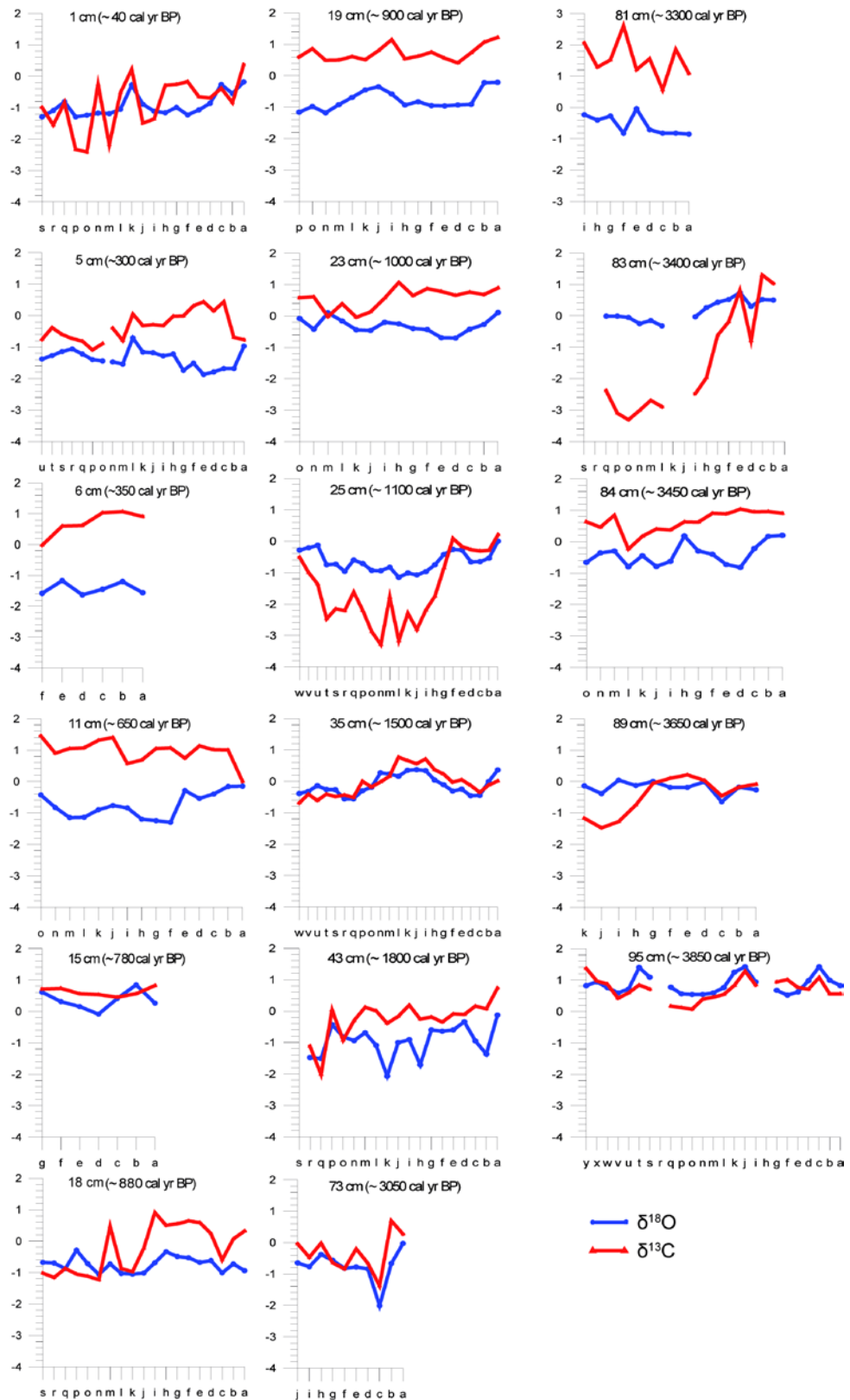**Figure 33: Sclerochronological δ^{18}O and δ^{13}C patterns of all *Radix* shells. The letter [a] represents the latest shell part.**

4.5 Discussion

4.5.1 Bulk isotope compositions of the Radix shells

The mean $\delta^{18}O$ values of the *Radix* shells exhibit a long-term trend to more negative values from 4200 cal yr BP until present which is similar to the ostracod calcite values reported in Mischke et al. (2010; Figure 34C). The notional equilibrium lines (Figure 34C) are based on the assumption of a steady state of the lake when the input by precipitation and meltwater equals the output by evaporation. The similar isotope trends provide evidence that *Radix* and ostracods shared the same habitat in the deeper water column of the relatively shallow eastern basin of Lake Karakul, in contrast to the assumption by Mischke et al. (2010) that the analyzed ostracod species lived within the uppermost sediments. The long-term trend is caused by a decrease of the isotope fractionation during evaporation of the lake water, which is dependent on humidity and temperature. Changes of temperature and relative humidity in turn, are controlled by changes of solar insolation intensity which has decreased since 4200 cal yr BP (Laskar et al. 2004; Figure 34A). The decreasing $\delta^{18}O$ trend (Figure 34C) is a result of decreasing air temperature but follows a long-term equilibrium. Changes of the meltwater flux to the lake disturb this equilibrium on much shorter time scales.

The dynamic of the *Radix* $\delta^{18}O$ curve mirrors several environmental parameters such as changes in the meltwater flux, water temperature, or dry periods (Figure 34C). Therefore a detailed interpretation of individual mean $\delta^{18}O$ values is difficult. However, the characterization of these processes can be provided by the sclerochronological *Radix* shell patterns which exemplify seasonal climatic and environmental changes (Taft et al. 2012, 2013).

The range of the $\delta^{18}O$ *Radix* shell values is higher than that of the ostracod shells (Figure 34C). This is probably caused by different temporal resolutions of the archives. Whereas one mean oxygen isotope value of a *Radix* shell averages a maximum of 1.5-2.5 years, each ostracod sample of ten individual shells may integrate the summer months of about 30 years (Mischke et al. 2010). However, both archives show similar trends in most core sections, even considering that $\delta^{18}O$ values of *Radix* aragonite should be generally about 0.6 ‰ higher than that of ostracod calcite if any vital-effects can be excluded (Grossman and Ku 1986; Abell and Williams 1989; Leng and Marshall 2004). It is assumed that an individual ostracod shell represents calcification during a

period as short as a day in the summer half year. The detailed sclerochronological *Radix* patterns indicate that the bottom lake water has a 0.5-1.0 ‰ lower $\delta^{18}O$ value during the summer months compared to the annual mean which explains the similarity of *Radix* and ostracod isotope ratios. In their multi-proxy study, Mischke et al. (2010) concluded that the studied Ostracoda taxon from Lake Karakul is probably not suitable for palaeoecological inferences in this region due to its assumed endobenthic habitat. However, the similarity between the *Radix* and the ostracod shell isotope data demonstrates that the ostracod dataset provides significant information.

$\delta^{18}O$ values of authigenic aragonite and ostracod calcite have different ranges and are partly opposite (Mischke et al. 2010; Figure 34C). This is most likely due to the fact that authigenic aragonite precipitates in the near surface water reflecting its isotope composition and temperature, and ostracod calcite is formed in the deeper water column primarily depending on the isotope composition of the water. A strong warming of the surface water is indicated for the period around 1500 cal yr BP (Figure 34C) which caused a higher evaporation mirrored by high *Radix* and ostracod $\delta^{18}O$ values. The following signal of glacial meltwater flux between ca. 1400 and 1200 cal yr BP, indicated by lower ostracod $\delta^{18}O$ values, most likely overprints the temperature effect in the $\delta^{18}O$ values of authigenic aragonite.

Interpreting the sclerochronological *Radix* shell pattern (Figure 33) is helpful to understand the $\delta^{18}O$ compositions of ostracod shells and authigenic aragonite from the sediment core in more detail. For this reason we grouped the isotope patterns in three sections of different inferred climate and environmental conditions.

4.5.2 Sclerochronological isotope patterns

Zone I (~ 4200-1800 cal yr BP, 104-45 cm core depth)

Core section 95 cm (~3850 cal yr BP): $\delta^{18}O$ and $\delta^{13}C$ shell values run nearly parallel which is typical for closed-basin lakes (Figure 33 and Figure 34D; Taft et al. 2013). This covariance mirrors the equilibration of the DIC in the lake water with atmospheric CO_2 (Talbot 1990; Li and Ku 1997; Lamb et al. 2002). Furthermore, because the $\delta^{13}C$ follows the $\delta^{18}O$ shell values, this pattern represents lake internal processes and not a signal from the catchment. The absolute $\delta^{18}O$ value is the highest in the whole core which indicates high evaporation and reduced meltwater input. The sclerochronological pattern is characterized by three peaks and subsequent decreasing values. This pattern points to a *Radix* specimen which lived more than two years. This inference is remarkable because modern *Radix* shells usually have a life span of about 12 to 16 months (Taft

et al. 2012, 2013). The sections from [t] to [m] and from [j] to [f] probably reflect meltwater input of two consecutive years which is supported by slightly decreasing δ^{13}C values representing inflow of allochthonous carbon with low δ^{13}C values from the catchment area. The increasing δ^{18}O and δ^{13}C values from [m] to [j] and from [f] to [c] mirror increasing evaporation and increasing biological activity in the lake. In general, the meltwater signal in this *Radix* shell is not well pronounced and the oxygen isotope values are high (> 0.00 ‰) during the whole life span of this specimen. Thus, at ~ 3850 cal yr BP glacial meltwater input during the summer months was most likely relatively low. Considering the life span of more than one year, it remains uncertain why the sclerochronological pattern does not mirror distinct ice cover periods during the winter months indicated by relatively constant isotope values. Probably the ice cover duration was reduced due to the warm conditions. Alternatively, the temperature effect overprinted the ice cover signal during the winter. The pollen composition and the ostracod oxygen isotope data for that period indicate warm and wet conditions (Mischke et al. 2010; Figure 34B,C).

Core section 89 cm (~3650 cal yr BP): The mean δ^{18}O value is lower than in the previous section indicating conditions near a steady state of the lake system (Figure 34C). Relatively balanced conditions concerning the amount of meltwater input and evaporation are therefore assumed. There is no distinct meltwater signal in the sclerochronological pattern. The δ^{13}C values between sub-samples [g] and [d] may represent biological productivity in the lake during the summer months.

Core section 84 cm (~3450 cal yr BP): The isotope shell pattern (Figure 33) shows a pronounced meltwater signal with decreasing δ^{18}O values from sub-samples [h] to [d]. If we consider that the meltwater input begins after the ice cover has disappeared in late May (Mischke et al. 2010), this shell section represents end of May to August / September. Increasing values to the latest shell [a] most likely mirror the increasing influence of evaporation. Increasing δ^{13}C values during and after the ice cover period indicate high lake productivity, comparable with the previous core section. The mean δ^{18}O value is rather low most likely as a result of decreasing air temperatures which is supported by more positive δ^{18}O values of authigenic aragonite (Mischke et al. 2010; Figure 34C) reflecting a cooling of the surface water .

Core section 83 cm (~3400 cal yr BP): The relatively high mean δ^{18}O value indicates another decrease of the meltwater flux compared to the previous section. The sclerochronological isotope pattern shows a slight meltwater signal in form of decreasing δ^{18}O values and subsequently increasing values as a result of evaporation. The δ^{13}C values are low from sub-sample [q] to [l] indicating input of light carbon originating from the catchment area. The ostracod calcite and authigenic aragonite δ^{18}O analyses give equivalent results (Mischke et al. 2010).

Core section 81 cm (~3300 cal yr BP): The lower mean $\delta^{18}O$ value points to increasing meltwater fluxes which is confirmed by $\delta^{18}O$ of authigenic aragonite (Mischke et al. 2010). The lower $\delta^{18}O$ ostracod value is concordant with the *Radix* shell value (Figure 34C). Because this shell was small and partly broken, the sclerochronological isotope pattern (Figure 33) is hard to interpret. However, the $\delta^{13}C$ values are high which indicates a lake internal source like biological productivity and not an input from the catchment. Mischke et al. (2010) reconstructed an abrupt shift to colder conditions around 3500 cal yr BP based on the TOC content, but such a sharp shift is not recorded in the *Radix* shells, most likely due to differing sample resolutions at this core section.

Core section 73 cm (~3050 cal yr BP): The lower mean $\delta^{18}O$ value indicates further increasing meltwater flux which is confirmed by lower ostracod $\delta^{18}O$ values (Mischke et al. 2010).The low TOC content and the higher $\delta^{18}O$ of authigenic aragonite suggest lower lake productivity and rather cooler conditions (Mischke et al. 2010; Figure 34C). The $\delta^{18}O$ and $\delta^{13}C$ values of the sclerochronological pattern run relatively parallel which points to a "lake-signal" not significantly influenced by processes originating in the catchment. Further information is hardly to provide due to the curtness of this pattern.

Zone II (~ 1800-500 cal yr BP, 44-8 cm core depth)

Core section 43 cm (~1800 cal yr BP): The low mean $\delta^{18}O$ value indicates a higher meltwater flux. The sclerochronological pattern represents two negative $\delta^{18}O$ and $\delta^{13}C$ peaks at sub-samples [k] and [h] indicating freshwater input followed by an evaporation signal. Compared to core section 95 and 84 cm, these meltwater fluxes are short-term events. In contrast, Mischke et al. (2010) reconstructed a rather low freshwater inflow based on $\delta^{18}O$ values of authigenic aragonite. However, TOC values in the core increase as a result of higher lake productivity and palynological data indicate increasing temperatures (Mischke et al. 2010; Figure 34B).

Core section 35 cm (~1500 cal yr BP): The higher mean $\delta^{18}O$ value indicates strong evaporation which is supported by the ostracod oxygen isotope data (Mischke et al. 2010; Figure 34C), most likely as a result of warmer conditions. The isotope composition of authigenic aragonite mirrors a warming of the surface water. A meltwater signal is not detectable in the sclerochronological shell pattern (Figure 33 andFigure 34D) and it is noticeable that the $\delta^{18}O$ and $\delta^{13}C$ pattern run relatively parallel indicating a high evaporation rate and a lake-intern signal. From sub-samples [q] to [h] both isotope values increase as a result of increasing evaporation and increasing biological productivity in the lake and/or exchange with atmospheric CO_2.

Core section 25 cm (~1100 cal yr BP): The mean $\delta^{18}O$ value indicates near steady state conditions of the lake system (Figure 34C) compared to the previous section. However, the sclerochronological $\delta^{18}O$ pattern shows a high meltwater flux represented by decreasing values from sub-sample [u] to [i] and synchronously decreasing $\delta^{13}C$ values. From sub-sample [j] to [a] the meltwater discharge decreases and the $\delta^{13}C$ values mirror probably both the increasing biological productivity in the lake and the reduced input of allochthonous carbon. Increasing oxygen isotope values from [i] to [a] represent increasing evaporation. Lower $\delta^{18}O$ values of authigenic aragonite indicate warm surface water (Mischke et al. 2010; Figure 34C).

Core section 23 cm (~1000 cal yr BP): The mean $\delta^{18}O$ value is higher compared to the previous section and is interpreted as a return of drier conditions which is supported by warmer surface water represented by negative $\delta^{18}O$ values of authigenic aragonite and a positive peak of $\delta^{18}O$ in the Ostracoda data set (Mischke et al. 2010; Figure 34C). The sclerochronological pattern shows two different aspects: a "lake-signal" represented by synchronously decreasing $\delta^{18}O$ and $\delta^{13}C$ values from [m] to [k], and a "catchment-signal" represented by still decreasing $\delta^{18}O$ values but increasing $\delta^{13}C$ values from [k] to [d] caused by biological productivity in the lake. A high TOC content was recorded in the core (Mischke et al. 2010). Palynological data indicate a tendency to slightly warmer but drier conditions (Mischke et al. 2010; Figure 34B).

Core section 19 cm (~900 cal yr BP): The lower mean $\delta^{18}O$ value indicates meltwater flux which is supported by the ostracod data (Mischke et al. 2010; Figure 34C). However, the sclerochronological pattern exhibits relatively parallel $\delta^{18}O$ and $\delta^{13}C$ trends and does not show a clear meltwater signal. Increasing $\delta^{18}O$ values from [n] to [j] most likely represent increasing evaporation and decreasing values between [j] and [h] probably mirror a slight meltwater influx. The high $\delta^{13}C$ values indicate a high biological productivity in the lake during the whole life span of this specimen.

Core section 18 cm (~880 cal yr BP): The mean $\delta^{18}O$ value is only slightly higher indicating relatively similar conditions to that of the previous section. Lower $\delta^{18}O$ values of authigenic aragonite and higher $\delta^{18}O$ values ostracod calcite mirror slightly warmer water and air temperature (Mischke et al. 2010; Figure 34C). The sclerochronological pattern (Figure 33) shows decreasing $\delta^{18}O$ values from [p] to [j] which probably indicate meltwater inflow to the lake. This is probably also indicated by decreasing $\delta^{13}C$ values from [m] to [k]. Close to the shell aperture, increasing biological productivity in the lake is mirrored by high $\delta^{13}C$ values. From [j] to [a] both isotope patterns run relatively parallel, indicating a "lake-signal".

Core section 15 cm (~780 cal yr BP): The mean δ^{18}O value shows a positive shift due to a higher evaporation rate most likely as a result of warmer conditions compared to the previous section. This is confirmed by a positive trend in the δ^{18}O ostracod data and decreasing δ^{18}O values of authigenic aragonite (Mischke et al. 2010, Figure 34C). The high δ^{13}C shell values indicate a low inflow and / or that the climate conditions were favorable for biological productivity. Because this shell was partly broken and the upper part was lacking, the sclerochronological pattern is too short to infer further information about seasonal changes.

Core section 11 cm (~650 cal yr BP): The lower mean δ^{18}O value indicates conditions relatively similar to the sections 19 cm and 18 cm, mirroring near steady state conditions which is supported by lower δ^{18}O ostracod values (Mischke et al. 2010; Figure 34C). However, the ^{18}O ratios of authigenic aragonite decreases at the same time, which points to a change in the isotope water composition, possibly by increasing evaporation due to warmer conditions. The sclerochronological isotope pattern (Figure 33) shows increasing δ^{18}O values from sub-samples [f] to [a] representing increasing evaporation. A slight meltwater signal is possibly shown from [i] to [f]. The δ^{13}C values are relatively high and stable along the whole pattern indicating a high biological productivity in the lake which is supported by a relatively high TOC content (Mischke et al.2010).

Zone III (~500 cal yr BP-present, 7-0 cm core depth)

Core section 6 cm (~350 cal yr BP): The mean δ^{18}O value is the lowest of all samples which maybe indicates high meltwater flux to the lake confirmed by δ^{18}O values of ostracods showing a positive peak at the same time indicating warmer conditions (Mischke et al. 2010; Figure 34C). The positive peak of the authigenic aragonite δ^{18}O values indicates rather cold surface water conditions maybe as a result of the cold meltwater input. Because the shell was very small and only a few sub-samples could be obtained, the sclerochronological shell pattern is difficult to interpret. However, the δ^{13}C values are high which point to a high biological productivity in the lake.

Core section 5 cm (~300 cal yr BP): The mean δ^{18}O value is still low during this period indicating high meltwater flux which is supported by low δ^{18}O ostracod values (Mischke et al. 2010; Figure 34C). The sclerochronological isotope pattern (Figure 33) shows a meltwater signal from [l] to [e] by decreasing δ^{18}O values. However, the δ^{13}C values do not indicate a high flux of light carbon from the catchment into the lake, instead, the values increase from [i] to [c]. Most likely the meltwater signal is overlain by a temperature signal during the summer months.

Core section 1 cm (~40 cal yr BP): The higher mean δ^{18}O value indicates less meltwater input likely due to slightly colder conditions compared to the previous section which is confirmed by lower δ^{18}O ostracod values (Mischke et al. 2010; Figure 34C). However, the reduced meltwater flux can also be a result of lacking glaciers masses in the catchment because it is assumed that they had melted in the period after 1500 cal yr BP. The slightly higher δ^{18}O values of authigenic aragonite point to relatively cold surface water, however, the general trend to more negative values from ca. 300 cal yr BP until present indicates increasingly warmer conditions. The sclerochronological δ^{18}O values show again a distinct signal of meltwater input to Lake Karakul at sub-samples [k] to [f] which probably reflect the period from ~May to July with decreasing values due to the significantly more negative δ^{18}O values of inflowing streams in comparison to the lake water (Figure 33 and Figure 34C). From [f] to [c] the values increase again as a result of increasing evaporation. The ice cover period for that winter period is probably reflected by the shell section from [p] to [l]. The δ^{13}C signal shows a relatively high variability even during the ice cover period. It can be assumed that the snow cover on the lake ice was reduced which enabled the light to penetrate deeper through the ice. Thus, the primary production could continue during the winter months. Increasing δ^{13}C shell values from [j] to [a] reflect increasing biological productivity during the summer months.
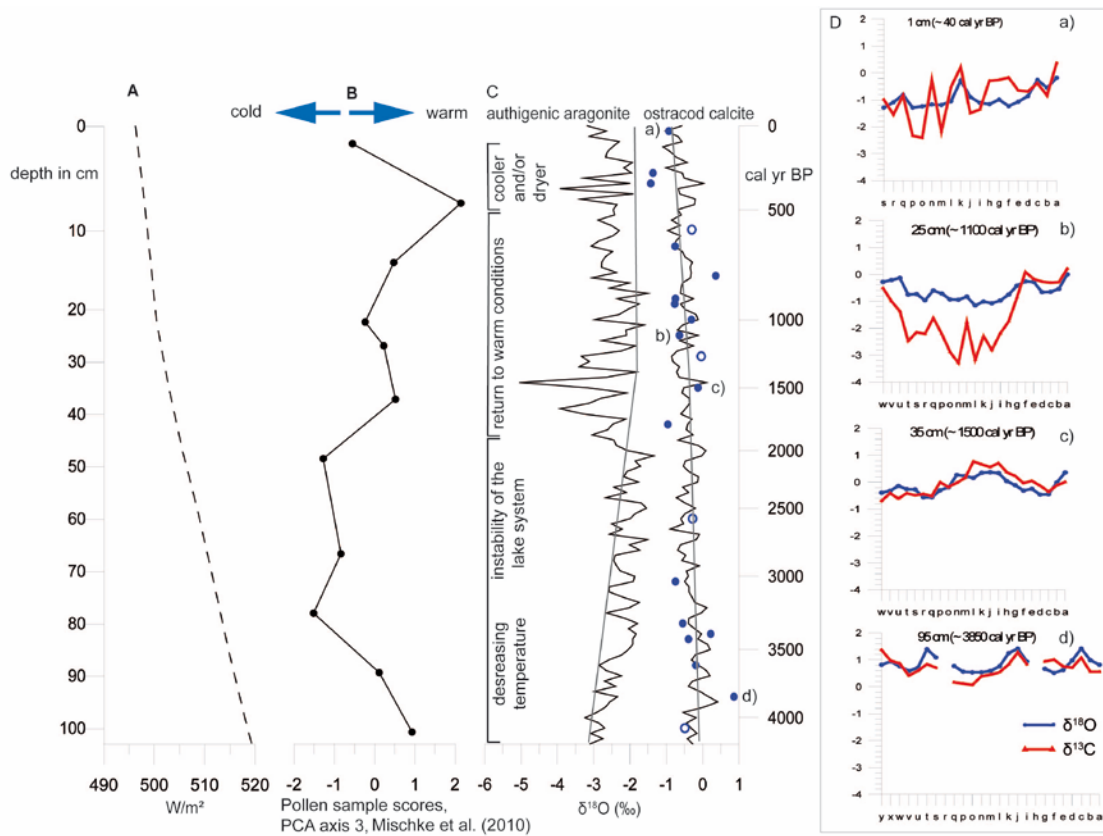
Figure 34: A) Summer (JJA) insolation curve for 39°N from 4200 cal yr BP until present generated following Laskar et al. 2004). B) Palynological data from the sedimen core of Lake Karakul after Mischke et al. (2010). The sample scores of pollen principle component analysis (PCA) axis 3 mainly indicate air temperatures. C) Mean δ18O values from *Radix* shells (filled blue circles) in comparison to ostracod calcite, which represents the same habitat conditions, and authigenic aragonite, which represents surface water conditions. Four *Radix* shells were isotopically measured as bulk samples (open blue circles). The grayish lines represent notional equilibrium-lines. Lower-case letters illustrate the sections of the sclerochronological patterns representing the four different zones characterizing varying climate and environmental conditions at Lake Karakul (D).

4.6 Summary and comparison with other records

Zone I (~ 4200-1800 cal yr BP, 104-45 cm core depth): Low lake level, increasing instability of the lake system, glacier advance, cooling

The mean δ18O shell values show a slight negative trend (Figure 34C) which primarily indicates decreasing air temperatures during this period. This is most likely a result of a decreasing summer insolation intensity (Figure 34A). The *Radix* shell data as well as the ostracod data from Mischke et al. (2010) indicate a decreasing glacial meltwater input flux to Lake Karakul during this period. It is assumed that the reduced input caused a lowering of the lake level and a reduced water surface area. At the same time, the δ18O values of authigenic aragonite increase which is probably caused

103

by a cooling of the surface lake water by up to 4°C, following the equation after Dettman et al. (1999). The cooling and the reduction of the meltwater input flux occurred in several steps, interrupted by warmer phases with enhanced meltwater input. It is assumed that the glaciers in the catchment generally expanded between ca. 4200 and 3000 cal yr BP.

Advancing glaciers and colder conditions were reconstructed for ca. 4200 and 3300 cal yr BP in the Muztag Ata and Kongur Shan region located about 150 km east-southeast of Lake Karakul, based on remote sensing, geomorphic mapping, and [10]Be terrestrial cosmogenic nuclide (TCN) surface-exposure dating of boulders (Seong et al. 2009). Hedrick et al. (2011) dated moraines in the Ladakh and Zanskar Ranges of Transhimalaya by using cosmogenic [10]Be and inferred glacier advances around 4.2 and 3.6 ka. A cold-period was also inferred for other Central Asian records, e.g. from Bosten Lake in northwestern China from 3.4-3.2 ka cal yr BP (Wünnemann et al. 2006), the central Tienshan between 3.5-2.1 ka cal yr BP (Zhang et al. 2009) or the Guliya ice core on the northwestern Tibetan Plateau between 3.5-3.0 ka cal yr BP (Thompson et al. 2005).

$\delta^{18}O$ values of *Radix*, ostracods and authigenic aragonite indicate oscillations of climate conditions and lake levels (Mischke et al. 2010; Figure 34C) but in general still relatively cold conditions until ca. 1800 cal yr BP. This period is characterized by an increasing instability of the lake system. It is assumed that the glaciers in the catchment had built up the ice volume during the previous period. The lake level was most likely still low because it is assumed that the glacial meltwater input to Lake Karakul was still reduced.

High evaporation but wet conditions and a low water level have been reported for the period between ca. 3200 and 2100 cal yr BP at lake Bangong Co located at the westernmost Tibetan Plateau (Gasse et al. 1996). A lake level low stand due to a long dry period was also suggested for ca. 3700-2400 cal yr BP for Lake Qinghai located on the northeastern Tibetan Plateau (Liu et al. 2011). Wünnemann et al. (2010) reconstructed mostly dry conditions and a shallow water level for the Tso Kar basin in Ladakh in India which is supported by a low moisture index value for the lake Tso Moriri area in the northwestern Himalaya (Leipe et al. 2013).

Zone II (~1800-500 cal yr BP, 44-8 cm core depth): Increasing meltwater input, increasing lake level, glacier retreat, warming

Between ca. 1800 and 1500 cal yr BP, the $\delta^{18}O$ values of authigenic aragonite, ostracod and *Radix* shells point to a strong warming of the surface water indicated by sharp declines and rises, respectively (Mischke et al. 2010; Figure 34C). The sclerochronological pattern of the *Radix* shell

from 35 cm core depth confirms the change to warmer and probably drier conditions which caused a higher evaporation rate (Figure 33 and Figure 34D). This period is characterized by a turnaround of the climate and environmental conditions at Lake Karakul which was already foreshadowed by the previous period. Until ca. 1800 cal yr BP, the glaciers in the catchment were thus far built up and the albedo was relatively high that a longer warm phase was needed to trigger an extensive glacier retreat. It is assumed that large masses of meltwater flowed into the lake and changed the isotope composition of the water which is indicated by negative $\delta^{18}O$ values of authigenic aragonite and ostracod calcite between ca. 1400 and 1200 cal yr BP (Mischke et al. 2010; Figure 34C). It is assumed that the isotope composition of the lake water deviated from the long-term isotopic equilibrium caused by this effective interference of the lake system.

Subsequently, as a result of the glacier retreat, the albedo decreased in this area. This self-reinforcing process most likely caused even warmer local conditions. These assumptions are primarily based on the core record from Mischke et al. (2010) due to the lack of a sclerochronological pattern. Between ca. 1200 and 500 cal yr BP the lake system seemed to approach a new steady state which is characterized by fluctuations of warmer and slightly cooler conditions and varying lake levels.

Narama (2002) found evidence for a retreat of the large Raigorodskogo Glacier (Pamir-Altai) as a result of a warm period shortly before 1545 cal yr BP. In contrast, Seong et al. (2009) dated moraines by [10]Be surface-exposure dating indicating a glacier advance around 1400 cal yr BP in the Muztag Ata and Kongur Shan region in westernmost Tibet. Boomer et al. (2000) found evidence for a maximum regression phase of Lake Aral around 1600 cal yr BP. The assumed strong warming around 1500 cal yr BP at Lake Karakul corresponds with the onset of the North Atlantic Medieval Warm Period and a maximum of the Indian monsoon intensity (Gupta et al. 2003).

Zone III (~500 cal yr BP-present, 8-0 cm core depth): Cool and dry (?) between ~500-300 cal yr BP, since ~ 300 cal yr BP increasing lake level and temperature?

As it can be seen in the ostracod dataset, the $\delta^{18}O$ of the lake has not been moved from the equilibrium (steady state; Figure 34C). Relatively cold and dry conditions are suggested for the period between around 350 cal yr BP possibly representing the LIA of Europe and the North Atlantic region. Subsequently increasing meltwater flux and an increasing lake level due to a slight warming is assumed for the period from ca. 300 cal yr BP until present. This inference of recent warming corresponds to several studies which confirm negative glacier mass balances for Central Asia since the first half of the 19th century due to warmer conditions (Unger-Shayesteh et al.

2013). However, the ice volume of the glaciers in the catchment of Lake Karakul was relatively small after the previous melting period and the amount of the meltwater flux is assumed to be low.

The first cooler and probably drier phase corresponds to inferred drier conditions from the Aral Sea, parts of the catchment are located only ca. 200 km south of Lake Karakul, between 500 and 400 cal yr BP (Boomer et al. 2000; Filippov and Riedel 2009) and from Sumxi Co at ca. 400 cal yr BP (Gasse et al. 1996).

4.7 Conclusions

The aim of this study was to test the hypothesis whether changes of the hydrologic system of Lake Karakul were primarily triggered by changing meltwater flux since 4200 cal yr BP as it was previously suggested by Mischke et al. (2010). The δ^{18}O and δ^{13}C record of 21 fossil *Radix* shells were compared with δ^{18}O ratios of ostracod shells and authigenic aragonite which have been interpreted by Mischke et al. (2010). Our results demonstrate that changes of the hydrologic system are not only triggered by meltwater fluxes but are more complex and additionally triggered by changes in temperature.

The decreasing long term δ^{18}O trend of *Radix* and ostracod shells mainly indicates decreasing air temperature causing a higher relative humidity. Over the last 4200 years, the general isotopic composition of the lake water follows the decreasing solar insolation. This isotopic trend is overprinted by short-term meltwater flux rates. The similarity between the *Radix* and the ostracod δ^{18}O values reflects the same benthic habitat conditions. Furthermore, the similarity demonstrates that palaeoecological conclusions can be inferred by the studied, probably endemic ostracod taxon, although Mischke et al. (2010) interpreted the data with certain limitation.

The period between 4200-3000 cal yr BP is characterized by cooling, and stepwise decreasing lake level and, most likely, a glacier advance in the catchment. From ca. 3000-1800 cal yr BP, the lake system became instable but the lake level remained low. The period 1800-1200 cal yr BP is characterized by a turnaround of the climate and environmental conditions, marked by increasing meltwater input due to warmer conditions, a glacier retreat and an increasing lake level. The assumed strong warming around 1500 cal yr BP probably represents the onset of the Medieval Warm Period. Warmer conditions and a higher lake level are indicated for the period until ca. 500 cal yr BP. A short relatively cold and probably dry period associated with a change of the lake level is assumed for the phase from around 350 cal yr BP, probably indicating the LIA.

106

Subsequently, an increasing lake level and a higher temperature until present are indicated by our results.

However, further studies are required to quantify the amount of former meltwater discharge, associated lake level changes, and to investigate the glacial history in the catchment area.

5. Synthesis and outlook

This doctoral thesis was composed of three major working steps and key questions. In the first step, it was tested whether sclerochronological $\delta^{18}O$ and $\delta^{13}C$ ratios in shells of the gastropod *Radix* mirror modern climate and environmental conditions on the TP at all. The study of a total of six modern shells from two lakes which are located under monsoonal influence provides valuable information on various parameters characterizing regional climate and lake environments. The oxygen isotope compositions in the shells are mainly dominated by precipitation and inflows if water residence times are short. If the water residence time is long (~ several tens of years), the isotope shell patterns exhibit less variation. An essential conclusion of the first working step is that the sclerochonological isotope shell patterns show a distinct "monsoon signal" composed of steep increasing $\delta^{18}O$ values during the first monsoon rains and subsequently gradually decreasing values during the peak of the monsoon. Thereby the isotopically light carbon in the shells is coupled with the monsoon precipitation (Chapters 2 and 3). Compared with meteorological data recorded during the life span of the *Radix* specimens, the sclerochronological shell patterns provide an archive with sub-monthly resolution.

In the second step, this study was spatially extended and a total of 14 shells from seven lakes across the TP were isotopically analysed to learn more about the interannual variability of precipitation patterns and how different hydrologic systems react to different climatic factors. The main result is that that sclerochronological $\delta^{18}O$ and $\delta^{13}C$ values of modern *Radix* shells mirror the different climate conditions, which are a result of the different lake settings, without noticeable dependence on the particular lake system. In comparison to other climate archives from the TP, the sclerochronological isotope patterns from the archive *Radix* mirror general climatic differences and trends as well as interannual and even sub-monthly changes on a plateau-wide scale. The sclerochronological patterns exhibit an increasing influence of precipitation and a decreasing influence of evaporation on the isotope compositions from west to east. The $\delta^{18}O$ values of shells from lakes on the eastern and central TP mirror monsoon signals, indicated by more negative values and higher variabilities compared to the more western lakes.

The last step of this study was to test whether the isotope compositions of fossil shells indicate different climatic and environmental parameters for the last 4200 cal yr BP at Lake Karakul. The main aim was to test the hypothesis whether changes in the hydrologic system of the lake were primarily triggered by changing meltwater flux as was previously suggested by Mischke et al., (2010). The $\delta^{18}O$ and $\delta^{13}C$ record of 21 fossil *Radix* shells from a lake sediment core were

compared with $\delta^{18}O$ ratios of ostracod shells and authigenic aragonite which have been interpreted by Mischke et al., (2010). The results demonstrate that changes in the hydrologic system are not only triggered by meltwater fluxes but are more complex and additionally triggered by changes in temperature. With the aid of sclerochronological patterns of the fossil shells, it is possible to distinguish between meltwater fluxes and precipitation, which is an essential step for the interpretation of multi-proxy studies of lake sediment cores.

5.1 Do we need another climate archive?

Considering the multitude of archives which are used for palaeoclimate reconstructions, it is a valid question whether we really need another archive. In this doctoral thesis it has been demonstrated that the interpretation of sclerochronological $\delta^{18}O$ and $\delta^{13}C$ patterns provides important additional information on single seasonal climate events. This information not only supplements limnological multi-proxy studies but also provides a more detailed insight into limnologic and climatic processes. This extra knowledge facilitates the understanding of the hydrology and moisture transport pathways on the TP, which is essential for more than 1 billion people in Asia. Moreover, with the aid of the new archive which provides a deeper insight into single climate processes and interactions, the understanding of natural climate (extreme) events improve. This knowledge is important for future climate predictions particularly in respect of the anthropogenic factor.

The question whether another climate archive is needed can be clearly affirmed. The sclerochronological isotope patterns of *Radix* shells are able to validate assumptions based on limnological multi-proxy studies and should be involved whenever fossil shells are found.

Because the $\delta^{18}O$ and $\delta^{13}C$ shell patterns mirror a distinct monsoon signal in regions which are monsoon influenced, studying lake level highstands in respect of monsoon evolution and intensity is a promising further approach.

5.2 Moisture transport pathways to the TP: implications from the new archive *Radix*

Stable isotope compositions of living *Radix* as well as fossil shells were studied from various lake systems. These lake systems are scattered across the TP, being located in different climatic and tectonic settings. This doctoral thesis has demonstrated that climatic and environmental signals preserved in modern and fossil shells allow conclusions about moisture transport pathways to the TP. Lakes which are beyond monsoon influence at the present time may have been reached by

monsoon precipitation in the past, which can be proved by the sclerochonological isotope patterns in the shells. $\delta^{18}O$ values in shells obtained from lakes which are located under monsoon influence mirror a characteristic "monsoon pattern" (Manuscript I and II). These signals can be compared to and integrated with geomorphological evidence of former lake level highstands such as palaeoshorelines providing detailed information about former atmospheric circulation patterns and moisture pathways. Because the ^{18}O ratios of precipitation are dependent on altitude and rainout history (Lee and Fung, 2007), it is possible to localize the moisture sources. This signal is mirrored in the shells, which represent a potential means by which to study changes of moisture sources in the past on the TP and in surrounding regions.

5.3 Outlook and open questions

The results of this doctoral thesis have demonstrated that the new archive *Radix* provides valuable information about climate and environmental conditions on the TP and in surrounding regions. Comparing the isotope compositions of fossil shells with multi-proxy analyses of lacustrine sediments, as was conducted at Lake Karakul in Tajikistan, is an essential step towards understanding different influencing parameters on lake systems. Sclerochronological isotope patterns in the shells clearly mirror the influence of meltwater on Lake Karakul. Deciphering meltwater and precipitation cannot be done using conventional multi-proxy analyses due to the lower temporal resolution. Thus, the approach of combining sclerochronological *Radix* datasets with geochemical results of lacustrine sediments and geomorphological observations in the catchment should be developed in the future whenever fossil shells are found. Varved sediments are most adequate in such studies due to the seasonal resolution at best. However, lakes with varved sediments are not known on the TP. In my opinion, it would be helpful if actual sedimentary trap data from a well monitored existent lake were available in order to compare it with modern *Radix* shells first. This would be essential to improve our understanding of the sclerechronological isotope patterns and shell accretion. These results should be compared with meteorological datasets and water chemistry.

The sclerochronological shell $\delta^{18}O$ values mirror distinct monsoon signals in lakes which are located under monsoon influence (Taft et al., 2012, 2013). If this signal is found in fossil shells in regions which are nowadays not under monsoon influence, conclusions about former monsoon limits and moisture transport pathways can be drawn. Moreover, extreme precipitation events can be detected and compared with archaeological findings to study the effects on human history and settlements.

Topographic reliefs have an intensely strong effect on the isotopic composition of precipitation. The ^{18}O composition becomes lighter with increasing altitude because air masses hold less water when they are cooled (Sharp, 2007). More rainout of the heavier oxygen isotope occurs. This "altitude effect" can be used to model palaeoaltitudes of the TP. This approach will be focused on the basis of fossil *Radix* shells from the Zhada Basin in the south-western part of the TP. This basin is located ca. 4,000 m a.s.l. and represents a potential pathway for the Indian monsoon moisture onto the TP in the past. Today, the basin is not reached by the monsoon (Clift and Plumb, 2008). Fossil shells from Miocene lacustrine sediments will be studied and if there is a monsoon signal in the shells, the Himalayan mountain range must have been lower during a certain time period. These results will contribute to an understanding of the uplift history of the TP. Moreover, if the Indian monsoon reached the Zhada Basin in the past, what are the possible effects on the atmospheric circulation in this area?
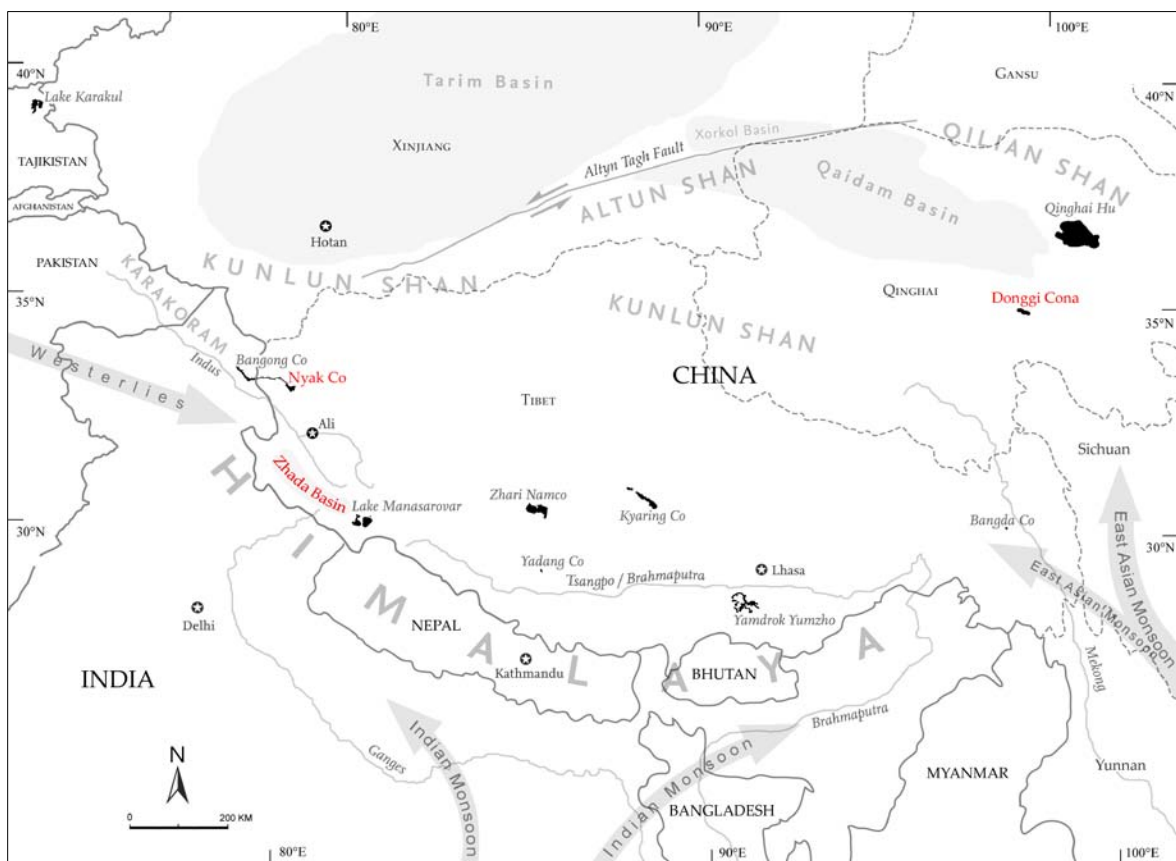
Figure 35: Overview map illustrating the two lake systems of Nyak Co and Donggi Cona and the intramontane Zhada Basin. Future studies with fossil *Radix* shells will be conducted at these locations.

The comparison of two extant lake systems on the TP each exhibiting Late Glacial and Holocene sediments in the catchment will help in the investigation of changes of moisture conditions and hydrological dynamics in the past. Lake Donggi Cona is located on the eastern margin of the TP and fossil *Radix* shells have been found in sediment outcrops in the catchment. The lake system is

111

located in a transition zone between the East Asian monsoon, the Indian monsoon and the westerlies, which makes this lake particularly sensitive to climate changes. The other lake, Nyak Co, is located on the western TP, influenced by the westerlies and only exceptionally influenced by the Indian monsoon. Fossil *Radix* shells were found ca. 370 m above the present lake level; a study will be conducted to determine whether this lake highstand was caused by intensified monsoon precipitation during the Holocene Climate Optimum. Both lake systems will be compared in order to characterize and quantify hydrological changes in the past and its trigger factors.

In summary, the new climate and environmental archive *Radix* opens up various options, to answer many open questions concerning changes in atmospheric and hydrologic conditions on the TP and in surrounding regions.

6. Overall references

Abell, P.I., 1985. Oxygen isotope ratios in modern African gastropod shells: A data base for paleoclimatology. *CHEMICAL GEOLOGY* 58, 183-193.

Abel,l P.I., Williams, A.J., 1989. Oxygen and Carbon isotope ratios in gastropod shells as indicators of paleoenvironments in the Afar Region of Ethiopia. *PALAEOGEOGRAPHY, PALAEOCLIMATOLOGY, PALAEOECOLOGY* 74, 265-278.

Abramovski, U., Bergau, A., Seebach, D., Zech, R., Glaser, B., Sosin, P., Kubik, P.W., Zech, W., 2006. Pleistocene glaciations of Central Asia: results from ^{10}Be surface exposure ages of erratic boulders from the Pamir (Tajikistan), and the Alay–Turkestan range (Kyrgyzstan). *QUATERNARY SCIENCE REVIEWS* 25, 1080-1096.

Aizen, V., Aizen, E., Melack, J., Martma, T., 1996. Isotopic measurements of precipitation on central Asian glaciers (southeastern Tibet, northern Himalayas, central Tien Shan). *JOURNAL OF GEOPHYSICAL RESEARCH* 101, 9185-9196.

An, Z.S., Clemens, S.C., Shen, J., Qiang, X.O., Jin, Z.D., Sun, Y.B., Prell, W.L., Luo, J.J., Wang, S.M., Xu, H., Cai, Y.J., Zhou, W.J., Liu, X.D., Liu, W.G., Shi, Z.G., Yan, L.B., Xiao, X.Y., Chang, H., Wu, F., Ai, L., Lu, F.Y., 2011. Glacial-interglacial Indian summer monsoon dynamics. *SCIENCE* 333, 719-723.

An, Z.S., Kutzbach, J.E., Prell, W.L., Porter, S.C., 2001. Evolution of Asian monsoons and phased uplift of the Himalyan-Tibetan plateau since Late Miocene times. *NATURE* 411, 62-66.

An, Z.S., Porter, S.C., Kutzbach, J.E., Wu, X.H., Wang, S.M., Liu, X.D., Li, X.Q., Zhou, W.J., 2000. Asynchronous Holocene optimum of the East Asian monsoon. *QUATERNARY SCIENCE REVIEWS* 19, 743-762.

Anderson, D.M., Overpeck, J.T., Gupta, A.K., 2002. Increase in the Asian southwest monsoon during the past four centuries. *SCIENCE* 297, 596-599.

Araguás-Araguás, L., Froehlich, K., Rozanski, K., 1998. Stable isotope composition of precipitation over southeast Asia. *JOURNAL OF GEOPHYSICAL RESEARCH* 103, 28,721-28,742.

Arrowsmith, J.R., Strecker, M.R., 1999. Seismotectonic range-front segmentation and mountain-belt growth in the Pamir-Alai region, Kyrgyzstan (India-Eurasia collision zone). *GEOLOGICAL SOCIETY OF AMERICA BULLETIN* 111, 1665-1683.

Battarbee, R.W., 2000. Palaeolimnological approaches to climate change, with special regard to the biological record. *QUATERNARY SCIENCE REVIEWS* 19, 107-124.

Benn, D.I., Owen, L.A., 1998. The role of the Indian summer monsoon and the mid-latitude westerlies in Himalayan glaciations: review and speculative discussion. *JOURNAL OF THE GEOLOGICAL SOCIETY, LONDON* 155, 353-363.

Blisniuk, P.M., Hacker, B.R., Glodny, J., Ratschbacher, L., Bik, S., Wuk, Z., McWilliams, M.O., Calvert, A., 2001. Normal faulting in central Tibet since at least 13.5 Myr ago. *NATURE* 412, 628-632.

Bolch, T., 2007. Climate change and glacier retreat in northern Tien Shan (Kazakhstan/Kyrgyzstan) using remote sensing data. *GLOBAL AND PLANETARY CHANGE* 56, 1-12.

Bonadonna, F.P., Leone, G., Zanchetta, G., 1999. Stable isotope analyses on the last 30 ka molluscan fauna from Pampa grassland, Bonaerense region, Argentinia. *PALAEOGEOGRAPHY PALAEOCLIMATOLOGY PALAEOECOLOGY* 153, 289-308.

Bookhagen, B., Burbank, D.W., 2006. Topography, relief, and TRMM-derived rainfall variations along the Himalaya. *GEOPHYSICAL RESEARCH LETTERS* 33, L08405, doi: 10.1029/2006GL026037.

Boomer, I., Aladin, N., Plotnikov, I., Whatley, R., 2000. The palaeolimnology of the Aral Sea: a review. *QUATERNARY SCIENCE REVIEWS* 19, 1259-1278.

Boos, W.R., Kuang, Z.M., 2010. Dominant control of the South Asian monsoon by orographic insulation versus plateau heating. *NATURE* 463, 218-223.

Bräuning, A., 2001. Climate history of the Tibetan Plateau during the last 1000 years derived from a network of Juniper chronologies. *DENDROCHRONOLOGIA* 19, 127-137.

Bräuning, A., Mantwill, B., 2004. Summer temperature and summer monsoon history on the Tibetan Plateau during the last 400 years recorded by tree rings. *GEOPHYSICAL RESEARCH LETTERS* 31, p. L24205.

Breitenbach, S.F.M., Adkins, J.F., Meyer, H., Marwan, N., Kumar, K.K., Haug, G.H., 2010. Strong influence of water vapor source dynamics on stable isotopes in precipitation observed in Southern Meghalaya, NE India. *EARTH AND PLANETARY SCIENCE LETTERS* 292, 212-220.

Brown, E.T., Bendick, R., Bourlès, D.L., Gaur, V., Molnar, P., Raisbeck, G.M., Yiou, F., 2003. Early Holocene climate recorded in geomorphological features in Western Tibet. *PALAEOGEOGRAPHY, PALAEOCLIMATOLOGY, PALAEOECOLOGY* 199, 141-151.

Burla, H., 1972. Die Abundanz von *Anodonta, Unio pictorum, Viviparus ater, Lymnaea auricularia* und *Lymnaea ovata* im Zürichsee in Abhängigkeit von der Wassertiefe und zu verschiedenen Jahreszeiten. *VIERTELJAHRSSCHRIFT DER NATURFORSCHENDEN GESELLSCHAFT IN ZÜRICH* 117, 129-151.

Cai, Y.J., Tan, L.C., Cheng, H., An, Z.S., Edwards, R.L., Kelly, M.J., Kong, X.G., Wang, X.F., 2010. The variation of summer monsoon precipitation in central China since the last deglaciation. *EARTH AND PLANETARY SCIENCE LETTERS* 291, 21-31.

Caley, T., Malaizé, B., Revel, M., Ducassou, E., Wainer, K., Ibrahim, M., Shoeaib, D., Migeon, S., Marieu, V., 2011. Orbital timing of the Indian, Easi Asian and African boreal monsoons and the concept of a 'global monsoon'. *QUATERNARY SCIENCE REVIEWS* 30, 3705-3715.

Chen, F., 2012. A discussion on the westerly-dominated climate model in mid-latitude Asia during the modern interglacial period. *QUATERNARY INTERNATIONAL* 279-280, 86-87.

Chen, F., Chen, J., Holmes, J., Boomer, I., Austin, P., Gates, J.B., Wang, N., Brooks, S., Zhang, J., 2010. Moisture changes over the last millennium in arid central Asia: a review, synthesis and comparison with monsoon region. *QUATERNARY SCIENCE REVIEWS* 29, 1055-1068.

Chengdu Institute of Geology and Mineral Resources, 2004. Geological map of the Qinghai-Xizang (Tibet) Plateau and adjacent areas. China Geological Survey, Chengdu.

Chinese Central Meteorological Office, 2010. Meteorological data of China. Meteorology Press, Beijing.

Clarke, A.H., 1973. The freshwater mollusks of the Canadian Interior Basin. *MALACOLOGIA* 13, 1-509.

Clemens, S., Prell, W., Murray, D., Shimmield, G., Weedon, G., 1991. Forcing mechanisms of the Indian Ocean monsoon. *NATURE* 353, 720-725.

Cook, E.R., Anchukaitis, K.J., Buckley, B.M., D'Arrigo, R.D., Jacoby, G.C., Wright, W.E., 2010. Asian monsoon failure and megadrought during the last millennium. *SCIENCE* 328, 486-489.

Cook, C.G., Jones, R.T., Langdon, P.G., Leng, M.J., Zhang, E.L., 2011. New insights on late Quaternary Asian palaeomonsoon variability and the timing of the last glacial maximum in southwestern China. *QUATERNARY SCIENCE REVIEWS* 30, 808-820.

Crowley, T.J., 2000. Causes of climate change over the past 1000 years. *SCIENCE* 289: 270-277.

Cui, X.F., Graf, F., 2009. Recent land cover changes on the Tibetan Plateau: A review. *CLIMATIC CHANGE* 94, 47-61.

Dansgaard, W., 1964. Stable isotopes in precipitation. *TELLUS* 16, 436-468.

Daut, G., Mäusbacher, R., Baade, J., Gleixner, G., Kroemer, E., Mügler, I., Wallner, J., Wang, J., Zhu, L., 2010. Late Quaternary hydrological changes inferred from lake level fluctuations of Nam Co (Tibetan Plateau, China). *QUATERNARY INTERNATIONAL* 218, 86-93.

Dettman, D.L., Kohn, M.J., Quade, J., Ryerson, F.J., Ojha, T.P., Hamidullah, S., 2001. Seasonal stable isotope evidence for a strong Asian monsoon throughout the past 10.7 m.y. *GEOLOGY* 29, 31-34.

Dettman, D.L., Reische, A.K., Lohmann, K.C., 1999. Controls on the stable isotope composition of seasonal growth bands in aragonitic fresh-water bivalves (unionidae). *GEOCHIMICA ET COSMOCHIMICA ACTA* 63, 1049-1057.

Dietze, E., Wünnemann, B., Diekmann, B., Aichner, B., Hartmann, K., Herzschuh, U., IJmker, J., Jin, H., Kopsch, C., Lehmkuhl, F., Li, S., Mischke, S., Niessen, F., Opitz, S., Stauch, G., Yang, S., 2010. Basin morphology and seismic stratigraphy of Lake Donggi Cona, north-eastern Tibetan Plateau, China. *QUATERNARY INTERNATIONAL* 218, 131-142.

Domrös, M., Peng,G.B., 1988. The climate of China. Springer. New York, Berlin, Heidelberg, 361 pp.

Dyckmans, J., n.d. Stable isotopes in terrestrial ecology – Introduction. Tutorial. Centre for stable isotope research and analysis. Georg August University Göttingen, Germany. Online access: http://www.uni-goettingen.de/en/71205.html.

Dykoski, C.A., Edwards, R.L., Cheng, H., Yuan, D.X., Cai, Y.J., Zhang, M.L., Lin, Y.S., Qing, J.M., An, Z.S., Revenaugh, J., 2005. A high-resolution, absolute-dated Holocene and deglacial Asian monsoon record from Dongge Cave, China. *EARTH AND PLANETARY SCIENCE LETTERS* 233, 71-86.

ESRI, 2011. ArcGIS Desktop: Release 10. Environmental Systems Research Institute, Redlands, CA.

Fan, Z.X., Bräuning, A., Tian, Q.H., Yang, B., Cao, K.F., 2010. Tree ring recorded May-August temperature variations since A.D. 1585 in the Gaoligong Mountains, southeastern Tibetan Plateau. *PALAEOGEOGRAPHY, PALAEOCLIMATOLOGY, PALAEOECOLOGY* 296, 94-102.

Fan, H., Gasse, F., Huc, A., Li, Y.F., Sifeddine, A., Soulié-Märsche, I., 1996. Holocene environmental changes in Bangong Co basin (Western Tibet). Part 3: Biogenic remains. *PALAEOGEOGRAPGY, PALAEOCLIMATOLOGY, PALAEOECOLOGY* 120, 65-78.

Feng, X.H., Cui, H.T., Tang, K.L., Conkey, L.E., 1999. Tree-ring δD as an indicator of Asian monsoon intensity. *QUATERNARY RESEARCH* 51, 262-266.

Filippov, A., Riedel, F., 2009. The late Holocene mollusk fauna of the Aral Sea and its biogeographical and ecological interpretation. *LIMNOLOGICA* 39, 67-85.

Fleitmann, D., Burns, S.J., Mangini, A., Mudelsee, M., Kramers, J., Villa, I., Neff, U., Al-Subbary, A.A., Buettner, A., Hippler, D., Matter, A., 2007. Holocene ITCZ and Indian monsoon dynamics recorded in stalagmites from Oman and Jemen. *QUATERNARY SCIENCE REVIEWS* 26, 170-188.

Fleitmann, D., Burns, S.J., Mudelsee, M., Neff, U., Kramers, J., Mangini, A., Matter, A., 2003. Holocene forcing of the Indian monsoon recorded in a stalagmite from southern Oman. *SCIENCE* 300, 1737-1739.

Fontes, J.C., Gasse, F., Gibert, E., 1996. Holocene environmental changes in Lake Bangong basin (Western Tibet). Part 1: Chronology and stable isotopes of carbonates of a Holocene lacustrine core. *PALAEOGEOGRAPHY, PALAEOCLIMATOLOGY, PALAEOECOLOGY* 120, 25-47.

Fritz, P., Poplawski, S., 1974. ^{18}O and ^{13}C in the shells of freshwater molluscs and their environments. *EARTH AND PLANETARY SCIENCE LETTERS* 24, 91-98.

Frömming, E., 1956. Biologie der mitteleuropäischen Süßwasserschnecken. Duncker & Humblot, Berlin.

Gadgil, S., 2003. The Indian monsoon and its variability. *ANNUAL REVIEW OF EARTH AND PLANETARY SCIENCES* 31, 429-467.

Gajurel, A.P., France-Lanord, C., Huyghe, P., Guilmette, C., Gurung, D., 2006. C and O isotope compositions of modern fresh-water mollusk shells and river waters from the Himalaya and Ganga plain. *CHEMICAL GEOLOGY* 233, 156-183.

Gasse, F., Arnold, M., Fontes, J.C., Fort, M., Gibert, E., Huc, A., Bingyan, L., Yuanfang, Y., Qing, L., Mélières, F., Van Campo, E., Wang, F., Zhang, Q., 1991. A 13,000-year climate record from western Tibet. *NATURE* 353, 742-745.

Gasse, F., Fontes, J.C., Van Campo, E., Wei, K., 1996. Holocene environmental changes in Bangong Co basin (Western Tibet). Part 4: Discussion and conclusions. *PALAEOGEOGRAPHY, PALAEOCLIMATOLOGY, PALAEOECOLOGY* 120, 79-92.

Gaten, E., 1986. Life cycle of *Lymnaea peregra* (Gastropoda: Pulmonata) in the Leicester canal, U.K., with an estimate of annual production. *HYDROBIOLOGIA* 135, 45-54.

Gautam, P.K., 2012. Climate change and conflict in South Asia. *STRATEGIC ANALYSIS* 36, 32-40.

Gittenberger, E., Janssen, A.W., Kuijper, W.J., Kuiper, J.G.J., Meijer, T., van der Velde, G., de Vries, J.N., 1998. De nederlandse zoetwatermollusken. Recente en fossiele weekdieren uit zoet en brak water. - Nederlandse Fauna 2. Nationaal Natuurhistorisch Museum Naturalis, KNNV Uitgeverij & EIS-Nederland, Leiden.

Gloaguen, R., Ratschbacher, L., (eds.), 2011. Growth and collapse of the Tibetan Plateau. Geological Society, London, Special Publications 353, 1-8.

Glöer, P., 2002. Die Süßwassergastropoden Nord- und Mitteleuropas. Conchbooks, Hackenheim.

Goehring, B.M., Vacco, D.A., Alley, R.B., Schaefer, J.M., 2012. Holocene dynamics of the Rhone Glacier, Switzerland, deduced from ice flow models and cosmogenic nuclides. *EARTH AND PLANETARY SCIENCE LETTERS* 351-352, 27-35.

Gopal, B., Ghosh, D., 2010. Lakes and reservoirs of Asia. Encyclopedia of inland waters, Lake ecosystem ecology. Likens, G.E. (ed.), Academic Press, 480 pp.

Grimes, S.T., Mattey, D.P., Hooker, J.J., Collinson, M.E., 2003. Paleogene paleoclimate reconstruction using oxygen isotopes from land and freshwater organisms: the use of multiple paleoproxies. *GEOCHIMICA ET COSMOCHIMICA ACTA* 67, 4033-4047.

Gröcke, D.R., Gillikin, D.P., 2008. Advances in mollusc sclerochronology and sclerochemistry: tools for understanding climate and environment. *GEO-MARINE LETTERS* 28, 265-268.

Grossman, E.L., Ku, T., 1986. Oxygen and carbon isotope fractionation in biogenic aragonite: temperature effects. *CHEMICAL GEOLOGY* 59, 59-74.

Gupta, A.K., Anderson, D.M., Overpeck, J.T., 2003. Abrupt changes in the Asian southwest monsoon during the Holocene and their links to the North Atlantic Ocean. *NATURE* 421, 354-357.

Gurov, E.P., Gurova, H.P., Rakitskaya, R.B., Yamnichenko, A.Y., 1993. The Karakul depression in Pamirs: The first impact structure in Central Asia. Abstract Volume of the 24th Lunar and Planetary Science Conference, Lunar and Planetary Institute, Lyndon B. Johnson Space Center Houston, 591-592.

Hailemichael, M., Aronson, J.L., Savin, S., Tevesz, M.J.S., Carter, J.G., 2002. $\delta^{18}O$ in mollusk shells from Pliocene Lake Hadar and modern Ethiopian lakes: implications for history of the Ethiopian monsoon. *PALAEOGEOGRAPHY, PALAEOCLIMATOLOGY, PALAEOECOLOGY* 186, 81-99.

Hammer, U.T., 1986. Saline Lake Ecosystems of the World. Monographiae Biologicae 59. Kluwer Academic Publishers, Dordrecht.

Harding, R., 2012. Water resources – How severe will freshwater resource shortages be on a regional scale? *PAGES NEWS* 20, 38.

Harris, N., 2006. The elevation history of the Tibetan Plateau and its implications for the Asian monsoon. *PALAEOGEOGRAPHY, PALAEOCLIMATOLOGY, PALAEOECOLOGY* 241, 4-15.

He, Y., Theakstone, W.H., Zhang, Z.L., Zhang, D., Yao, T.D., Chen, T., Shen, Y.P., Pang, H.X., 2004. Asynchronous Holocene climatic change across China. *QUATERNARY RESEARCH* 61, 52-63.

Hedrick, K.A., Seong, Y.B., Owen, L.A., Caffee, M.W., Dietsch, C., 2011. Towards defining the transition in style and timing of Quaternary glaciations between the monsoon-influenced Greater Himalaya and the semi-arid Transhimalaya of Northern India. *QUATERNARY INTERNATIONAL* 236, 21-33.

Henderson, A.C.G., Holmes, J.A., Zhang, J.W., Leng, M.J., Carvalho, L.R., 2003. A carbon- and oxygen-isotope record of recent environmental change from Qinghai Lake, NE Tibetan Plateau. *CHINESE SCIENCE BULLETIN* 48, 1463-1468.

Herzschuh, U., 2006. Palaeo-moisture evolution in monsoonal Central Asia during the last 50,000 years. *QUATERNARY SCIENCE REVIEWS* 25, 163-178.

Herzschuh, U., Zhang, C., Mischke, S., Herzschuh, R., Mohammadi, F., Mingram, B., Kürschner, H., Riedel, F., 2005. A late Quaternary lake record from the Qilian Mountains (NW China): evolution of the primary production and the water depth reconstructed from macrofossil, pollen, biomarker, and isotope data. *GLOBAL AND PLANETARY CHANGE* 46, 361-379.

Hölting, B., Coldewey, W.G., 2009. Hydrogeologie. Spektrum Akademischer Verlag, Heidelberg.

Hövermann, J., Süssenberger, H., 1986. Zur Klimageschichte Hoch- und Ostasiens. *BERLINER GEOGRAPHISCHE STUDIEN* 20, 173-186.

Hou J, D'Andrea WJ, Liu Z. 2012. The influence of ^{14}C reservoir age on interpretation of paleolimnological records from the Tibetan Plateau. *QUATERNARY SCIENCE REVIEWS* 48: 67-79.

Hua, O.Y., 2009. The Himalayas - water storage under threat. Sustainable Mountain Development 56, ICIMOD, 3-5.

IAEA/WMO, 2006. Global Network of Isotopes in Precipitation. The GNIP Database. [http://www-naweb.iaea.org/napc/ih/IHS_resources_gnip.html].

Immerzeel, W.W., van Beek, L.P.H., Bierkens, M.F.P., 2010. Climate change will affect the Asian water towers. *SCIENCE* 328, 1382-1385.

India Meteorological Department, 2012. Rainfall Data for the SW Monsoon. http://www.imd.gov.in/section/nhac/dynamic/Monsoon_frame.htm.

Intergovernmental Panel on Climate Change IPCC, 2007. Contribution of Working Group I to the Fourth Assessment Report of the Intergovernmental Panel on Climate Change. Solomon,

S.D., Qin, M., Manning, Z., Chen, M., Marquis, K.B., Averyt, M., Tignor, M.M.B., Miller, H.L. (eds.). Cambridge University Press, Cambridge, United Kingdom and New York, NY, USA, 996 pp.

Jin, H.J., Li, S.X., Cheng, G.D., Shaoling, W., Li, X., 2000. Permafrost and climatic change in China. *GLOBAL AND PLANETARY CHANGE* 26, 387-404.

Johnson, K.R., Ingram, B.L., Sharp, W.D., Zhang, P.Z., 2006. East Asian summer monsoon variability during Marine Isotope Stage 5 based on speleothem $\delta^{18}O$ records from Wanxiang Cave, central China. *PALAEOGEOGRAPHY, PALAEOCLIMATOLOGY, PALAEOECOLOGY* 236, 5-19.

Jones, M.D., Leng, M.J., Eastwood, W.J., Keen, D.H., Turney, C.S.M., 2002. Interpreting stable-isotope records from freshwater snail-shell carbonate: a Holocene case study from Lake Gölhisar, Turkey. *THE HOLOCENE* 12, 629-634.

Kang, S.C., Zhang, Y.L., Zhang, Y.J., Grigholm, B., Kaspari, S., Qin, D.H., Ren, J.W., Mayewski, P., 2010. Variability of atmospheric dust loading over the central Tibetan Plateau based on ice core glaciochemistry. *ATMOSPHERIC ENVIRONMENT* 44, 2980-2989.

Khromova, T.E., Osipova, G.B., Tsvetkov, D.G., Dyurgerov, M.B., Barry, R.G., 2006. Changes in glacier extent in the eastern Pamir, Central Asia, determined from historical data and ASTA imagery. *REMOTE SENSING OF ENVIRONMENT* 102, 24-32.

Knecht, A., Walter, E., 1977. Vergleichende Untersuchung der Diäten von *Lymnaea auricularia* und *L. peregra* (Gastropoda: Basommatophora) im Zürichsee. *SCHWEIZERISCHE ZEITSCHRIFT FÜR HYDROLOGIE* 39, 299-305.

Komatsu, T., 2009. Field photographs of geomorphic features in the lake Karakul region, eastern Pamirs. *GEOGRAPHICAL STUDIES* 84, 44-50.

Komatsu, T., Watanabe, T., Hirakawa, K., 2010. A framework for Late Quaternary lake-level fluctuations in Lake Karakul, eastern Pamir, focusing on lake–glacier landform interaction. *GEOMORPHOLOGY* 119, 198-211.

Kong, P., Na, C., Fink, D., Huang, F., Ding, L., 2007. Cosmogenic [10]Be inferred lake-level changes in Sumxi Co basin, Western Tibet. *JOURNAL OF ASIAN EARTH SCIENCES* 29, 698-703.

Krishnan, R., Mujumdar, M., Vaidya, V., Ramesh, K.V., Satyan, V., 2003. The abnormal Indian summer monsoon of 2000. *JOURNAL OF CLIMATE* 16, 1177-1194.

Kuhle, M., 1998. Reconstruction of the 2.4 million km² late Pleistocene ice sheet on the Tibetan Plateau and its impact on the global climate. *QUATERNARY INTERNATIONAL* 45-46, 71-108.

Kutuzov, S., Shahgedanova, M., 2009. Glacier retreat and climatic variability in the eastern Terskey–Alatoo, inner Tien Shan between the middle of the 19th century and beginning of the 21st century. *GLOBAL AND PLANETARY CHANGE* 69, 59-70.

Kutzbach, J.E., Guetter, P.J., Ruddiman, W.F., Prell, W.L., 1989. The sensitivety of climate to late Cenozoic uplift in southern Asia and the American West: Numerical experiments. *JOURNAL OF GEOPHYSICAL RESEARCH* 94, 18393-18407.

Lamb, A.L., Leng, M.J., Lamb, H.F., Telford, R.J., Mohammed, M.U., 2002. Climatic and non-climatic effects on the $\delta^{18}O$ and $\delta^{13}C$ compositions of Lake Awassa, Ethiopia, during the last 6.5 ka. *QUATERNARY SCIENCE REVIEWS* 21, 2199-2211.

Lang, A., Bishop, M.A., Le Sueur, A., 2007. An annotated list of birds wintering in the Lhasa river watershed and Yamzho Yumco, Tibet Autonomous Region, China. *FORKTAIL* 23, 1-11.

Laskar, J., Robutel, P., Joutel, F., Gastineau, M., Correia, A.C.M., Levrard, B., 2004. A long term numerical solution for the insolation quantities of the Earth. *ASTRONOMY & ASTROPHYSICS* 428, 261-285.

Latal, C., Piller, W.E., Harzhauser, M., 2004. Palaeoenvironmental reconstructions by stable isotopes of Middle Miocene gastropods of the Central Paratethys. *PALAEOGEOGRAPHY PALAEOCLIMATOLOGY PALAEOECOLOGY* 211, 157-169.

Lee, J.-E., Fung, I., 2007. "Amount effect" of water isotopes and quantitative analysis of post-condensation processes. *HYDROLOGICAL PROCESSES* 22, 1-8.

Lee, J., Li, S.-H., Aitchison, J.C., 2009. OSL dating of paleoshorelines at Lagkor Tso, western Tibet. *QUATERNARY GEOCHRONOLOGY* 4, 335-343.

Lehner, B., Döll, P., 2004. Development and validation of a global database of lakes, reservoirs and wetlands. *JOURNAL OF HYDROLOGY* 296, 1-22.

Lehner, B., Verdin, K., Jarvis, A., 2006. HydroSHEDS Technical Documentation. World Wildlife Fund US, Washington, DC. http://hydrosheds.cr.usgs.gov

Leipe, C., Demske, D., Tarasov, P., 2013. A Holocene pollen record from the northwestern Himalayan lake Tso Moriri: Implications for palaeoclimatic and archaeological research. *QUATERNARY INTERNATIONAL*, doi: http://dx.doi.org/10.1016/j.quaint.2013.05.005

Leng, M.J., Henderson, A.C.G., 2013. Recent advances in isotopes as palaeolimnological proxies. *JOURNAL OF PALEOLIMNOLOGY* 49, 481-496.

Leng, M.J., Lamb, A.L., Lamb, H.F., Telford, R.J., 1999. Palaeoclimatic implications of isotopic data from modern and early Holocene shells of the freshwater snail *Melanoides tuberculata*, from lakes in the Ethiopian Rift Valley. *JOURNAL OF PALEOLIMNOLOGY* 21, 97-106.

Leng, M.J., Marshall, J.D., 2004. Palaeoclimate interpretation of stable isotope data from lake sediment archives. *QUATERNARY SCIENCE REVIEWS* 23, 811-831.

Leng, M.J., Telford, R.J., Ayenew, T., Umer, M., 2007. Oxygen and carbon isotope composition of authigenic carbonate from an Ethiopian lake: a climate record of the last 2000 years. *THE HOLOCENE* 17, 517-526.

Li, C.F., Yanai, M., 1996. The onset and interannual variability of the Asian summer monsoon in relation to land-sea thermal contrast. *JOURNAL OF CLIMATE* 9, 358-375.

Li, H.C., Ku, T.L., 1997. $\delta^{13}C$-$\delta^{18}O$ covariance as a paleohydrological indicator for closed-basin lakes. *PALAEOGEOGRAPHY, PALAEOCLIMATOLOGY, PALAEOECOLOGY* 133, 69-80.

Li, X.Z., Liu, W.G., Xu, L.M., 2012. Carbon isotopes in surface-sediment carbonates of modern Lake Qinghai (Qinghai-Tibet Plateau): Implications for lake evolution in arid areas. *CHEMICAL GEOLOGY* 300-301, 88-96.

Liang, E.Y., Shao, X.M., Qin, N.S., 2008. Tree-ring based summer temperature reconstruction for the source region of the Yangtze River on the Tibetan Plateau. *GLOBAL AND PLANETARY CHANGE* 61, 313-320.

Lin, Z.J., Niu, F.J., Liu, H., Lu, J.H., 2011. Hydrothermal processes of Alpine Tundra Lakes, Beiluhe Basin, Qinghai-Tibet Plateau. *COLD REGIONS SCIENCE AND TECHNOLOGY* 65, 446-455.

Linnaeus, C., 1758. Systema naturæ per regna tria naturæ, secundum classes, ordines, genera, species, cum characteribus, differentiis, synonymis, locis. Tomus I. Editio decima, reformata, Holmiæ. (Salvius), 824 pp.

Linz, E., Müller, G., 1981. Isotopen-geochemische Untersuchungen an Mollusken-Schalen verschiedener Seen Mitteleuropas. *TSCHERMAKS MINERALOGISCHE UND PETROGRAPHISCHE MITTEILUNGEN*. 29, 55-65.

Lister, G.S., Kelts, K., Zao, C.K., Yu, J.-Q., Niessen, F., 1991. Lake Qinghai, China: closed-basin lake levels and the oxygen isotope record for ostracoda since the latest Pleistocene. *PALAEOGEOGRAPHY, PALAEOCLIMATOLOGY, PALAEOECOLOGY* 84, 141-162.

Liu, J.J., Yang, B., Qin, C., 2011. Tree-ring based annual precipitation reconstruction since AD 1480 in south central Tibet. *QUATERNARY INTERNATIONAL* 236, 75-81.

Liu, J.R., Song, X.F., Yuan, G.F., Sun, X.M., Liu, X., Wang, S.Q., 2010. Characteristics of δ18O in precipitation over Eastern Monsoon China and the water vapor sources. *CHINESE SCIENCE BULLETIN* 55, 200-211.

Liu, T.C., 1995. Changes of Yamzho Lake water stage in Xizang. *SCIENTIA GEOGRAPHICA SINICA* 15, 55-62. (in Chinese with English abstract).

Liu, X.J., Lai Z.P., Madsen D., Yu, L.P., Liu, K., Zhang, J.R., 2011. Lake level variations of Qinghai Lake in northeastern Qinghai-Tibetan Plateau since 3.7 ka based on OSL dating. *QUATERNARY INTERNATIONAL* 236, 57-64.

Liu, X.H., Shao, X.M., Liang, E.Y., Chen, T., Qin, D.H., An, W.L., Xu, W.B., Sun, W.Z., Wang, Y., 2009. Climatic significance of tree-ring δ18O in the Qilian Mountains, northwestern China and its relationship to atmospheric circulation patterns. *CHEMICAL GEOLOGY* 268, 147-154.

Liu, X., Shen, J., Wang, S., Wang, Y., Liu, W., 2007. Southwest monsoon changes indicated by oxygen isotope of ostracode shells from sediments in Qinghai Lake since the late Glacial. *CHINESE SCIENCE BULLETIN* 52, 539-544.

Liu, Z., Tian, L., Yao, T., Yu, W., 2010. Characterization of precipitation $\delta^{18}O$ variation in Nagqu, central Tibetan Plateau and its climatic controls. *THEORETICAL AND APPLIED CLIMATOLOGY* 99, 99-104.

McConnaughey, T.A., Burdett, J., Whelan, J.F., Paull, C.K., 1997. Carbon isotopes in biological carbonates: Respiration and photosynthesis. *GEOCHIMICA ET COSMOCHIMICA ACTA* 61, 611-622.

McConnaughey, T.A., Gillikin, D.P., 2008. Carbon isotopes in mollusk shell carbonates. *Geo-Marine Letters* 28, 287-299.

McCrea, J.M., 1950. On the isotopic chemistry of carbonates and a paleotemperature scale. *Journal of Chmical Physics* 18, 849-857.

Mischke, S., Aichner, B., Diekmann, B., Herzschuh, U., Plessen, B., Wünnemann, B., Zhang, C., 2010a. Ostracods and stable isotopes of a late glacial and Holocene lake record from the NE Tibetan Plateau. *Chemical Geology* 276, 95-103.

Mischke, S., Bößneck, U., Diekmann, B., Herzschuh, U., Jin, H., Kramer, A., Wünnemann, B., Zhang, C., 2010b. Quantitative relationship between water-depth and sub-fossil ostracod assemblages in Lake Donggi Cona, Qinghai Province, China. *Journal of Paleolimnology* 43, 589-608.

Mischke, S., Kramer, M., Zhang, C.J., Shang, H.M., Herzschuh, U., Erzinger, J., 2008. Reduced early Holocene moisture availability in the Bayan Har Mountains, northeastern Tibetan Plateau, inferred from a multi-proxy lake record. *Palaeogeography, Palaeoclimatology, Palaeoecology* 267, 59-76.

Mischke, S., Rajabov, I., Mustaeva, N., Zhang, C.J., Herzschuh, U., Boomer, I., Brown, E., Andersen, N., Myrbo, A., Ito, E., Schudack, M.E., 2010b. Modern hydrology and late Holocene history of Lake Karakul, eastern Pamirs (Tajikistan): A reconnaissance study. *Palaeogeography, Palaeoclimatology, Palaeoecology* 289, 10-24.

Mischke, S., Zhang, C.J., 2010. Holocene cold events on the Tibetan Plateau. *Global and Planetary Change* 72, 155-163.

Molchanov, L.A., 1929. Lakes of Central Asia. Trudy Sredneaziat. Gos. Univ., *Geografiya* 3, 26-31. Tashkent. (in Russian)

Molnar, P., Boos, W.R., Battisti, D.S., 2009. Orographic controls on climate and paleoclimate of Asia: Thermal and Mechanical Roles for the Tibetan Plateau. *Annual Review of Earth and Planetary Sciences* 38, 77-102.

Mook, W.G., Bommerson, J.C., Staverman, W.H., 1974. Carbon isotope fractionation between dissolved bicarbonate and gaseous carbon dioxide. *Earth and Planetary Science Letters* 22, 169-176.

Mordan, P., Wade, C., 2008. Heterobranchia II: The pulmonata. In: Ponder, W.F., Lindberg, D.R., (eds.) Phylogeny and evolution of the mollusca, 409-426.

Morrill, C., Overpeck, J.T., Cole, J.E., 2003. A synthesis of abrupt changes in the Asian summer monsoon since the last deglaciation. *The Holocene* 13, 465-476.

Morrill, C., Overpeck, J.T., Cole, J.E., Liu, K., Shen, C., Tang, L., 2006. Holocene variations in the Asian monsoon inferred from the geochemistry of lake sediments in central Tibet. *Quaternary Research* 65, 232-243.

Murphy, M.A., Burgess, W.P., 2006. Geometry, kinematics, and landscape characteristics of an active transtension zone, Karakoram fault system, Southwest Tibet. *Journal of Structural Geology* 28, 268-283.

Murphy, M.A., Sanchez, V., Taylor, M.H., 2010. Syncollisional extension along the India–Asia suture zone, south-central Tibet: Implications for crustal deformation of Tibet. *Earth and Planetary Science Letters* 290, 233-243.

Narama, C., Kääb, A., Duishonakunov, M., Abdrakhmatov, K., 2010. Spatial variability of recent glacier area changes in the Tien Shan Mountains, Central Asia, using Corona (~1970), Landsat (~2000), and ALOS (~2007) satellite data. *Global and Planetary Change* 71, 42-54.

Ni, A., Nurtayev, B., Petrov, M., Tikhanovskaya, A., Tomashevskaya, I., 2004. The share of glacial feeding in water balance of Aral Sea and Karakul Lake. *Journal of Marine Systems* 47, 143-146.

Økland, J., 1990. Lakes and Snails. Environment and Gastropoda in 1,500 Norwegian lakes, ponds and rivers. Universal Book Services / Dr. W. Backhuys, Oegstgeest.

Opitz, S., Wünnemann, B., Aichner, B., Dietze, E., Hartmann, K., Herzschuh, U., IJmker, J., Lehmkuhl, F., Li, S., Mischke, S., Plotzki, A., Stauch, G., Diekmann, B., 2012. Late Glacial and Holocene development of Lake Donggi Cona, north-eastern Tibetan Plateau, inferred from sedimentological analysis. *Palaeogeography, Palaeoclimatology, Palaeoecology* 337-338, 159-176.

Osipov, E.Y., Khlystov, O.M., 2010. Glaciers and meltwater flux to Lake Baikal during the Last Glacial Maximum. *Palaeogeography Palaeoclimatology Palaeoecology* 294, 4-15.

Overpeck, J., Anderson, D., Trumbore, S., Prell, W., 1996. The southwest Indian monsoon over the last 18.000 years. *Climate Dynamics* 12, 213-225.

Overpeck, J., Cole, J., 2008. The rhythm of the rains. *Nature* 451, 1061-1063.

Owen, L.A., Chen, J., Hedrick, K.A., Caffee, M.W., Robinson, A.C., Schoenbohm, L.M., Yuan, Z., Li, W.Q., Imrecke, D.B., Liu, J.F., 2012. Quaternary glaciations of the Tashkurgan Valley, Southeast Pamir. *Quaternary Science Reviews* 47, 56-72.

Owen, L.A., Kamp, U., Spencer, J.Q., Haserodt, K., 2002. Timing and style of Late Quaternary glaciation in the eastern Hindu Kush, Chitral, northern Pakistan: a review and revision of the glacial chronology based on new optically stimulated luminescence dating. *Quaternary International* 97-98, 41-55.

Pang, H.X., He, Y.Q., Zhang, N.N., Li, Z.X., Theakstone, W.H., 2010. Observed glaciohydrological changes in China´s typical monsoonal temperate glacier region since 1980s. *Journal of Earth Science* 21, 179-188.

Peel, M.C., Finlayson, B.L., McMahon, T.A., 2007. Updated world map of the Köppen-Geiger climate classification. *Hydrology and Earth System Sciences* 11, 1633-1644.

Piao, S.L., Ciais, P., Yao, H.A., Shen, Z.H., Peng, S.S., Li, J.S., Zhou, L.P., Liu, H.Y., Ma, Y.C., Ding, Y.H., Friedlingstein, P., Liu, C.Z., Tan, K., Yu, Y.Q., Zhang, T.Y., Fang, J.Y., 2010. The impacts of climate change on water resources and agriculture in China. *NATURE* 467, 43-51.

Prell, W.L., Kutzbach, J.E., 1992. Sensitivity of the Indian monsoon to forcing parameters and implications for its evolution. *NATURE* 360, 647-652.

Qian, W.H., Ding, T., Hu, H.R., Lin, X.A., Qin, A.M., 2009. An overview of dry-wet climate variability among monsoon-westerly regions and the monsoon northernmost marginal active zone in China. *ADVANCES IN ATMOSPHERIC SCIENCES* 26, 630-641.

Qin, C., Yang, B., Bräuning, A., Sonechkin, D.M., Huang, K., 2011. Regional extreme climate events on the northeastern Tibetan Plateau since AD 1450 inferred from tree rings. *GLOBAL AND PLANETARY CHANGE 75*, 143-154.

Qiu, J., 2008. The Third Pole. *NATURE* 454, 393-396.

Raymo, M.E., Ruddiman, W.F., 1992. Tectonic forcing of late Cenozoic climate change. *NATURE* 359, 117-122.

Rhode, D., Ma, H., Madsen, D.B., Brantingham, P.J., Forman, S.L., Olsen, J.W., 2010. Paleoenvironmental and archaeological investigation at Qinghai Lake, western China: geomorphic and chronometric evidence of lake level history. *QUATERNARY INTERNATIONAL* 218, 29-44.

Rhodes, T.E., Gasse, F., Lin, R., Fontes, J.C., Keqin, W., Bertrand, P., Gibert, E., Mélières, F., Tucholka, P., Wang, Z.X., Cheng, Z.Y., 1996. A Late Pleistocene-Holocene lacustrine record from Lake Manas, Zunggar (northern Xinjiang, western China). *PALAEOGEOGRAPHY PALAEOCLIMATOLOGY PALAEOECOLOGY* 120, 105-121.

Ricketts, R.D., Johnson, T.C., Brown, E.T., Rasmussen, K.A., Romanovsky, V.V., 2001. The Holocene paleolimnology of Lake Issyk-Kul, Kyrgyzstan: trace element and stable isotope composition of ostracods. *PALAEOGEOGRAPHY PALAEOCLIMATOLOGY PALAEOECOLOGY* 176, 207-227.

Riedel, F., 1993. Early ontogenetic shell formation in some freshwater gastropods and taxonomic implications of the protoconch. *LIMNOLOGICA* 23, 349-368.

Robinson, A.C., Yin, A., Manning, C.E., Harrison, T.M., Zhang, S.H., Wang, X.F., 2007. Cenozoic evolution of the eastern Pamir: Implications for strain-accommodation mechanisms at the western end of the Himalayan-Tibetan orogen. *GEOLOGICAL SOCIETY OF AMERICA BULLETIN* 119, 882-896.

Röpstorf, P., Riedel, F., 2004. Deep-water gastropods endemic to Lake Baikal - An Sem study on protoconchs and radulae. *JOURNAL OF CONCHOLOGY* 38, 253-282.

Rohlf, F.J., 2007. Morphometrics at SUNY Stony Brook. Morpho-Tool, online access http://life.bio.sunysb.edu/morph/index.html

Rozanski, K., Araguás-Araguás, L., Gonfiantini, R., 1993. Isotopic patterns in modern global precipitation. *GEOPHYSICAL MONOGRAPH* 78, 1-36.

Royden, L.H., Burchfiel, B.C., Hilst van der, R.D., 2008. The Geological Evolution of the Tibetan Plateau. SCIENCE 321, 1054-1058.

Rupper, S., Roe, G., Gillespie, A., 2009. Spatial patterns of Holocene glacier advance and retreat in Central Asia. QUATERNARY RESEARCH 72, 337-346.

Safarov, N.M., 2006. Republic of Tajikistan. National Environmental Action Plan. www.unpei.org/PDF/National_Environmental_Action_Plan_eng.pdf.

Sarikaya, M.A., Zreda, M., Çiner, A., 2009. Glaciations and paleoclimate of Mount Erciyes, central Turkey, since the Last Glacial Maximum, inferred from [36]Cl cosmogenic dating and glacier modeling. QUATERNARY SCIENCE REVIEWS 28, 2326-2341.

Sato, T., 2009. Influences of subtropical jet and Tibetan Plateau on precipitation pattern in Asia: Insights from regional climate modeling. QUATERNARY INTERNATIONAL 194, 148-158.

Scherler, D., Bookhagen, B., Strecker, M.R., 2011. Spatially variable response of Himalayan glaciers to climate change affected by debris cover. NATURE GEOSCIENCE 4, 156-159.

Schlolaut, G., Marshall, M.H., Brauer, A., Nakagawa, T., Lamb, H.F., Staff, R.A., Ramsey, C.B., Bryant, C.L., Brock, F., Kossler, A., Tarasov, P.E., Yokoyama, Y., Tada, R., Haraguchi, T., Suigetsu 2006 project members, 2012. An automated method for varve interpolation and its application to the Late Glacial chronology from Lake Suigetsu, Japan. Quaternary Geochronology 13, 52-69.

Schmitz, B., Andreasson, F.P., 2001. Air humidity and lake $\delta^{18}O$ during the latest Paleocene–earliest Eocene in France from recent and fossil fresh-water and marine gastropod $\delta^{18}O$, $\delta^{13}C$, and $^{87}Sr/^{86}Sr$. GEOLOGICAL SOCIETY OF AMERICA BULLETIN 113, 774-789.

Schöne, B.R., Gillikin, D.P., 2013. Unraveling environmental histories from skeletal diaries – Advances in sclerochronology. PALAEOGEOGRAPHY PALAEOCLIMATOLOGY PALAEOECOLOGY 373, 1-5.

Schöne, B.R., Oschmann, W., Tanabe, K., Dettman, D., Fiebig, J., Houk, S.D., Kanie, Y., 2004. Holocene seasonal environmental trends at Tokyo Bay, Japan, reconstructed from bivalve mollusk shells—implications for changes in the East Asian monsoon and latitudinal shifts of the Polar Front. QUATERNARY SCIENCE REVIEWS 23, 1137-1150.

Seong, Y.B., Owen, L.A., Bishop, M.P., Bush, A., Clendon, P., Copland, L., Finkel, R., Kamp, U., Shroder, J.F., 2007. Quaternary glacial history of the Central Karakoram. QUATERNARY SCIENCE REVIEWS 26, 3384-3405.

Seong, Y.B., Owen, L.A., Yi, C., Finkel, R.C., 2009. Quaternary glaciations of Muztag Ata and Kongur Shan: evidence for glacier response to rapid climate changes throughout the Late Glacial and Holocene in westernmost Tibet. THE GEOLOGICAL SOCIETY OF AMERICA BULLETIN 121, 348-365.

Shanahan, T.M., Pigati, J.S., Dettman, D.S., Quade, J., 2005. Isotopic variability in the aragonite shells of freshwater gastropods living in springs with nearly constant temperature and isotopic composition. GEOCHIMICA ET COSMOCHIMICA ACTA 69, 3949-3966.

Sharp, Z., 2007. Principles of stable isotope geochemistry. Pearson Prentice Hall, Upper Saddle River, NY, USA, 344 pp.

Sinha, A., Stott, L., Berkelhammer, M., Cheng, H., Edwards, R.L., Buckley, B., Aldenderfer, M., Mudelsee, M., 2011. A global context for megadroughts in monsoon Asia during the past millennium. *QUATERNARY SCIENCE REVIEWS* 30, 47-62.

Solomina, O., Barry, R., Bodnya, M., 2004. The retreat of Tien Shan glaciers (Kyrgyzstan) since the Little Ice Age estimated from aerial photographs, lichenometric and historical data. *GEOGRAFISKA ANNALER* 86, 205-215.

Sorrel, P., Popescu, S.M., Head, M.J., Suc, J.P., Klotz, S., Oberhänsli, H., 2006. Hydrographic development of the Aral Sea during the last 2000 years based on a quantitative analysis of dinoflagellate cysts. *PALAEOGEOGRAPHY PALAEOCLIMATOLOGY PALAEOECOLOGY* 234, 304-327.

Stevens, R.E., Metcalfe, S.E., Leng, M.J., Lamb, A.L., Sloane, H.J., Naranjo, E., González, S., 2012. Reconstruction of late Pleistocene climate in the Valsequillo Basin (Central Mexico) through isotopic analysis of terrestrial and freshwater snails. *PALAEOGEOGRAPHY, PALAEOCLIMATOLOGY, PALAEOECOLOGY* 319-320, 16-27.

Stift, M., Michel, E., Sitnikova, T.Y., Mamonova, E. Y., Sherbakov, D. Y., 2004. Palaearctic gastropod gains a foothold in the dominion of endemics: range expansion and morphological change of *Lymnaea* (*Radix*) *auricularia* in Lake Baikal. *HYDROBIOLOGIA* 513, 101-108.

Stone, R., 2010. Severe droughts puts spotlight on Chinese dams. *SCIENCE* 327, 1311.

Tapponnier, P., Xu, Z.Q., Roger, F., Meyer, B., Arnaud, N., Wittlinger, G., Yang, J.S., 2001. Oblique stepwise rise and growth of the Tibet Plateau. *SCIENCE* 294: 1671-1677.

Taft, L., Wiechert, U., Riedel, F., Weynell, M., Zhang, H.C., 2012. Sub-seasonal oxygen and carbon isotope variations in shells of modern *Radix* sp. (Gastropoda) from the Tibetan Plateau: Potential of a new archive for palaeoclimatic studies. *QUATERNARY SCIENCE REVIEWS* 34, 44-56.

Taft, L., Wiechert, U., Zhang, H.C., Lei, G.L., Mischke, S., Plessen, B., Weynell, M., Winkler, A., Riedel, F., 2013. Oxygen and carbon isotope patterns archived in shells of the aquatic gastropod *Radix*: Hydrologic and climatic signals across the Tibetan Plateau in sub-monthly resolution. *QUATERNARY INTERNATIONAL* 290-291, 282-298.

Talbot, M.R., 1990. A review of the palaeohydrological interpretation of carbon and oxygen isotope ratios in primary lacustrine carbonates. *CHEMICAL GEOLOGY* 80, 261-279.

Tan, L.C, Cai, Y.J., Cheng, H., An, Z.S., Edwards, R.L., 2009. Summer monsoon precipitation variations in central China over the past 750 years derived from a high-resolution absolute-dated stalagmite. *PALAEOGEOGRAPHY, PALAEOCLIMATOLOGY, PALAEOECOLOGY* 280, 432-439.

Tian, L., Liu, Z., Gong, T., Yin, C., Yu, W., Yao, T., 2008. Isotopic variation in the lake water balance at the Yamdruk-tso basin, southern Tibetan Plateau. *HYDROLOGICAL PROCESSES* 22, 3386-3392.

Tian, L.D., Yao, T.D., MacClune, K., White, J.W.C., Schilla, A., Vaughn, B., Vachon, R., Ichiyanagi, K., 2007. Stable isotopic variations in west China: A consideration of moisture sources. *Journal of Geophysical Research* 112, D10112, doi:10.1029/2006JD007718.

Tian, L., Yao, T., Numaguti, A., Sun, W., 2001. Stable isotope variations in monsoon precipitation on the Tibetan Plateau. *Journal of the Meteorological Society of Japan* 79, 959-966.

Thompson, L.G., 2000. Ice core evidence for climate change in the Tropics: implications for the future. *Quaternary Science Reviews* 19, 19-35.

Thompson, L.G., Davis, M.E., Mosley-Thompson, E., Lin, P., Henderson, K.A., Mashiotta, T.A., 2005. Tropical ice core records: evidence for asynchronous glaciation on Milankovitch timescales. *Journal of Quaternary Sciences* 20, 723-733.

Thompson, L.G., Mosley-Thompson, E., Davis, M.E., Bolzan, J.F., Dai, J., Yao, T., Gundestrup, N., Wu, X., Klein, L., Xie, Z., 1989. Holocene-Late Pleistocene climatic ice core records from Qinghai-Tibetan Plateau. *Science* 246, 474-477.

Thompson, L.G., Mosley-Thompson, E., Davis, M.E., Mashiotta, T.A., Henderson, K.A., Lin, P.N., Yao, T.D., 2006, Ice core evidence for asynchronous glaciation on the Tibetan Plateau. *Quaternary International* 154-155, 3-10.

Thompson, L.G., Yao, T., Davis, M.E., Henderson, K.A., Mosley-Thompson, E., Lin, P.-N., Beer, J., Synal, H.-A., Cole-Dai, J., Bolzan, J.F., 1997. Tropical climate instability: The last glacial cycle from a Qinghai-Tibetan ice core. *Science* 276, 1821-1825.

Thompson, L.G., Yao, T., Mosley-Thompson, E., Davis, M.E., Henderson, K.A., Lin, P.-N., 2000. A high-resolution millennial record of the South Asian monsoon from Himalayan ice cores. *Science* 289, 1916-1919.

Tütken, T., Vennemann, T.W., Janz, H., Heizmann, E.P.J., 2006. Palaeoenvironment and palaeoclimate of the Middle Miocene lake in the Steinheim basin, SW Germany: A reconstruction from C, O, and Sr isotopes of fossil remains. *Palaeogeography, Palaeoclimatology, Palaeoecology* 241, 457-491.

Unger-Shayesteh, K., Vorogushyn, S., Farinotti, D., Gafurov, A., Duethmann, D., Mandychey, A., Merz, B., 2013. What do we know about past changes in the water cycle of Central Asian headwaters? A review. *Global and Planetary Change*, doi: 10.1016/j.gloplacha.2013.02.004

Vasskog, K., Paasche, Ø., Nesje, A., Boyle, J.F., Birks, H.J.B., 2012. A new approach for reconstructing glacier variability based on lake sediments recording input from more than one glacier. *Quaternary Research* 77 192-204.

Van der Woerd, J., Tapponnier, P., Ryerson, F.J., Meriaux, A.-S., Meyer, B., Gaudemer, Y., Finkel, R.C., Caffee, M.W., Guoguang, Z., Zhiqin, X., 2002. Uniform postglacial slip-rate along the central 600 km of the Kunlun Fault (Tibet), from 26Al, 10Be, and 14C dating of riser offsets, and climatic origin of the regional morphology. *Geophysical Journal International* 148, 356–388.

von Oheimb, P.V., Albrecht, C., Riedel, F., Du, L., Yang, J.X., Aldrige, D.C., Bößneck, U., Zhang, H.C., Wilke, T., 2011. Freshwater biogeography and limnological evolution of the Tibetan

Plateau - Insights from a plateau-wide distributed gastropod taxon (*Radix* spp.). *PLoS ONE* 6, e26307, doi:10.1371/journal.pone.0026307.

Walter, J.E., 1977. Lebenszyklen von *Lymnaea peregra* im Zürichsee. *ARCHIV FÜR MOLLUSKENKUNDE* 108, 177-184.

Wanamaker, A.D. Jr., 2010. Visions: the future of sclerochronology. Abstract 2nd International Sclerochronology Conference, Mainz, Germany. *TERRA NOSTRA*, 85.

Wang, B., French, H.M., 1995. Permafrost on the Tibetan Plateau, China. *QUATERNARY SCIENCE REVIEWS* 14, 255-274.

Wang, B., Huang, F., Wu, Z.W., Yang, J., Fu, X.H., Kikuchi, K., 2009. Multi-scale climate variability oft he South China Sea monsoon: A review. *DYNAMICS OF ATMOSPHERES AND OCEANS* 47, 15-37.

Wang, P.X., Clemens, S., Beaufort, L., Braconnot, P., Ganssen, G., Jian, Z.M., Kershaw, P., Sarntheim, M., 2005. Evolution and variability of the Asian monsoon system: state of the art and outstanding issues. *QUATERNARY SCIENCE REVIEWS* 24, 595-629.

Wang, R.L., Scarpitta, S.C., Zhang, S.C., Zheng, M.P., 2002. Later Pleistocene/Holocene climate conditions of Qinghai-Xizhang Plateau (Tibet) based on carbon and oxygen stable isotopes of Zabuye Lake sediments. *EARTH AND PLANETARY SCIENCE LETTERS* 203, 461-477.

Wang, S.F., Zhang, W.L., Gang, X.M., Dai, S.A., Kempf, O., 2008. Magnetostratigraphy of the Zanda basin in southwest Tibet Plateau and its tectonic implications. *CHINESE SCIENCE BULLETIN* 53, 1393-1400.

Wang, Y.B., Liu, X.Q., Herzschuh, U., 2010. Asynchronous evolution of the Indian and East Asian summer monsoon indicated by Holocene moisture patterns in monsoonal central Asia. *EARTH-SCIENCE REVIEWS* 103, 135-153.

Wang, Y.D., Zheng, J.J., Zhang, W.L., Li, S.Y., Liu, X.W., Yang, X., Liu, Y.H., 2012. Cenozoic uplift of the Tibetan Plateau: Evidence from the tectonic-sedimentary evolution of the western Qaidam Basin. *GEOSCIENCE FRONTIERS* 3, 175-187.

Wang, Y.J., Cheng, H., Edwards, R.L., An, Z.S., Wu, J.Y., Shen, C.C., Dorale, J.A., 2001. A high-resolution absolute-dated late Pleistocene monsoon record from Hulu Cave, China. *SCIENCE* 294, 2345-2348.

Wang, Y.J., Cheng, H., Edwards, R.L., He, Y.Q., Kong, X.G., An, Z.S., Wu, J.Y., Kelly, M.J., Dykoski, C.A., Li, X.D., 2005. The Holocene Asian monsoon: links to solar changes and North Atlantic climate. *SCIENCE* 308, 854-857.

Wang, Y.,Wang, X., Xu,Y., Zhang, C., Li, Q., Tseng, Z.J., Takeuchi, G., Deng, T., 2008. Stable isotopes in fossil mammals, fish and shells from Kunlun Pass Basin, Tibetan Plateau: Paleo-climatic and paleo-elevation implications. *EARTH AND PLANETARY SCIENCE LETTERS* 270, 73-85.

Webster, P.J., Toma, V.E., Kim, H.-M., 2011. Were the 2010 Pakistan floods predictable? *GEOPHYSICAL RESEARCH LETTERS* 38, L04806, doi:10.1029/2010GL046346.

Wefer, G., Berger, W.H., 1991. Isotope paleontology: Growth and composition of extant calcareous species. *MARINE GEOLOGY* 100, 207-248.

Wei, K., Gasse, F., 1999. Oxygen isotopes in lacustrine carbonates of West China revisited: implications for post glacial changes in summer monsoon circulation. *QUATERNARY SCIENCE REVIEWS* 18 13615-1334.

White, D., Preece, R.C., Shchetnikov, A.A., Parfitt, S.A., Dlussky, K.G., 2008. A Holocene molluscan succession from floodplain sediments of the upper Lena River (Lake Baikal region), Siberia. *QUATERNARY SCIENCE REVIEWS* 27, 962-987.

White, R.M.P., Dennis, P.F., Atkinson, T.C., 1999. Experimental calibration and field investigation of the oxygen isotope fractionation between biogenic aragonite and water. *RAPID COMMUNICATIONS IN MASS SPECTROMETRY* 13, 1242-1247.

Wischnewski, J., Mischke, S., Wang, Y.B., Herzschuh, U., 2011. Reconstructing climate variability on the northeastern Tibetan Plateau since the last Lateglacial – a multi-proxy, dual-site approach comparing terrestrial and aquatic signals. *QUATERNARY SCIENCE REVIEWS* 30, 82-97.

World Glacier Monitoring Service WGMS, 2012. Global Glacier Changes: facts and figures. http://www.grid.unep.ch/glaciers/pdfs/glaciers.pdf

Wu, J., Li, S., Luecke, A., Wang, S., 2002. Climatic signals in the last 200 years from stable isotope record in the shells of freshwater snails in Lake Xingcuo, Eastern Tibet Plateau, China. *CHINESE JOURNAL OF GEOCHEMISTRY* 21, 234-243.

Wu, Y., Cui, Z., Liu, G., Ge D., Yin, J., Xu, Q. & Pang, Q., 2001. Quaternary geomorphological evolution of the Kunlun Pass area and uplift of the Qinghai-Xizang (Tibet) Plateau. *GEOMORPHOLOGY* 36, 203-216.

Wu, Y.H., Lücke, A., Jin, Z.D., Wang, S.M., Schleser, G.H., Batterbee, R.W., Xia, W.L., 2006. Holocene climate development on the central Tibetan Plateau: A sedimentary record from Cuoe Lake. *PALAEOGEOGRAPHY, PALAEOCLIMATOLOGY, PALAEOECOLOGY* 234, 328-340.

Wu, Y.Q., Cui, Z.J., Liu, G.N., Ge, D.K., Yin, J.R., Xu, Q.H., Pang, Q.Q., 2001. Quaternary geomorphological evolution of the Kunlun Pass area and uplift of the Qinghai-Xizang (Tibet) Plateau. *GEOMORPHOLOGY* 36, 203-216.

Wünnemann, B., Demske, D., Tarasov, P., Kotlia, B.S., Reinhardt, C., Bloemendal, J., Diekmann, B., Hartmann, K., Krois, J., Riedel, F., Arya, N., 2010. Hydrological evolution during the last 15 kyr in the Tso Kar lake basin (Ladakh, India), derived from geomorphological, sedimentological and palynological records. *QUATERNARY SCIENCE REVIEWS* 29, 1138-1155.

Wünnemann, B., Mischke, S., Chen, F.H., 2006. A Holocene sedimentary record from Bosten Lake, China. *PALAEOGEOGRAPHY PALAEOCLIMATOLOGY PALAEOECOLOGY* 234, 223-238.

Xiao, G.Q., Guo, Z.T., Dupont-Nivet, G., Lu, H.Y., Wu, N.Q., Ge, J.Y., Hao, Q.Z., Peng, S.Z., Li, F.J., Abels, H.A., Zhang, K.X., 2012. Evidence for northeastern Tibetan Plateau uplift between 25 and 20 Ma in the sedimentary archive of the Xining Basin, northwestern China. *EARTH AND PLANETARY SCIENCE LETTERS* 317-318: 185-195.

Xu, H., Hou, Z.H., Ai, L., Tan, L.C., 2007. Precipitation at Lake Qinghai, NE Qinghai-Tibet Plateau, and its relation to Asian summer monsoons on decadal/interdecadal scales during the past 500 years. *PALAEOGEOGRAPHY, PALAEOCLIMATOLOGY, PALAEOECOLOGY* 254, 541-549.

Xu, X.D., Lu, C.G., Shi, X.H., Gao, S.T., 2008. World water tower: An atmospheric perspective. *GEOPHYSICAL RESEARCH LETTERS* 35, L20815, doi:10.1029/2008GL035867.

Yan, G., Wang, F.B., Shi, G.R., Li, S.F., 1999. Palynological and stable isotopic study of palaeoenvironmental changes on the northeastern Tibetan plateau in the last 30,000 years. *PALAEOGEOGRAPHY, PALAEOCLIMATOLOGY, PALAEOECOLOGY* 153, 147-159.

Yanai, M., Wu, G.-X., 2006. Effects of the Tibetan Plateau. Wang, B., (ed.). The Asian Monsoon. Springer Berlin Heidelberg, 788 pp.

Yang, B., Bräuning, A., Shi, Y.F., 2003. Late Holocene temperature fluctuations on the Tibetan Plateau. *QUATERNARY SCIENCE REVIEWS* 22, 2335-2344.

Yang, B., Bräuning, A., Yao, T.D., Davis, M.E., 2007. Correlation between the oxygen isotope record from Dasuopu ice core and the Asian Southwest monsoon during the last millennium. *QUATERNARY SCIENCE REVIEWS* 26, 1810-1817.

Yang, X., Scuderi, L.A., 2010. Hydrological and climatic changes in deserts of China since the late Pleistocene. *QUATERNARY RESEARCH* 73, 1-9.

Yang, X., Scuderi, L., Paillou, P., Liu, Z., Li, H., Ren, X., 2011. Quaternary environmental changes in the drylands of China - A critical review. *QUATERNARY SCIENCE REVIEWS* 30, 3219-3233.

Yang, Y.D., Man, Z.M., Zheng, J.Y., 2007. Reconstruction of the starting time series of rainy season in Yunnan and the evolvement of summer monsoon during 1711-1982. *JOURNAL OF GEOGRAPHICAL SCIENCES* DOI: 10.1007/s11442-007-0212-9.

Yao, T.D., Li, Z.X., Thompson, L.G., Mosley-Thompson, E., Wang, Y.Q., Tian, L.D., Wang, N.L., Duan, K.Q., 2006. δ18O records from Tibetan ice cores reveal differences in climatic changes. *ANNALS OF GLACIOLOGY* 43, 1-7.

Yao, Z.J., Liu, J., Huang, H.Q., Song, X.F., Dong, X.H., Liu, X., 2009. Characteristics of isotope in precipitation, river water and lake water in the Manasarovar basin of Qinghai-Tibet Plateau. *ENVIRONMENTAL GEOLOGY* 57, 551-556.

Ye, D.Z., Wu, G.X., 1998. The role of the heat source of the Tibetan Plateau in the general circulation. *METEOROLOGY AND ATMOSPHERIC PHYSICS* 67, 181-198.

Young, M.R., 1975. The life cycles of six species of freshwater molluscs in the Worcester-Birmingham Canal. *PROCEEDINGS OF THE MALACOLOGICAL SOCIETY OF LONDON* 41, 533-548.

Yu, G., Harrison, S.P., Xue, B., 2001. Lake status records from China: Data base documentation. Max Planck Institute for BiogeochemistryTechical Report 4. Online access http://www.bgc-jena.mpg.de/uploads/Publications/TechnicalReports/tech_report4.pdf.

Yu, S.Q., Shi, X.H., Lin, X.C., 2009. Interannual variation of East Asian summer monsoon and its impacts on general circulation and precipitation. *JOURNAL OF GEOGRAPHICAL SCIENCES* 19, 67-80.

Yu, W., Yao, T., Tian, L., Ma, Y., Ichiyanagi, K., Wang, Y., Sun, W., 2008. Relationships between δ18O in precipitation and air temperature and moisture origin on a south–north transect of the Tibetan Plateau. *ATMOSPHERIC RESEARCH* 87, 158-169.

Yue, Y., Ritts, B.D., Graham, S.A., Wooden, J.L., Gehrels, G.E., Zhang, Z., 2003. Slowing extrusion tectonics: lowered estimate of post-Early Miocene slip rate for the Altyn Tagh fault. *EARTH AND PLANETARY SCIENCE LETTERS* 217, 111-122.

Zech, R., Abramowski, U., Glaser, B., Sosin, P., Kubik, P.W., Zech, W., 2005. Late Quaternary glacial and climate history of the Pamir Mountains derived from cosmogenic [10]Be exposure ages. *QUATERNARY RESEARCH* 64, 212-220.

Zhang, C.J., Mischke, S., 2009. A Lateglacial and Holocene lake record from the Nianbaoyeze Mountains and inference of lake, glacier and climate evolution on the eastern Tibetan Plateau. *QUATERNARY SCIENCE REVIEWS* 28, 1970-1983.

Zhang, C.J., Zhang, W.Y., Feng, Z.D., Mischke, S., Gao, X., Gao, D., Sun, F.F., 2012. Holocene hydrological and climatic change on the northern Mongolian Plateau based on multi-proxy records from Lake Gun Nuur. *PALAEOGEOGRAPHY PALAEOCLIMATOLOGY PALAEOECOLOGY* 323-325, 75-86.

Zhang, J.W., Chen, F.H., Holmes, J.A., Li, H., Guo, X.Y., Wang, J.L., Li, S., Lü, Y.B., Zhao, Y., Qiang, M.R., 2011. Holocene monsoon climate documented by oxygen and carbon isotopes from lake sediments and peat bogs in China: A review and synthesis. *QUATERNARY SCIENCE REVIEWS* 30, 1973-1987.

Zhang, Y., Kong, Z.C., Yan, S., Yang, Z.J., Ni, J., 2009. "Medieval Warm Period" on the northern slope of central Tienshan Mountains, Xinjiang, NW China. *GEOPHYSICAL RESEARCH LETTERS* 36. doi:10.1029/2009GL037375

Zhao, Y., Yu, Z.C., Zhao, W.W., 2011. Holocene vegetation and climate histories in the eastern Tibetan Plateau: controls by insolation-driven temperature or monsoon-derived precipitation changes? *QUATERNARY SCIENCE REVIEWS* 30, 1173-1184.

Zheng, M.P., 1997. An introduction to saline lakes on the Qinghai-Tibet Plateau. Monographiae Biologicae 76. Kluwer Academic Publishers, Dordrecht.

Zheng, W., Yao, T.D., Joswiak, D.R., Xu, B.Q., Wang, N.L., Zhao, H.B., 2010. Major ions composition records from a shallow ice core on Mt. Tanggula in the central Qinghai-Tibetan Plateau. *ATMOSPHERIC RESEARCH* 97, 70-79.

7. Appendix

7.1 List of publications and presentations

<u>International peer-reviewed articles</u>

Taft, L., Mischke, S., Leipe, C., Rajabov, I., Riedel, F., Wiechert, U. Oxygen and carbon isotope ratios in *Radix* (Gastropoda) shells indicate changes of glacial meltwater flux and temperature since 4200 cal yr BP at Lake Karakul, eastern Pamirs (Tajikistan). *JOURNAL OF PALAEOLIMNOLOGY*, submitted.

Taft, L., Wiechert, U., Riedel, F., Weynell, M., Zhang, HC., 2012. Sub-seasonal oxygen and carbon isotope variations in shells of modern *Radix* sp. (Gastropoda) from the Tibetan Plateau: potential of a new archive for palaeoclimate studies. *QUATERNARY SCIENCE REVIEWS* 34, 44-56.

Taft, L., Wiechert, U., Zhang, HC., Lei, GL., Mischke, S., Plessen, B., Weynell, M., Winkler, A., Riedel, F., 2012. Oxygen and carbon isotope patterns archived in shells of the aquatic gastropod *Radix*: Hydrologic and climatic signals across the Tibetan Plateau in sub-monthly resolution. *QUATERNARY INTERNATIONAL* 290-291, 282-298.

<u>Talks, Abstracts and Poster Presentations</u>

Taft, L., Mischke, S., Wiechert, U., Zhang, HC., 2013. Sclerochronologic isotope patterns in shells of the aquatic gastropod *Radix*: A hydrologic and climatic archive for the Tibetan Plateau in sub-seasonal resolution. Abstract and talk Applied Isotope Geochemistry Conference, Budapest, Hungary.

Taft, L., Albrecht, C., Mischke, S., von Oheimb, P., Riedel, F., Wiechert, U., Wilke, T., Zhang, HC., 2013. The aquatic gastropod genus *Radix*: A new archive for inferring Neogene and Quaternary palaeoclimatic patterns across the Tibetan Plateau and its possible application in palaeoelevation studies. Abstract for Humboldt-Kolleg *"Third Pole Demands Protection (HOPE - 2013)* Nainital, India.

Taft, L., Wiechert, U., Zhang, HC., Mischke, S., Plessen, B., Weynell, M., Winkler, A., Riedel, F., 2012. Stable isotope compositions in modern gastropod shells from the Tibetan Plateau and the Pamirs mirror hydrologic and climatic signals in sub-seasonal resolution. Abstract in Journal of Nepal Geologic Society 45, 85.

Taft, L., Wiechert, U., Zhang, HC., Mischke, S., Plessen, B., Weynell, M., Winkler, A., Riedel, F., 2012. Hydrologic and climatic signals across the Tibetan Plateau inferred from $\delta^{18}O$ and

δ^{13}C patterns archived in shells of the gastropod *Radix* sp.: A window to the past? Abstract and talk Centenary Meeting of the Palaeontologic Society, Berlin, Germany.

Riedel, F., Fuchs, M., Henderson, A., Kossler, A., Leipe, C., Schmidt, M., **Taft, L.**, 2012. Evolution of the mega-lake Palaeo-Makgadikgadi (Kalahari, Botswana) during the last 100 ka. Abstract in Speciation in Ancient Lakes (SIAL) – 6, Bogor, Indonesia.

Taft, L., Wiechert, U., Riedel, F., Weynell, M., Zhang, HC., 2011. Oxygen and carbon isotope analyses in shells of the freshwater gastropod *Radix* sp.: a suitable method for reconstructing lake history on the Tibetan Plateau. Abstract and talk INQUA, Bern, Switzerland.

Taft, L., Riedel, F., Wiechert, U., Weynell, M., Zhang, HC., 2010. Monsoon signals in shells of the gastropod *Radix*: a new archive for lake history and palaeoclimate studies on the Tibetan Plateau. Abstract and Poster presentation AGU, San Francisco, United States of America.

7.2 Curriculum Vitae

For reasons of data protection,

the curriculum vitae is not included in the online version

For reasons of data protection,

the curriculum vitae is not included in the online version